

ENGINEERING APPLICATIONS

SOCIAL | TECHNOLOGY | ENGINEERING | MATHEMATICS



AI

Editor in Chief

Prof. Dr. Murat Yakar

Mersin University, Department of Geomatics Engineering (myakar@mersin.edu.tr)

Advisory Board

Prof. Dr. Mehmet Cihan AYDIN, BITLIS EREN UNIVERSITY (mcaudin@beu.edu.tr)

Associate Professor Ercan IŞIK, BITLIS EREN UNIVERSITY (eisik@beu.edu.tr)

Associate Professor Ümit BUDAK, BITLIS EREN UNIVERSITY (ubudak@beu.edu.tr)

Associate Professor. Mehmet Baran, Ankara Yıldırım Beyazıt University (mehmet.baran@ybu.edu.tr)

Associate Professor. Memduh Kara, Mersin University (memduhkara@mersin.edu.tr)

Associate Professor. Cafer Erkin Koyuncu, Mersin University (ckoyuncu@mersin.edu.tr)

Asst. Prof Atta-ur-Rahman, University of Peshawar (atta-ur-rehman@uop.edu.pk)

Abdell Aziiz Fathii Abdell Aziiz Elfadally, Basilicata University / Italian National Research Councils / National Authority for Remote Sensing and Space Sciences (abdelaziz.elfadaly@narss.sci.eq) / (abdelaziz.elfadaly@imaa.cnr.it)

Lec. Mustafa Buber, Selçuk University (mbuber@selcuk.edu.tr)

Technical Editor

Res. Asst. Aydın Alptekin

Engineering Applications (ENAP) is a multidisciplinary journal and covers all fields of basic science and engineering. The Journal is involved in both experimental and theoretical studies on the subject area of basic science and engineering. The Journal is a multidisciplinary journal and covers all fields of basic science and engineering. It is the main purpose of the Journal that to convey the latest development on science and technology towards the related scientists and to the readers. The Journal is also involved in both experimental and theoretical studies on the subject area of basic science and engineering. ADEJ is a fully free journal, which does not take any article processing charge from authors.

Engineering Applications (ENAP) is a multidisciplinary journal and covers all fields of basic science and engineering

- Aerospace Engineering
- Environmental Engineering
- Civil Engineering
- Geomatics Engineering
- Mechanical Engineering
- Geology Science and Engineering
- Mining Engineering
- Chemical Engineering
- Metallurgical and Materials Engineering
- Electrical and Electronics Engineering
- Mathematical Applications in Engineering
- Computer Engineering
- Food Engineering

CONTENTS

Volume 1 Issue 2

ARTICLES

- The function of artificial intelligence and its sub-branches in the field of health**
Hüseyin Fırat Kayıran 99-107
- Structural, petrographic and geochemical features of the calcite quarry in the Biga Peninsula (Çanakkale, Türkiye)**
Mustafa Kaya, Cihan Yalçın, Mustafa Kumral 108-116
- Overview of neurodegenerative disease**
Havva Türkben, Furkan Ayaz 117-123
- Direct pouring system design and optimization in steel castings**
Mustafa Murat Zor, Serdar Kesim, Buğra Erbakan, Ferhat Tülüce, Alper Yoloğlu, Kazım Çakır 124-131
- Components used in the vulcanization of rubber**
Ahmet Güngör 132-136
- Development of individualized education system with artificial intelligence Fuzzy logic method**
Hüseyin Fırat Kayıran, Ufuk Şahmeran 137-144
- Provenance, petrographic and geochemical signatures of sandstones in Çalarasın Formation: A unit of ophiolitic melange in eastern of Kargı District**
Cihan Yalçın, Nurullah Hanilçı, Mustafa Kumral, Mustafa Kaya 145-156
- Investigation of the effects of using steel cross and reinforced concrete shears earthquake performance in building**
Muhammed Mustafa Eser, Hüsnü Can 157-162
- Overview of multiple sclerosis (MS) and systemic lupus erythematosus (SLE)**
Ceren Canatar, Furkan Ayaz 163-169
- Detection of materials and material deterioration in historical buildings by spectroscopic and petrographic methods: The example of Mardin Tamir Evi**
Lale Karataş, Aydın Alptekin, Murat Yakar 170-187



The function of artificial intelligence and its sub-branches in the field of health

Hüseyin Fırat Kayıran*¹ 

¹ARDSI, Mersin Provincial Coordination Unit, Mersin, Türkiye, huseyinfirat kayiran@tkdk.gov.tr

Cite this study: Kayıran, H. F. (2022). The function of artificial intelligence and its sub-branches in the field of health. *Engineering Applications*, 1 (2), 99-107

Keywords

Composite materials
Hybrid composites
Artificial intelligence
Nano technology
Robots
Human health

Research Article

Received: 23.09.2022
Revised: 22.10.2022
Accepted: 01.11.2022
Published: 14.11.2022



Abstract

Nowadays, computers and smartphones, tablets and other electronic gadgets have become indispensable for human life. Human health is paramount. It is very important to know the use of robotic applications in the health sector and to closely follow the general developments related to this issue. The human brain is in a constant state of interaction with this technology. The specialties formed by the adaptation of nanotechnology to human health; tissue engineering is very important for people. Artificial intelligence is one of the greatest engineering works in the history of mankind and the world. Artificial Intelligence technology has become a field that humanity has often heard about with the increase of epidemic diseases. Artificial intelligence is the ability to exhibit human-like behavior. Artificial intelligence has the potential to make scientific research, an area where people focus, much more efficient and increase the speed of scientific research by a factor. In this study, the importance and usability of machine learning in human health were investigated by literature review. The results obtained from different studies are shown in the figures.

1. Introduction

Before defining artificial intelligence, we need to know the definition of intelligence. Intelligence can be briefly called the abilities of a person to think, reason, perceive, understand, judge and draw conclusions from real events. In addition, Intelligence can also be seen as the ability of the mind to learn, take advantage of what has been learned, adapt to new situations and find new solutions. Intelligence, in other words, can be called the ability to adapt to technological events that can be developed through education, training, knowledge, accumulation and experience [1]. Artificial intelligence is the process by which the human brain, non-organic systems (computer, program, robot, etc.) based on its functions. Who thinks like a human, perceives like a human, interprets like a human, analyzes like a human and makes decisions like a human after all these stages). Scientists have defined artificial intelligence differently. For example, artificial intelligence is the science of computer programs that imitate intelligent behavior, and artificial intelligence is the science of converting things into machines that require intelligence when done by humans [2-4]. Artificial intelligence is also used in other fields besides the health field. For example, when current studies are examined; the interaction of artificial intelligence and space design has been evaluated in today's design education. In the research, the interaction of artificial intelligence and space design was compared in today's design education [5]. The artificial intelligence index was investigated with the use of doubt in favor approach. In order to investigate the impact of artificial intelligence talent, capacity and potential levels of countries on their economic development, the relationship between Artificial Intelligence Index scores and category shares and economic development indicators has been deciphered with graphs [6]. The ability to control the military with artificial intelligence The global management of artificial intelligence from the

perspective of international security has been studied. At the end of the study; the idea that the global management of artificial intelligence can be realized with an effective international border organization emerges [7].

2. Material and Method

In this study, artificial intelligence and its sub-branch, machine learning, were investigated. Previous studies have been examined by conducting a literature review. The usability of the lower branches of artificial intelligence in the field of health has been investigated. The studies obtained at the end of the research are shared with reference to the photos.

2.1. Artificial Intelligence (AI)

A number of processes have been left behind by artificial intelligence scientists. Some scientists define artificial intelligence as "the study of mental abilities using computational models." Other scientists, artificial intelligence a modern approach', 4 AI can be classified under the title of description in the book of like-minded people, systems, system of systems that behave like rational human beings maintain a rational system [8-9]. Artificial Intelligence and its subsets are given in Figure 1 in the form of a photo.

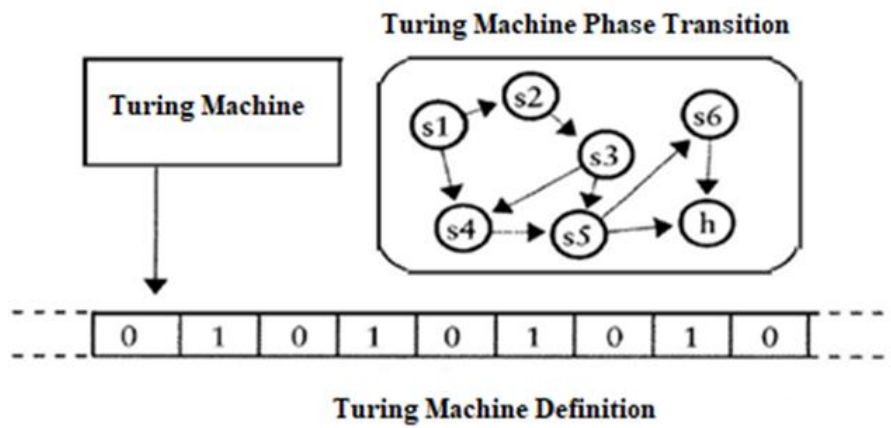


Figure 1. Artificial Intelligence and its subsets [10]

2.2. Literature Studies on Artificial Intelligence in the Health Sector

The use of artificial intelligence in the health sector continues rapidly. Artificial intelligence can also be used for dentists and oral health. At a time when human health is the most important; health services are one of the fastest growing sectors in the health sector, covering the diagnosis, treatment and prevention of oral diseases in general. For example, diagnosis is of great importance because tooth deficiencies cause malocclusion, loss of function and aesthetic problems in individuals. In dentistry, intraoral or extra-oral radiographs are used to detect tooth deficiencies. For example: in a study; the artificial atom algorithm of the individual-specific optimal nutrition program was used [11]. In a study, the lateral buckling behavior of hybrid composite materials was estimated using the Artificial Neural Networks (ANN) tool using test data on the effects of different environmental conditions and different fiber combinations [12]. In a different study, a pilot study on artificial intelligence was conducted to detect tooth deficiencies from panoramic radiography using the deep learning method [13]. In a different study, the diagnosis and predictions of periodontically weakened teeth were investigated using an artificial neural network algorithm [14]. They shared the software studies they developed on the detection of dental caries and dental problems in X-ray images using artificial neural networks and the diagnosis and classification of caries in digital radiographs with the literature [15-16]. In different studies, MRI images were associated with a deep learning model. In this way, it is believed that the specialist radiologist can reach the result more efficiently and in a short time [17].

2.3. Machine Learning

Machine Learning (Machine Learning) is a branch of artificial intelligence that uses statistics and computer science and has recently become very popular. Machine learning is all algorithms that mimic human intelligence. However, it does not need rules that we interpret and enter manually. In the machine learning model, learning occurs in the form of teaching-teaching (education) and testing (testing). At the learning stage, a learning model is created by learning algorithms and features to the system using examples from the dataset. At the experimental stage, estimation is made for the trial data with the learning model application Engine [11-18].

2.4. Deep Learning, Robotics, the Method of Artificial Neural Networks and Genetic Algorithms

Deep learning is a machine learning method consisting of multiple layers that predicts outcomes with a specific set of data. Deep learning, machine learning and artificial intelligence are terms that have different meanings from each other. Deep learning has been described as a class of machine learning techniques that use many nonlinear hidden layers for supervised or unsupervised feature extraction, transformation, pattern analysis, and classification [19]. Artificial intelligence is used in tumor diagnosis in the health sector. Early detection of tumors is very important for human life. To facilitate this situation, the Machine learning method and deep Learning Algorithms (DLAs) are based on a kind of artificial intelligence and machine learning, which occurs by imitating the way people acquire information [20-21]. The mathematical modeling given below can be used to detect tumor cells by deep learning [22]. The mathematical modeling equations used in this regard are given below [22].

$$Accuracy = \frac{TP+TN}{TP+FP+FN+TN} \quad (1)$$

$$Sensitivity = \frac{TP}{TP+FN} \quad (2)$$

$$Precision = \frac{TP}{TP+FP} \quad (3)$$

$$Specificity = \frac{TN}{TN+FP} \quad (4)$$

$$F1\ Score = \frac{2 \cdot (Precision \cdot Sensitivity)}{(Precision + Sensitivity)} \quad (5)$$

In different studies, more than one model has been identified to diagnose dental caries using deep learning or to detect lesions on dental x-ray images. The results obtained are close to the truth [23-26]. An example of a sample tooth structure analysis and caries labeling is given in Figure 2.

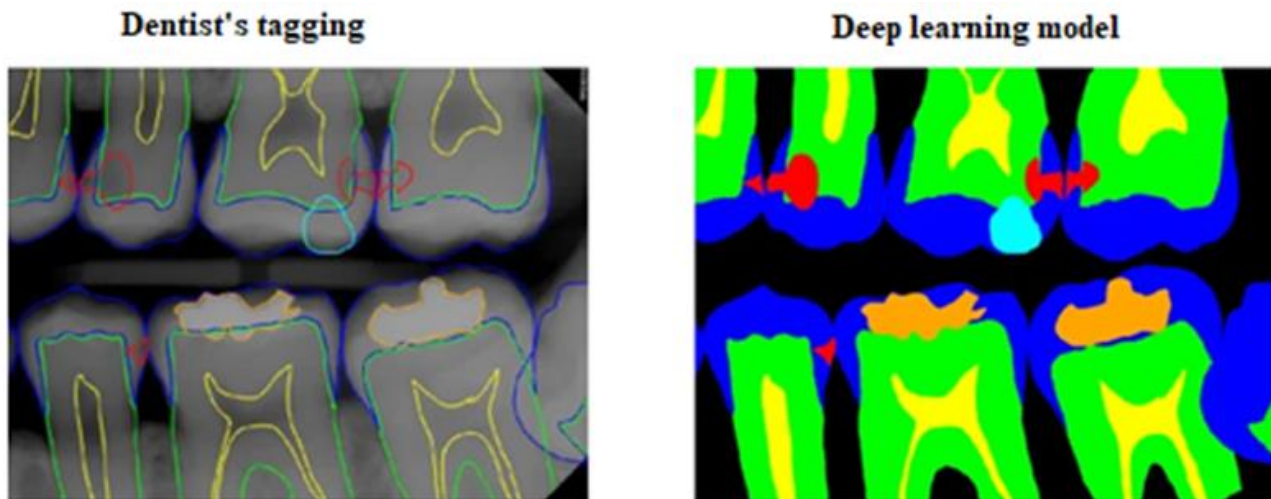


Figure 2. An example of tooth structure analysis [26]

Red: Caries, Blue: Enamel, Green: Dentin, Yellow: Pulp, Orange: Metal restoration, Sky blue: Restoration, Brown: Gutta percha, Black: Background [26].

In a different study, evaluations were calculated at the caries component level to evaluate the performance of dental caries detection [26-27].

For each object class, An Average Precision (AP) is defined [27].

FP-False Positive,
FN-False Negative,

$$AP = \frac{1}{11} \sum_{r \in \{0.0, 0.1, \dots, 1.0\}} P_{interp}(r) \quad (7)$$

Where $P_{interp}(r)$ is the maximum precision for any recall values exceeding [27].

$$P_{interp}(r) = \max_{\tilde{r} \geq r} p(\tilde{r}) \quad (8)$$

Finally, the mean average precision (mAP) is calculated as an average of Aps for all object classes:

$$mAP = \frac{1}{N_{class}} \sum AP \quad (9)$$

It is known that there will be a number of innovations in human life with robotic applications that are the basis of artificial intelligence. With robotic applications, computers and electronic robots are integrated with the principle of compatibility, the result of which is artificial intelligence, especially used in industry and cutting-edge technology, production and design robots are made with the help of computers. Figure 3 shows a symbolic robot produced by coding [28]. Artificial neural networks are a branch developed inspired by the human brain. Each one with its own memory and processing elements are connected through weighted links of parallel and distributed information processing structure. Artificial neural networks find wide application in many fields of science today due to these learning and generalization features and demonstrate the ability to solve complex problems successfully. Genetic algorithms, a sub-Dec branch of artificial intelligence, are a search and optimization method that works in a similar way to the evolutionary process observed in nature. It seeks the holistic best solution according to the principle of survival of the Dec in the complex multidimensional search space [28-30]. It has been researched with a literature study that it can be applied in the field of Artificial Intelligence, Food Engineering, Epidemic Artificial Intelligence (Robots) and Law [31-32]. As a situation where artificial intelligence becomes visible in every field as in the health sector. A photo of AI and Machine Learning is provided [33]. A photo of AI and Machine Learning is given in Figure 3.

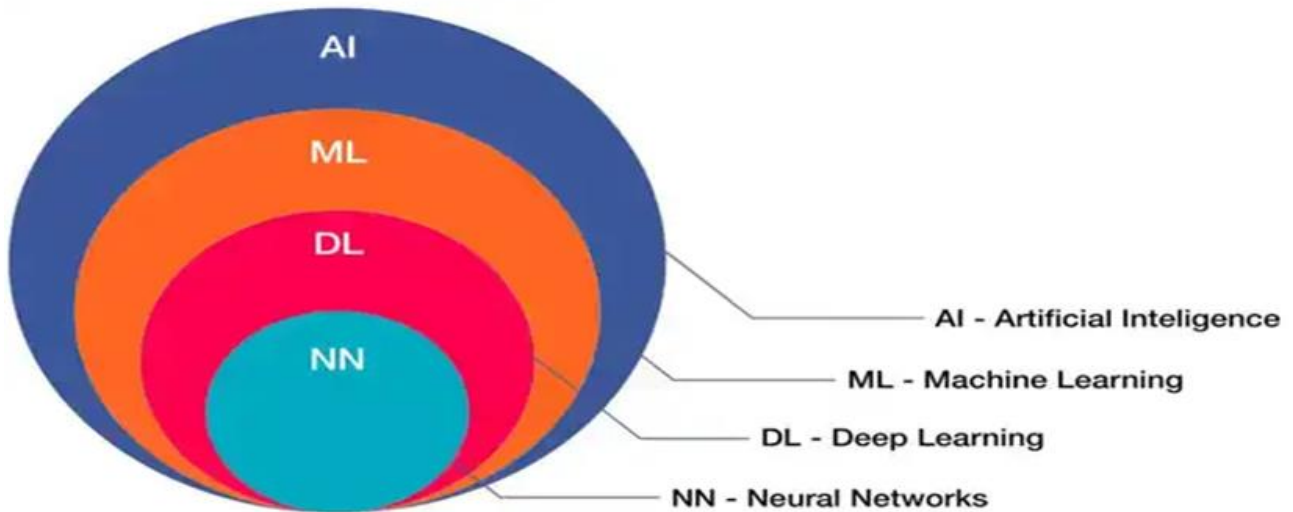


Figure 3. A photo of AI and Machine Learning [34]

Deep Learning is a large family of methods for machine learning based on artificial neural networks. Artificial neural networks are computational models based on the simplification of biological neural networks. Figure 4 shows an example of a neural network [35].

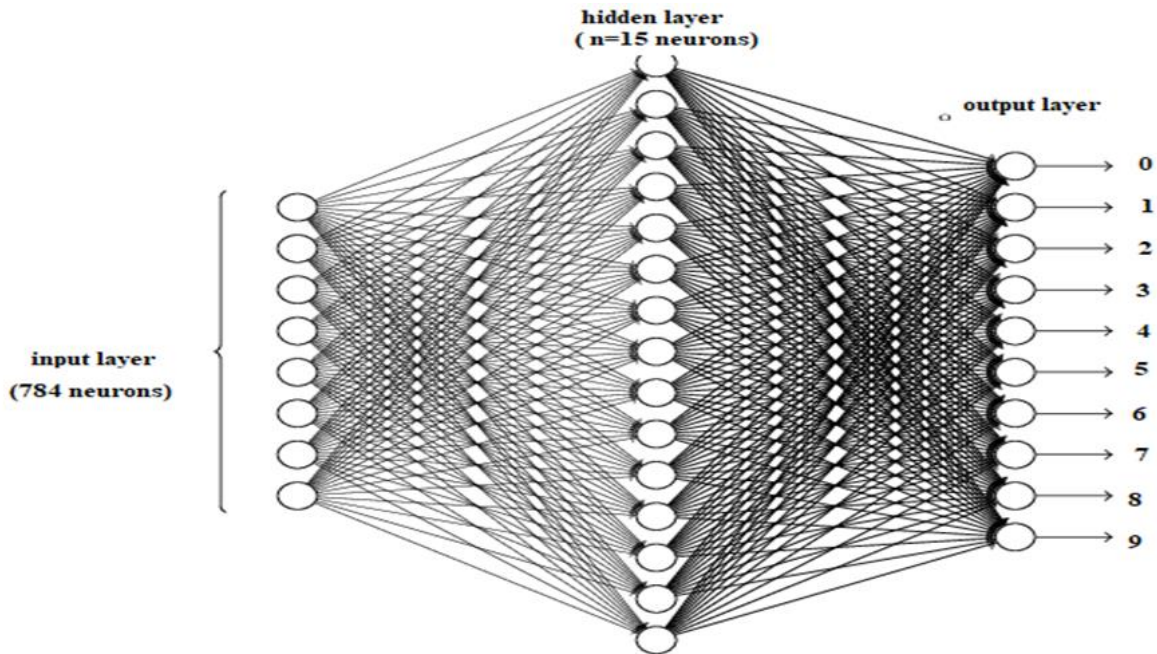


Figure 4. Example of neural network [35]

As can be seen in Figure 6, they can consist of many nodes or neurons and multiple layers of neurons. As the number of neurons and layers increases, the network can represent more complex nonlinear functions [36]. In a study, the classification of brain tumor images by deep learning methods was investigated. In another study, it was investigated that doctors can diagnose sick people early. In the study, Alexnet, Googlenet and Resnet50 architectures, which are deep learning architectures, were used to detect brain tumor images. The highest accuracy rate was achieved on the Resnet50 architecture. It is thought that the accuracy value of 85.71 percent obtained as a result of the experiments will be improved in future studies [37]. The experiment was conducted for automatic segmentation of the brain system. The BRATS2015 data set was used in the experiment [38]. In a different study, the semantic segmentation approach for volumetric 3D brain tumor segmentation from multimodal 3D MRI was investigated. The photo of the study is given in Figure 5.

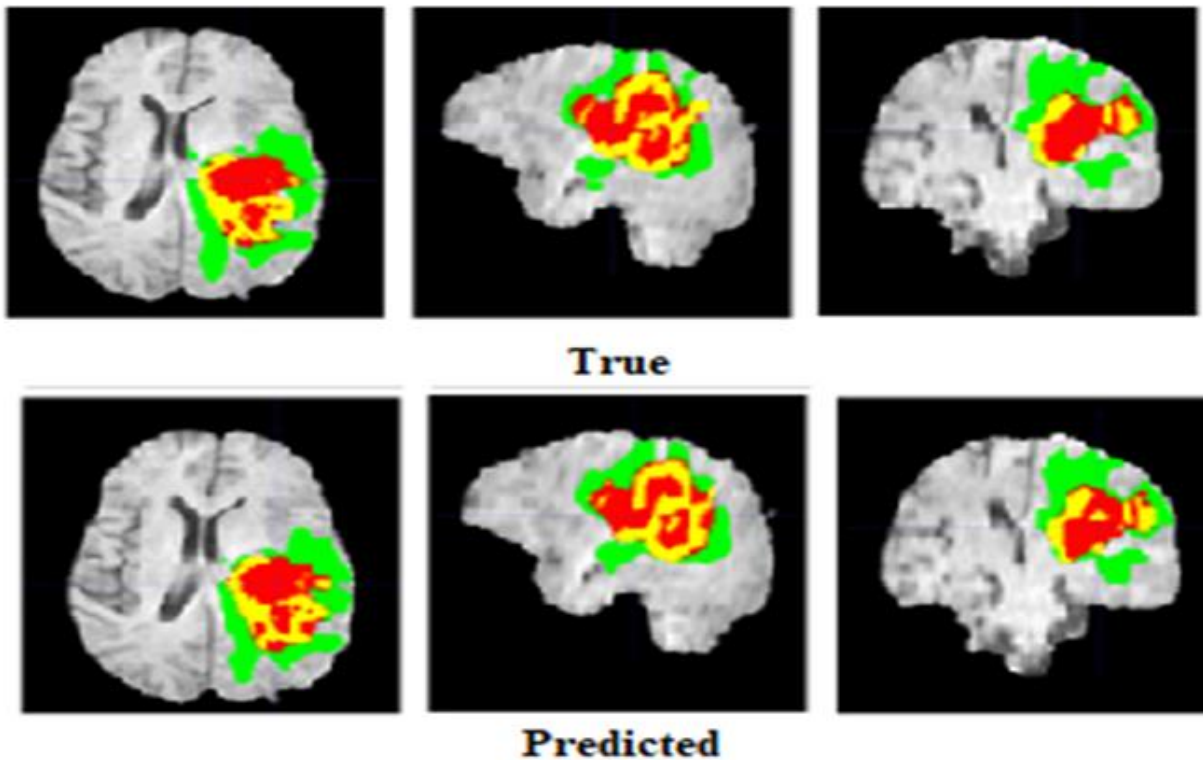


Figure 5. 3D brain tumor segmentation from multimodal 3D MRIs [38]

In a different study, it was estimated how quickly a malfunction in the machine could occur. Algorithm models between the generated sensor data and the malfunctions Decayed in the machines were used [39]. The segmentations obtained by Deciphering a Distinction between brain tumors and deep learning in a different study are given in Figure 6 [39].

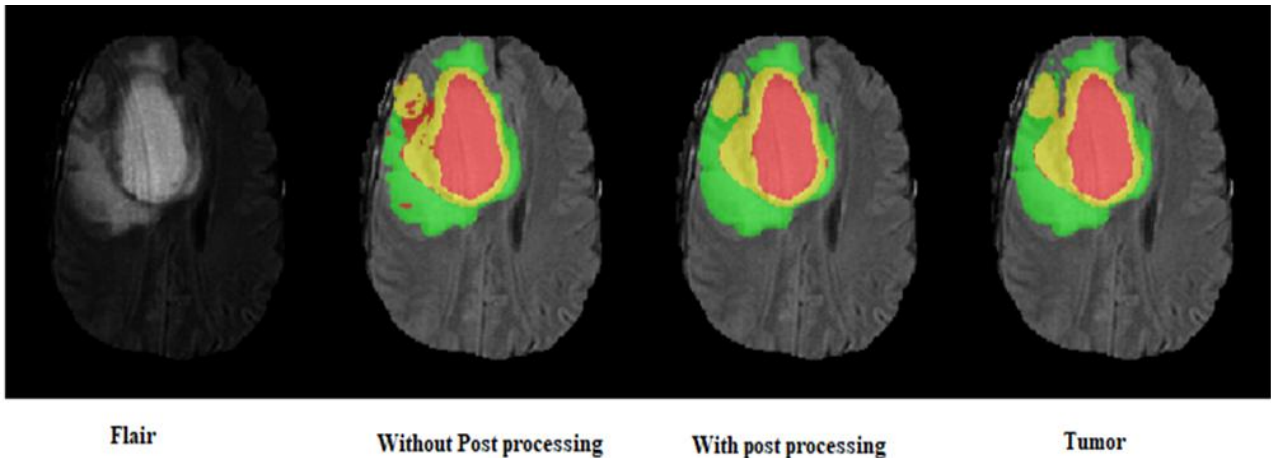
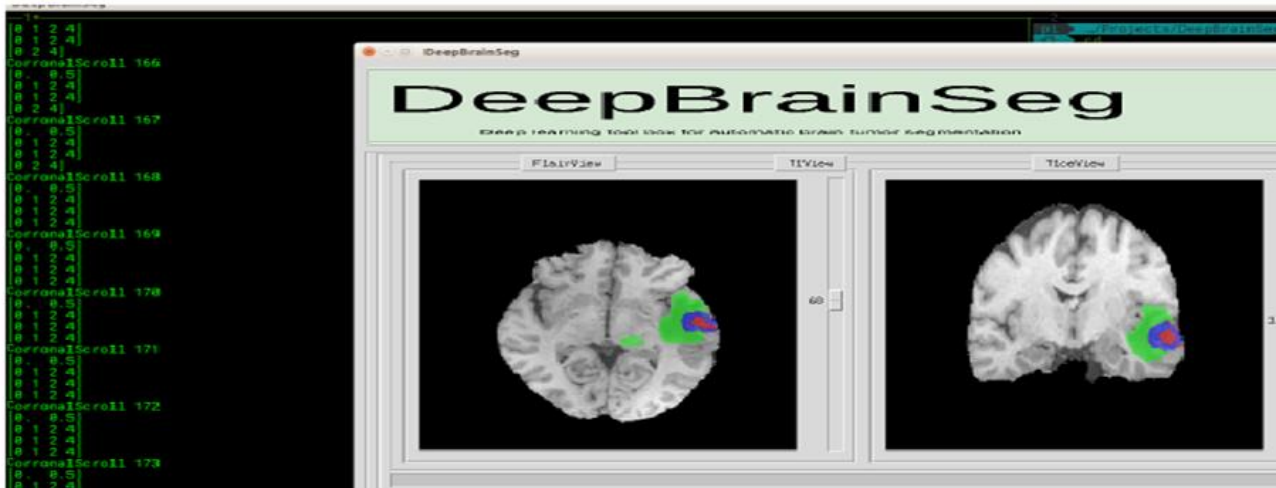


Figure 6. Telemetry data example literature [39]

In a different study; a user interface-based tool was produced for tumor segmentation visualization. The interfaced program obtained from brain tumor segmentation and commands is given in Figure 7 [40].



for data in BraTs format

```
from DeepBrainSeg import deepSeg
segmentor = deepSeg(quick=True)
segmentor.get_segmentation_brats(path)
```

for other formats

```
from DeepBrainSeg import deepSeg
t1_path =
t2_path =
t1ce_path =
flair_path =

segmentor = deepSeg(quick=True)
segmentor.get_segmentation(t1_path, t2_path, t1ce_path, flair_path, save = True)
```

Figure 7. Brain tumor segmentation and creation of commands [40]

Deep learning has been highly preferred in the field of health. Previous studies related to this are given in Table 1 [41].

Table 1. The use of deep learning in the field of health [41]

S/n	Author	Year Published	Title
1	Shin et al. [24]	2016	Deep convolutional neural networks for computer-aided detection: CNN architectures, dataset characteristics and transfer learning
2	Esteva et al. [69]	2017	Dermatologist-level classification of skin cancer with deep neural networks
3	Havaei et al. [78]	2017	Brain tumor segmentation with deep neural networks
4	Kamnitsas et al. [21]	2017	Efficient multi-scale 3D CNN with fully connected CRF for accurate brain lesion segmentation
5	Zhang et al. [120]	2015	Deep convolutional neural networks for multi-modality isointense infant brain image segmentation
6	Iglesias et al. [121]	2015	Multi-atlas segmentation of biomedical images: a survey
7	Greenspan et al. [14]	2016	Guest editorial deep learning in medical imaging: Overview and future promise of an exciting new technique
8	Tajbakhsh et al. [26]	2016	Convolutional neural networks for medical image analysis: Full training or fine tuning?
9	Pereira et al. [77]	2016	Brain tumor segmentation using convolutional neural networks in MRI images
10	Milletari et al. [20]	2016	V-net: Fully convolutional neural networks for volumetric medical image segmentation
11	Roth et al. [122]	2016	Improving computer-aided detection using convolutional neural networks and random view aggregation
12	Çiçek et al. [123]	2016	3D U-Net: learning dense volumetric segmentation from sparse annotation
13	Sirinukunwattana et al. [72]	2016	Locality sensitive deep learning for detection and classification of nuclei in routine colon cancer histology images
14	Anthimopoulos et al. [124]	2016	Lung pattern classification for interstitial lung diseases using a deep convolutional neural network
15	Setio et al. [125]	2016	Pulmonary nodule detection in CT images: false positive reduction using multi-view convolutional networks
16	Xu et al. [73]	2016	Stacked sparse autoencoder (SSAE) for nuclei detection on breast cancer histopathology images
17	Roth et al. [126]	2015	Deeporgan: Multi-level deep convolutional networks for automated pancreas segmentation
18	Moeskops et al. [76]	2016	Automatic segmentation of MR brain images with a convolutional neural network
19	Suk et al. [97]	2015	Latent feature representation with stacked auto-encoder for AD/MCI diagnosis
20	Bar et al. [127]	2015	Deep learning with non-medical training used for chest pathology identification

As can be seen in Table 1, there are studies related to cancer cells and tumors, especially through artificial intelligence. These studies are very important for the early diagnosis of diabetes, brain disorders, cysts that occur in the tooth and other diseases. Studies related to the analyzes made using artificial intelligence and mathematical programming are currently included in the literature [41-43].

3. Conclusion

In this study, literature studies on the applicability of Artificial Intelligence and its sub-branches in the field of health were examined. In the study, the definition of artificial intelligence, its sub-branches, and its applicability in health fields were investigated. The availability of artificial intelligence in the health and medical sector has emerged. As a result of the study, the following results were obtained: It is believed that artificial intelligence techniques can be successfully applied in the field of health and medical. It was concluded that it can be achieved with a high degree of success in solving various dental problems. It is thought that the use of robots can contribute to the health sector and physicians. It is thought that the desired goals can be fully achieved in the field of the health sector with the lower branches of artificial intelligence. Using the records in the hospital database, it is thought that online doctor robots, robots that can perform surgical procedures and nurse robots will play an important role in our lives in the future. In the field of health and medicine, health management with machine learning and artificial intelligence, artificial limb (arm, eye, etc.) applications, analysis of heart sounds, sound analysis for the deaf, classification of respiratory sounds, analysis of side effects of drugs, it is believed that useful studies can be produced by people.

Acknowledgement

This study was partly presented in 4th Advanced Engineering Days [43] on 8 June 2022. I would like to express my gratitude to my wife Nihal Kayıran for her moral support in this article.

Funding

This research received no external funding.

Conflicts of interest

The authors declare no conflicts of interest.

References

1. Elmas, Ç., (2003). Fuzzy logic controllers. Seçkin Publishing House, Ankara Faculty, Water Foundation First Edition, Istanbul, 189s.
2. Minsky, M. (1960). Steps toward artificial intelligence. Lexington, Lincoln Laboratory.
3. Brooks, R. A., (1991). Artificial intelligence without representation. Elsevier, 139-159.
4. Öztemel, E. (2003). Artificial neural networks. Papatya Publishing, 44s, Istanbul.
5. Bayrak, E., (2022). Evaluation of the interaction of artificial intelligence and space design in today's design education. Hacettepe University Institute of Fine Arts, Master's Thesis, 142 p.
6. Parlu, R. A. (2021). Development of artificial intelligence index with the use of doubt in favor approach, Istanbul University Institute of Social Sciences, Master's Thesis, 302p.
7. Türk, O. (2021). How to government military ai: On the global governance of artificial intelligence from an international security perspective, Graduate Education Institute, Istanbul Technical University, Master's Thesis, 146s.
8. Chen, F., Lv, H., Pang, Z., Zhang, J., Hou, Y., Gu, Y., ... & Yang, G. (2018). WristCam: A wearable sensor for hand trajectory gesture recognition and intelligent human-robot interaction. *IEEE Sensors Journal*, 19(19), 8441-8451.
9. Avanzini, G. B., Ceriani, N. M., Zanchettin, A. M., Rocco, P., & Bascetta, L. (2014). Safety control of industrial robots based on a distributed distance sensor. *IEEE Transactions on Control Systems Technology*, 22(6), 2127-2140.
10. Kurzweil, R. (2015). Creating a mind. İstanbul Bilgi University Press, 159 pp, İstanbul.
11. Sandhya, N., & Dhage, R. C. K. (2016). A review on machine learning techniques. In *International Journal on Recent and Innovation Trends in Computing and Communication*, 4(3), 139-159.
12. Yıldırım, A. E., & Karçı, A. (2015). Preparation of the optimum nutrition chart for the individual using artificial atom algorithm. *Mustafa Kemal University Medical Journal*, 6(24), 1-11.
13. Çelik, Ö., Odabaş, A., Bayraktar, İ. Ş., Bilgir, E., & Akkoca, K. F. (2019). Detection of missing teeth from panoramic radiography with deep learning method: An artificial intelligence pilot study. *Selcuk Dental Journal*, 6 (4), 168 – 172
14. Geetha, V., Aprameya, K. S., & Hinduja, D. M. (2020). Dental caries diagnosis in digital radiographs using back-propagation neural network. *Health Information Science and Systems*, 8(1), 1-14.
15. Lee, J. H., Kim, D. H., Jeong, S. N., & Choi, S. H. (2018). Diagnosis and prediction of periodontally compromised teeth using a deep learning-based convolutional neural network algorithm. *Journal of periodontal & implant science*, 48(2), 114-23.
16. Amasya, H., & Yıldırım, D. (2018). Artificial intelligence applications in dentistry. *Turkiye Klinikleri Journal of Dentistry Sciences*, 24, 227.
17. Chartrand, G., Cheng, P. M., Vorontsov, E., Drozdal, M., Turcotte, S., Pal, C. J., ... & Tang, A. (2017). Deep learning: a primer for radiologists. *Radiographics*, 37(7), 2113-2131.
18. Candan, H. (2019). Comparison of the performance of machine learning methods in the diagnosis of lung diseases with the speed of sound transmission. Ege University, Institute of Health Sciences, Department of Biostatistics and Medical Informatics, İzmir.
19. Endustri40, (2020). Access Address: <https://www.endustri40.com/robot-meslekleri-avukatlik-dis-hekimligi-polislik/>, Access Date: 01.05.2020.a
20. Badillo, S., Banfai, B., Birzele, F., Davydov, I. I., Hutchinson, L., Kam-Thong, T., ... & Zhang, J. D. (2020). An introduction to machine learning. *Clinical pharmacology & therapeutics*, 107(4), 871-885.
21. Goodfellow, I. & Bengio, Y. (2016). Courville, A. Deep Learning; M.I.T. Press: Cambridge, MA, USA.
22. Öztürk, T., & Katar, O. (2022). A Deep Learning Model Collaborates with an Expert Radiologist to Classify Brain Tumors from MR Images. *Turkish Journal of Science and Technology*, 17(2), 203-210.
23. Lee, J. H., Kim, D. H., Jeong, S. N., & Choi, S. H. (2018). Diagnosis and prediction of periodontally compromised teeth using a deep learning-based convolutional neural network algorithm. *Journal of periodontal & implant science*, 48(2), 114-123.
24. Lee, J. H., Kim, D. H., Jeong, S. N., & Choi, S. H. (2018). Detection and diagnosis of dental caries using a deep learning-based convolutional neural network algorithm. *Journal of dentistry*, 77, 106-111.
25. Srivastava, M. M., Kumar, P., Pradhan, L., & Varadarajan, S. (2017). Detection of tooth caries in bitewing radiographs using deep learning. *arXiv preprint arXiv:1711.07312*.
26. Nature, (2022). Access Address: <https://www.nature.com/articles/s41598-021-96368-7>, Access Date: 01.10.2022.

27. Chen, H., Zhang, K., Lyu, P., Li, H., Zhang, L., Wu, J., & Lee, C. H. (2019). A deep learning approach to automatic teeth detection and numbering based on object detection in dental periapical films. *Scientific reports*, 9(1), 1-11.
28. Dishekfak, (2020). Access Address: <http://dishekfak.ksbu.edu.tr/index/slide/4113/dis-hekimliginde-yapay-zeka-arastirmalari-atolyesi>, Access Date: 01.05.2020.
29. Deng, L., & Yu, D. (2014). Deep learning: methods and applications. *Foundations and trends® in signal processing*, 7(3-4), 197-387.
30. Widrow, B., (1960). Adaptive Adaline neuron using chemical memistors. Number Technical Report 1553-2. Stanford Electron. Labs. Stanford, CA.
31. Kükner, C. U., (2020). A comparative analysis of LSTM and XG Boost methods for day ahead electricity price forecasting, Istanbul Technical University, Energy Institute, Department of Energy Science and Technology, Master's Thesis, 105 pp.
32. Kayıran, H. F., (2020). Use of Artificial Intelligence in Food Engineering, 4th International Mersin Symposium, Mersin.
33. Kayıran, H. F., & Gökalp, H. (2020). Epidemics Artificial Intelligence (Robots) and Law, 4th International Mersin Symposium, Mersin.
34. Techblog, (2022). Access Address: <https://techblog.smc.it/en/2020-05-25/machine-learning-industry>, Access Date: 07.07.2022.
35. BMC, (2022). Access Address: <https://www.bmc.com/blogs/neural-network-introduction/>, Access Date: 07.07.2022.
36. Bingöl, H., & Alataş, B., (2021). Classification of brain tumor images using deep learning methods. *Turkish Journal of Science Technology*, 16(1), 137-143.
37. Dong, H., Yang, G., Liu, F., Mo, Y., & Guo, Y. (2017). Automatic brain tumor detection and segmentation using u-net based fully convolutional networks. In annual conference on medical image understanding and analysis, Springer, 506-517.
38. Nvidia Developer, (2022). Access Address: <https://developer.nvidia.com/blog/automatically-segmenting-brain-tumors-with-ai>, Access Date: 07.07.2022.
39. Koriavinash, (2022). Access Address: <https://github.com/koriavinash1/DeepBrainSeg>. Access Date: 01.10.2022.
40. Koriavinash, (2022). Access Address: <https://github.com/koriavinash1/DeepBrainSeg/blob/master/imgs/overlay2.png> Access Date: 01.10.2022.
41. Ker, J., Wang, L., Rao, J., Lim, T., (2018). Deep Learning Applications in Medical Image Analysis. Special Section on Soft Computing Techniques for Image Analysis in The Medical Industry Current Trends, Challenges and Solutions. Digital Object Identifier 10.1109/Access.2017.2788044. pp: 9375-9389.
42. Kayıran, H. F. (2022). Investigation of stress in rotating cylinders with gray irons (Grade G4000) materials by mathematical programming. *Advanced Engineering Days (AED)*, 4, 100-102.
43. Kayıran, H. F., & Şahmeran, U. (2022). Development of individualized education system with artificial intelligence fuzzy logic method. *Advanced Engineering Days (AED)*, 4, 103-105.



© Author(s) 2022. This work is distributed under <https://creativecommons.org/licenses/by-sa/4.0/>



Structural, petrographic and geochemical features of the calcite quarry in the Biga Peninsula (Çanakkale, Türkiye)

Mustafa Kaya ¹, Cihan Yalçın ², Mustafa Kumral ¹

¹Istanbul Technical University, Geological Engineering, İstanbul, Türkiye, kayamusta@itu.edu.tr, kumral@itu.edu.tr

²Ministry of Industry and Technology, General Directorate of Industrial Zones, Ankara, Türkiye, cihan.yalcin@sanayi.gov.tr

Cite this study: Kaya, M., Yalçın, C., & Kumral, M. (2022). Structural, petrographic and geochemical features of the calcite quarry in the Biga Peninsula (Çanakkale, Türkiye). *Engineering Applications*, 1(2), 108-116

Keywords

Calcite Quarry
Structural
Geochemical
Raw material

Research Article

Received: 23.09.2022

Revised: 22.10.2022

Accepted: 02.11.2022

Published: 14.11.2022



Abstract

Calcite is a significant industrial raw material used in many fields owing to its properties. For this reason, determining the calcite quarry's geological and geochemical characteristics promotes the sector. This study was carried out to explain the geological and geochemical properties of the marble blocks of Paleozoic metamorphics located in the Biga peninsula. The length of this area, operated as a calcite quarry, is 350 meters, and its width is around 50 meters. Although alterations are partially observed due to the effect of faulting, the alteration is quite low in the main production area. Secondary minerals are rarely seen in fractures and cracks in marbles that display texturally granular texture. In geochemical analyzes, CaO values are around 55%, and MgO values are quite low. Structural elements in the region show that the region has gone through two separate deformation phases. These are NW-SE direction compression and NW-SE direction tension, respectively. Rose and point-contour diagrams obtained from the joint values measured in the calcite field confirm these deformation phases. The structural condition of the calcite quarry in terms of operation is compatible with its other characteristics. These data show that the calcite quarry suggests remarkably useful properties in terms of industrial raw materials.

1. Introduction

Limestone consists of calcite, whose chemical formula is CaCO_3 (calcium carbonate). It is largely used in many sectors in aggregate, powder, block, etc., owing to its physical and chemical properties [1]. The most important sectors are metal, paper, ceramics, chemistry and construction. For this reason, it is inevitable to research limestone, an extremely remarkable industrial raw material, and determine its physical and chemical properties.

The quality of the calcite mineral is determined by its grain diameter, color and chemical purity [2-3]. The hardness of pure calcite is three according to Moh's scale, and its specific gravity is around 2.6-2.7 g/cm^3 at 20°C [3]. Carbonate rocks consisting of calcite with these properties are generally used as aggregates. To satisfy this need, the geological and geochemical characteristics of the calcite quarries should be explained.

When the geological framework of Turkey is reviewed, significant carbonate belts stand out. While some belts spread in relatively long and continual areas, a block or lenticular structure occurs in some areas for tectonic reasons. This study explained the geological and geochemical properties of the limestones in the Biga (Çanakkale) peninsula in Western Anatolia.

Western Anatolia has led to much research due to its complex geological structure. The stratigraphic base of the Biga peninsula consists of units belonging to the Sakarya continent. Sakarya Zone [4] consists of Kazdağ group

metamorphics and the Karakaya complex [5]. The Kazdağ group comprises pre-Permian amphibolite facies metamorphic rocks that have undergone metamorphism [6]. Metamorphic rocks are still cut by Upper Paleozoic granitoids (Çamlık meta granitoid [5], Söğüt granite [7], Kavsarali unit [8] and Yolindi metagranite [5]). In the region, which has a remarkably complex geological structure, there are large carbonate blocks in metamorphic rocks. These blocks are used as calcite quarries, and the geological and geochemical data of this quarry are exceedingly limited. For this reason, it will be very beneficial for the industry in the region to explain the geological features of the calcite quarry.

2. Material and Method

A 1/10,000-scaled geological map of the study area was drawn up. The contact relations of the units were completed in the field and redrawn in the Corel Draw program. In supplement, thin sections of the samples collected from the calcite quarry were made in ITU-JAL and examined under a polarizing microscope. Eventually, the geochemical analyzes of the samples were carried out with the X-ray fluorescence (XRF) spectrometer method. The X-ray diffraction analysis (XRD) method was preferred for mineralogical identification.

In addition to these basic analyses, joint measurements were carried out in the calcite field. In addition to the regional structural evaluations, point-contour and rose diagrams were prepared, and the states of the effective force regimes in the region were determined. For this study, the Stereo-net program was used.

The data gathered were described in the office.

2.1. Geological Background

Pre-Tertiary rocks in the district crop out in tectonic belts, which spread in a NE-SW direction [5]. These tectonic zones consist of the İzmir-Ankara zone, Sakarya zone, Çetmi mélange, and Ezine zones from east to west, respectively.

The study area is located in the Sakarya zone defined by Şengör and Yılmaz [9]. Kazdağ metamorphics and the Karakaya complex come together with tectonic contact. According to the Turkish Tectonic Units [10], the study area is located within the Paleozoic-Early Mesozoic subduction-subduction complex (Figure 1).

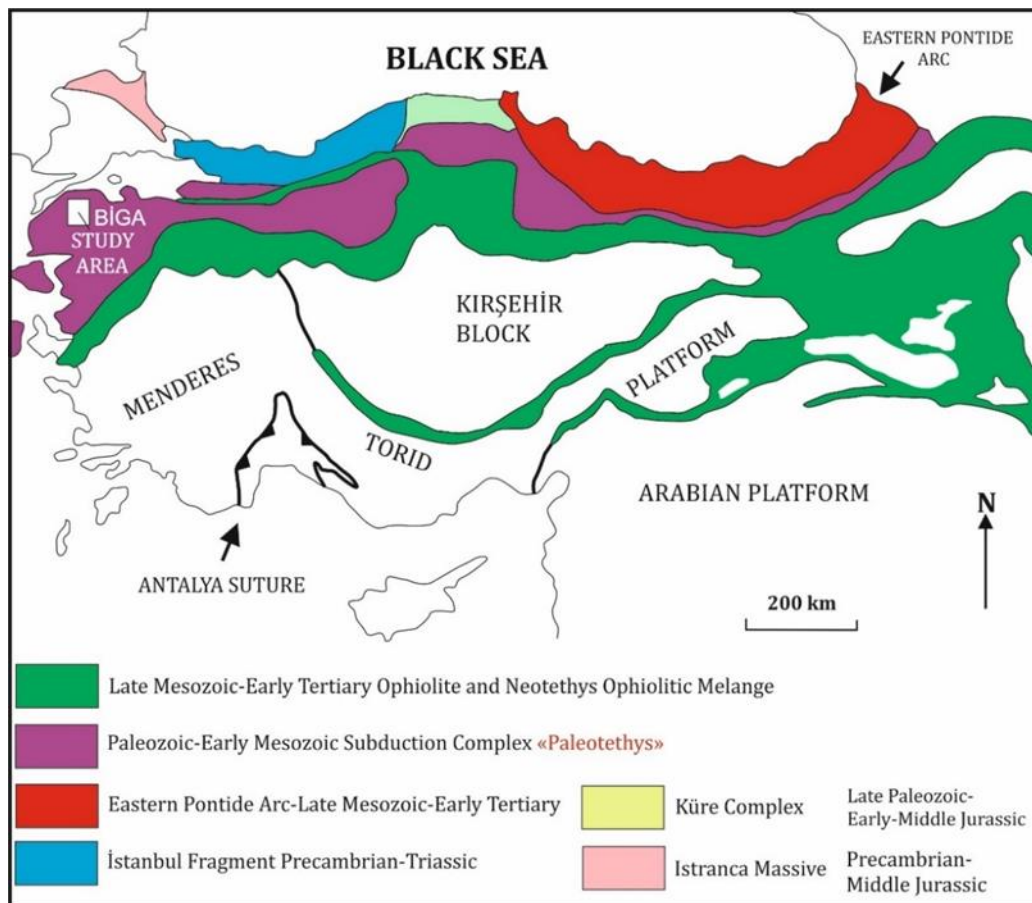


Figure 1. Tectonic location map of the study area (Modified from Şengör et al. [10])

The base of the study area is the Kalabak Unit. Within this unit, there are Torasan formations and Çamlık Metagranodiorites are observed. The Torasan formation, which mainly includes phyllites, schists, metarhyolite,

marble blocks and metaserpentinite blocks, is cut by the Çamlık Metagranodiorites. As a result of the deformations that occurred in the province, these two units belonging to the Kalabak Unit came together in some areas with a tectonic contact. The Karakaya formation of the Karakaya complex overlies this basement unit with angular unconformity. The contact of this unit, which consists of metamorphic rocks, with the basic units is generally tectonic (Figure 2).

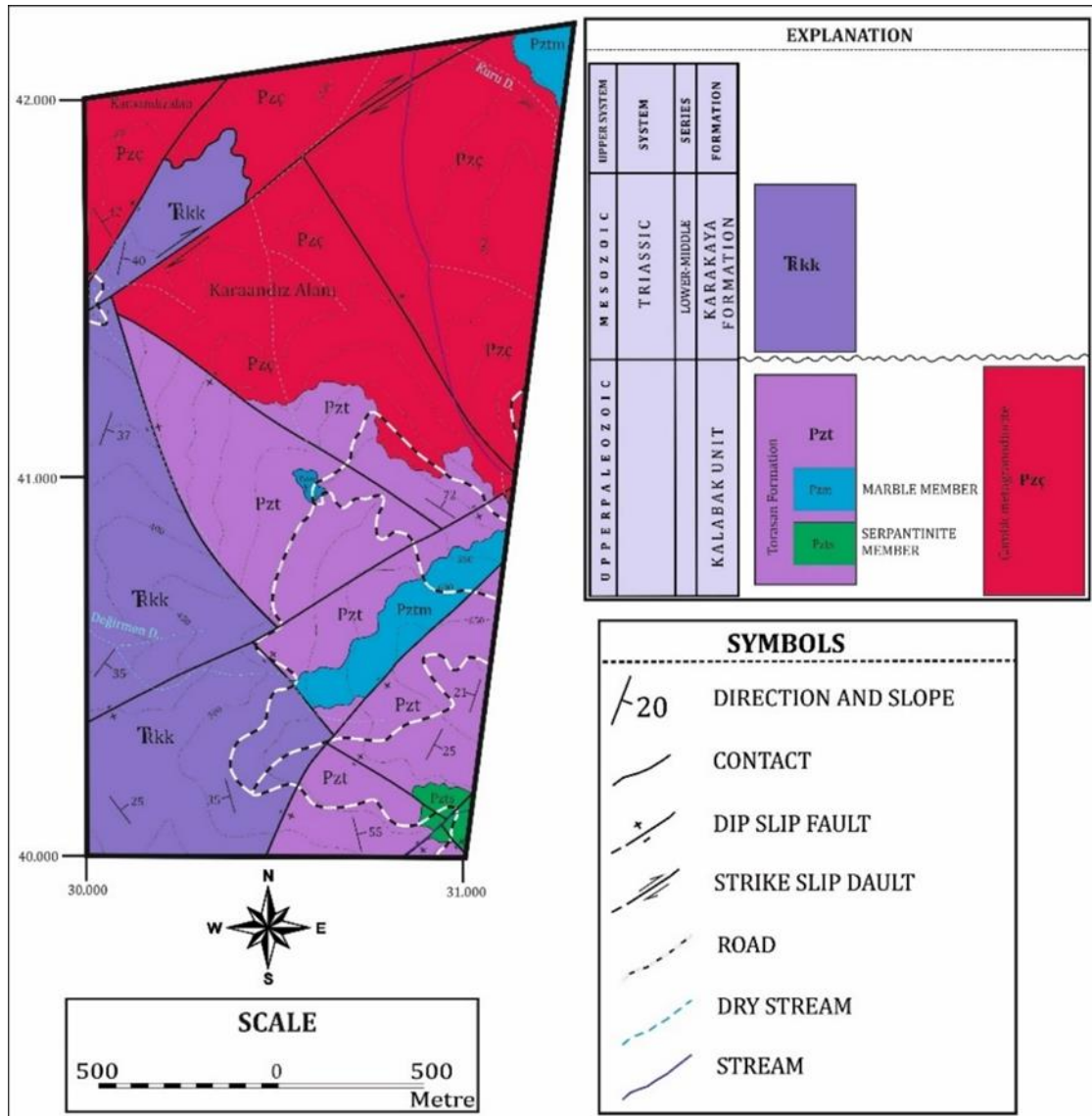


Figure 2. Geological map of the study area

Detailed investigations were implemented in the calcite quarry area, which is included in these lithologies and defined as the Marble member. The mineralogy, petrography and geochemistry of the rock, along with the structural relationship of the marble contact, are explained.

2.2. Characteristics of Calcite Quarry

The study area has an already operated calcite quarry east of Değirmen creek. This quarry operated using the calcite mineral belonging to the Marble blocks in the Torasan formation. Located on the site in a northwest-southeast direction, this marble block is approximately 350 meters long and 50 meters wide. This unit is cut by two NE-SW and NW-SE direction faults.

In the enterprise opened at 540 m elevations of the unit, it is observed that it is bordered by a fault along the dry stream and is in the form of a lens in the Torasan formation (Figure 3). The field easily recognizes its weathering color and morphological features (Figure 4a). In the continuation of the unit towards the northeast, it is observed that the alteration color turns dark grey-blackish grey (Figure 4b).

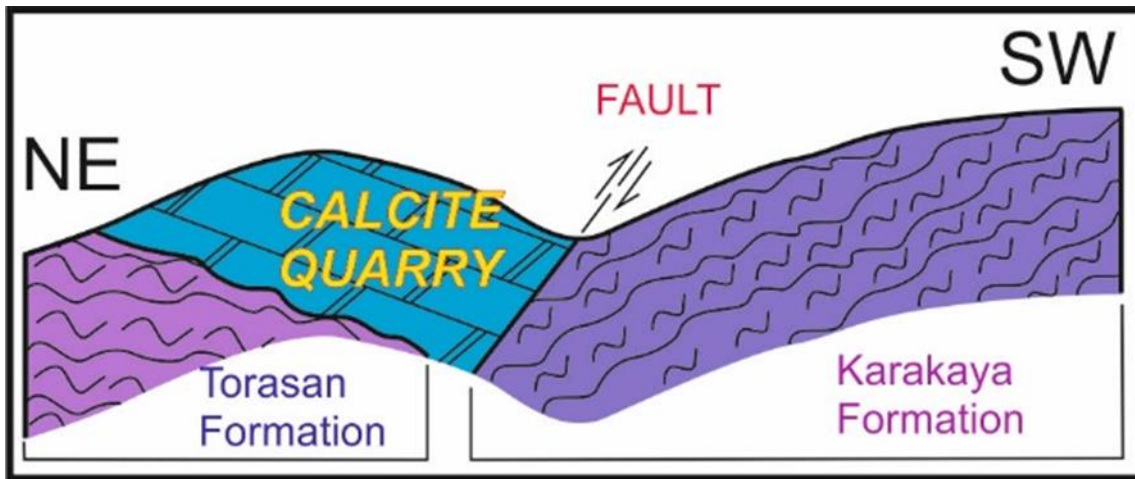


Figure 3. Geological cross-section of the calcite quarry district (without scale)



Figure 4. General view of a. calcite quarry; b. Marble

2.3. Petrography

When the macroscopic properties of the samples collected from the field were examined, it was determined that the color was white-grey, heterogeneous color distribution and medium-coarse grained. It reacts when treated with 10% HCl acid, and no decomposition is observed in the hand samples.

Thin sections of the same samples were examined under a polarizing microscope. The examination determined that the rock has a crystalline mosaic texture (Figure 5). The rock is monomineralic and consists entirely of calcite crystals. Opaque minerals and quartz-type silicate minerals are remarkably rare. No alteration-decomposition is observed except for the iron oxide yield. The frequency of fissures and cracks is low in micro terms of the rock. It is seen as very plain and homogeneous regarding mineral content and structural elements (Figure 5).

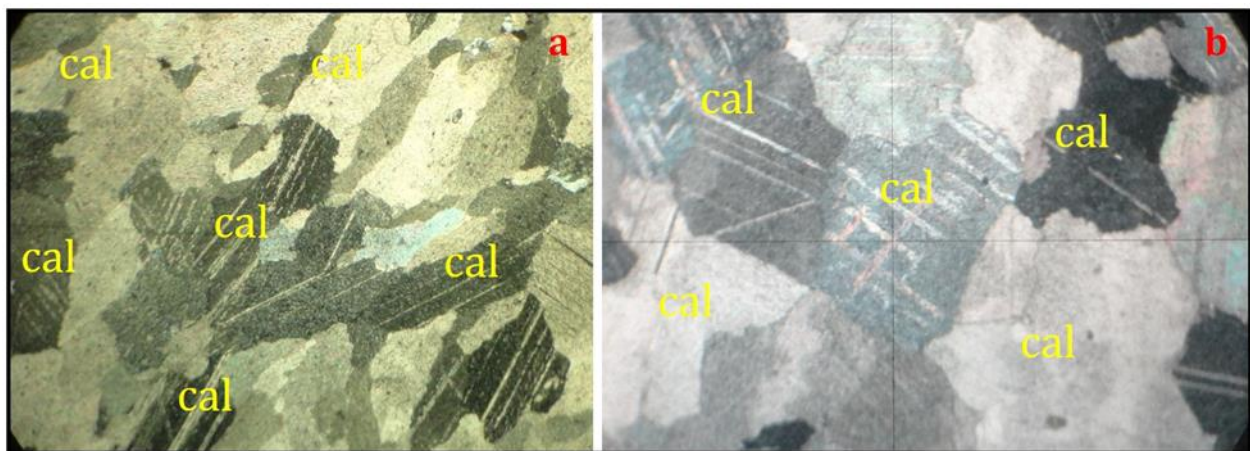


Figure 5. Microphotograph of marble (Abr: cal, calcite)

X-ray diffraction (XRD) analysis of the sample collected from the field was performed, and calcite mineral was detected (Figure 6).

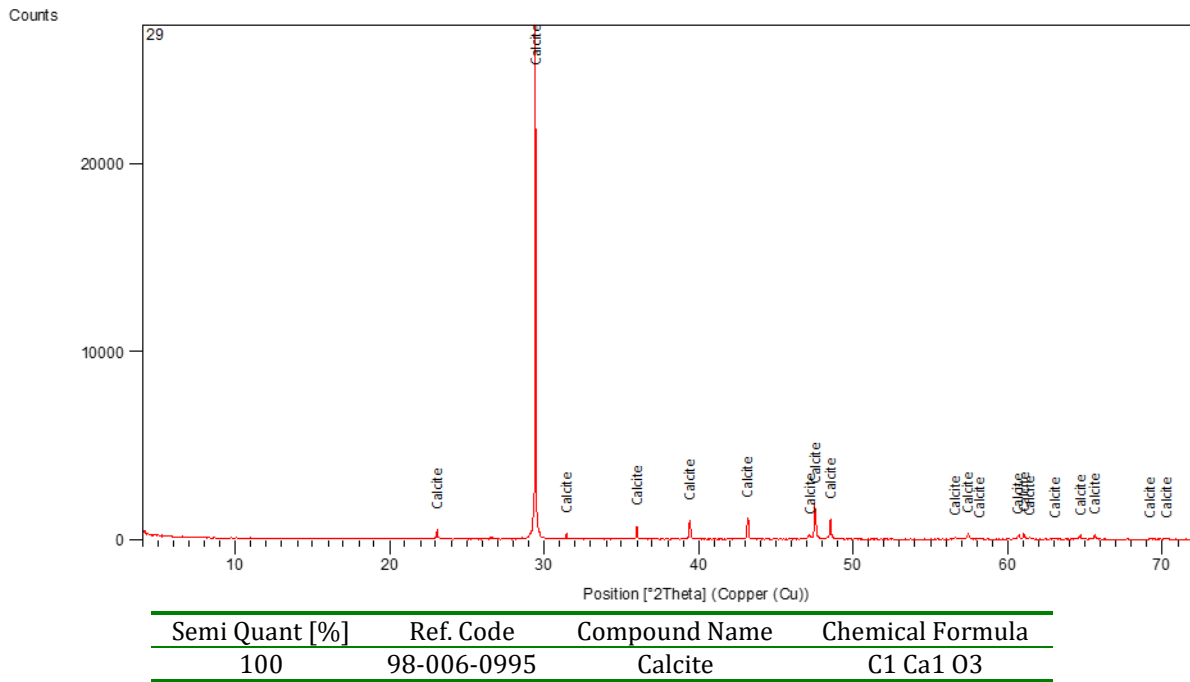


Figure 6. XRD analysis of the calcite sample

3. Geochemistry

In the calcite field, three drillings were made before. Samples representing the field were compiled from the cores of these drillings. Samples from 12, 15, 30, 82, 162, and 212 meters were selected in the sounding, where the calcite lens is the thickest. Detailed geochemical analyzes of the samples obtained from different meters were made.

The major oxide (%) values of the samples taken from the field are given in Table 1. It is recognized that the SiO₂ concentration in the samples is between 0.1-1%, the MgO concentration is between 0.27-0.66%, and the CaO concentration is around 55%, respectively.

Table 1. Major oxide concentration (%) of the calcite specimens

SAMPLE (%)	BC-1 (12m)	BC-2 (15 m)	BC-3 (30 m)	BC-4 (82 m)	BC-5 (162 m)	BC-6 (212 m)
SiO ₂	0,05	0,99	0,20	0,11	0,04	0,11
Al ₂ O ₃	0,03	0,10	0,03	0,05	0,00	0,04
Fe ₂ O ₃	0,01	0,03	0,05	0,05	0,02	0,02
MgO	0,66	0,48	0,27	0,57	0,62	0,60
CaO	55,73	55,91	55,66	55,75	55,25	55,82
K ₂ O	0,00	0,00	0,00	0,00	0,00	0,01
TiO ₂	0,00	0,00	0,00	0,00	0,00	0,00
P ₂ O ₅	0,01	0,01	0,01	0,02	0,01	0,00
MnO	0,00	0,01	0,01	0,00	0,00	0,00
LOI	43,47	42,42	43,74	43,41	44,01	43,35
TOTAL	99,95	99,95	99,97	99,96	99,95	99,95

4. Structural Geology

Metamorphic rocks constitute the dominant lithology in the study area. These rocks have lost their original position due to deformations in the region. Considering the structural elements in the region, it is possible to say that the region has undergone two separate deformation phases. When the types and directions of the faults are examined:

It can be said that NW-SE is trending dip-slip faults (Figure 7) and NE-SW trending strike-slip faults developed as a result of NW-SE trending compression in Phase 1 (Figure 8).

In Phase 2, due to an NW-SE trending tension, NE-SW trending dip-slip faults are observed to develop and cut the NW-SE trending dip-slip faults (Figure 2).



Figure 7. The general view of the NW-SE trending dip-slip fault cutting the Calcite Quarry (Looking from the Southwest to the Northeast). Abbreviations: Pzt; Torasan formation, Pztm; Marble Member



Figure 8. General view of the right-lateral strike-slip fault observed in the Karakaya formation west of the Karaandız district (looking from the southeast to the northwest)

The study area has undergone intense deformation, and the units have faulted within themselves. The contact relationship of the lithostratigraphic units is generally tectonic. It is seen that it is difficult to determine the contact relationships due to the dense vegetation. However, these faults can be detected, especially along eroded streams.

Joint measurements were carried out for the deformation analysis of the calcite quarry located in the study area. Fifty joint measurements and kinematic analyzes were made at two different locations.

For the kinematic analysis of the measured joints, point-contour and rose diagrams were prepared (Figure 9-10-11).

According to the rose diagrams (Figure 9), N50E tension and N40W compression were detected at Location 1, and N20E tension and N40W compression at Location 2.

In addition, the prepared point-contour diagrams (Figure 10-11) give a result that supports the rose diagrams.

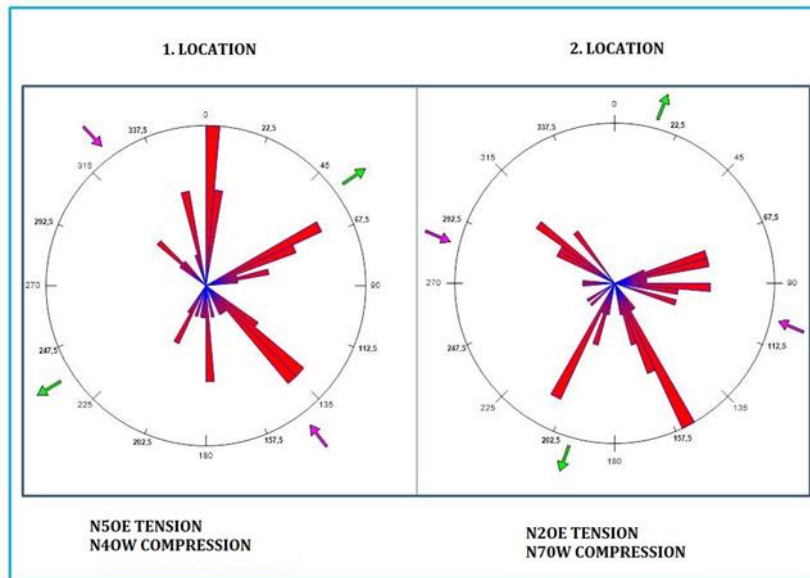


Figure 9. Rose diagram of the joints

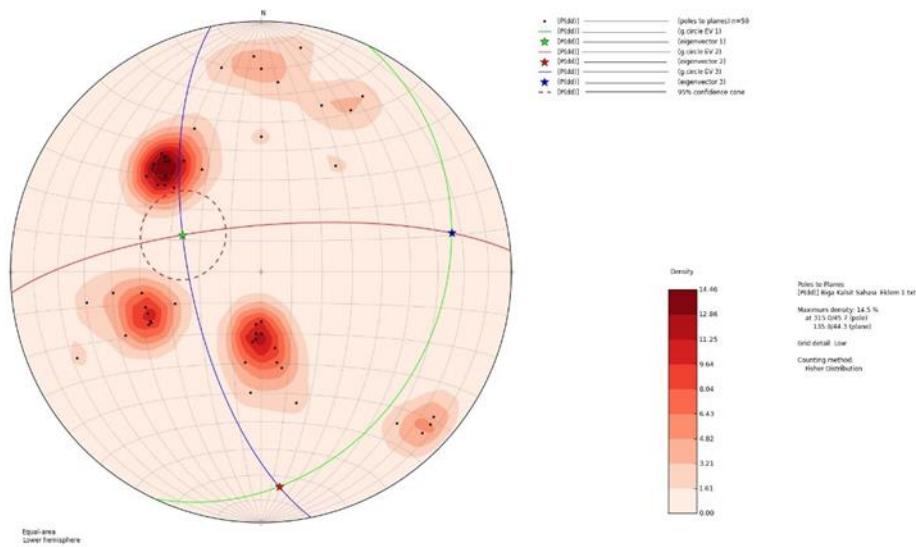


Figure 10. Point-contour diagram of the 1. Location's joints

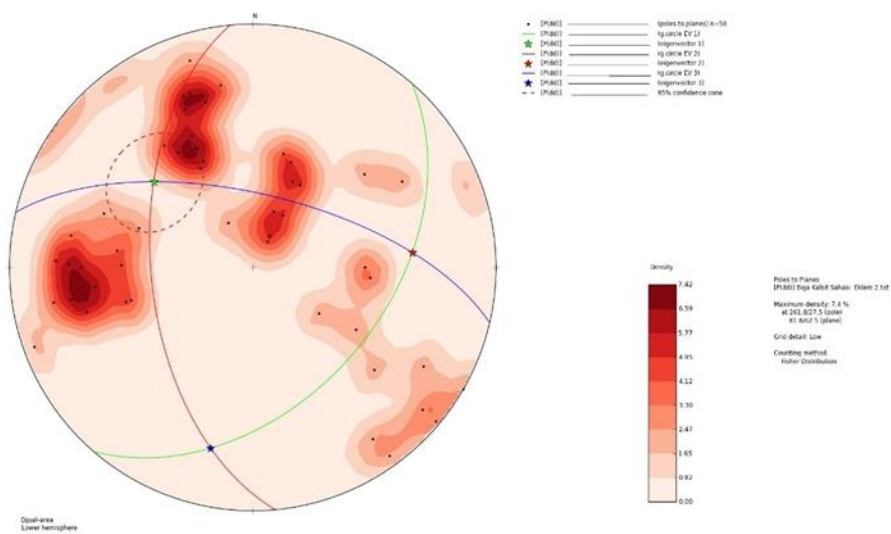


Figure 11. Point-contour diagram of the 2nd Location's joints

5. Conclusion

The geological and geochemical characteristics of the Marble member of the Torasan formation located on the Biga peninsula were explained. The contact relationships of the Marble member, considered a calcite quarry, were determined. This unit, which extends approximately NE-SW, has a length of approximately 350 meters and a width of approximately 50 meters. Petrographic and geochemical explanations of calcite, a useful mineral in the marble member, were carried out. As a result of the study, it was determined that the calcite in the quarry, which was observed as a block, was medium-coarse crystalline, was less affected by deformations in terms of fractures and cracks, the alteration was at low levels, the CaO value was around 55%, and the MgO content was quite low. The variation of CaO and MgO values according to the drilling points is given in Figure 12.

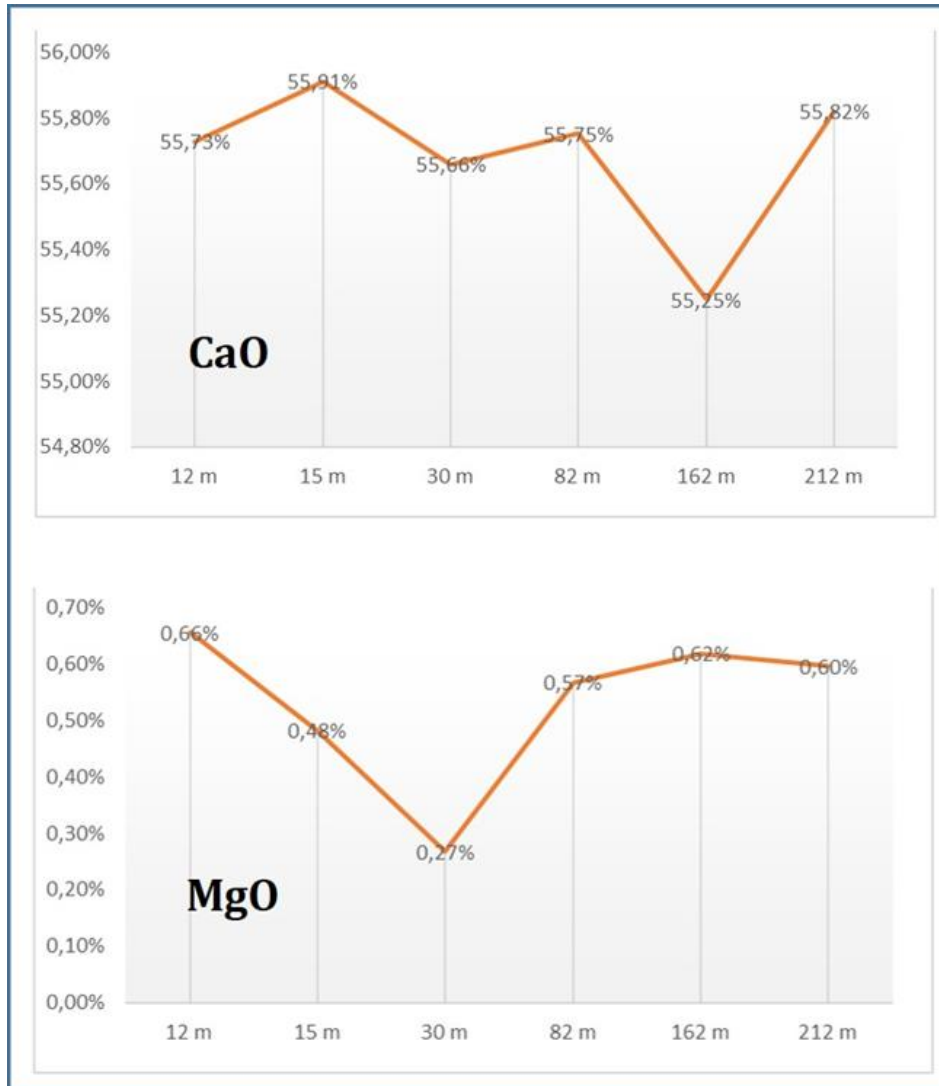


Figure 12. CaO and MgO concentrations (%) of the samples

When the region's structural elements and joint measurements were evaluated together, it was determined that there were similar compression and tension regimes. In terms of business, it is very important to reveal the deformation structures of the region and the calcite quarry.

Acknowledgement

This study is a part of Mustafa Kaya's PhD Thesis. This study was partly presented at the 4th Advanced Engineering Days [11] on 21 September 2022.

Funding

This research received no external funding.

Author contributions

Mustafa Kaya: Petrography, Geochemistry. **Cihan Yalçın:** Data curation, Methodology, Writing-Original draft preparation, Editing. **Mustafa Kumral:** Software, Visualization, Investigation.

Conflicts of interest

The authors declare no conflicts of interest.

References

1. Sanjeevi, S. (2008). Targeting limestone and bauxite deposits in southern India by spectral unmixing of hyperspectral image data. *The International Archives of the Photogrammetry, Remote Sensing and Spatial Information Sciences*, 37(B8), 1189-1194.
2. DPT-Devlet Planlama Teşkilatı. (2001). Madencilik özel ihtisas komisyonu raporu, Endüstriyel Hammaddeler Alt Komisyonu Genel Endüstri Mineralleri I, 8. Kalkınma Planı (2001-2005), Yayın No: 2618, ISBN 975- 19-2853-2, Ankara, Türkiye.
3. Şahin, N. (2008). Kalsit hakkında bazı bilgiler. *Madencilik Bülteni*, 86, 48-51.
4. Yılmaz, Y. (1981). Sakarya kıtası güney kenarının tektonik evrimi. *İstanbul Yerbilimleri*, 1(1-2), 33-52.
5. Okay, A. I., Siyako, M., & Bürkan, K. A. (1990). Biga Yarımadası'nın jeolojisi ve tektonik evrimi. *Türkiye Petrol Jeologları Derneği Bülteni*, 2(1), 83-121.
6. Bingöl, E. (1968). Contribution a Le etude geologikue de la partie centale et sudest du Massif de Kazdağ (Turque), These du doctorat, Fac. Sci. Univ. Nancy, 191 s.
7. Çoğulu, H.E., Delaloye, M. & Chessez, R. (1965). Sur l'age de quelques roches plutoniques acides dans la region d'Eskişehir - Turquie. *Arch. Sci. Geneve. Aust. Bull.* 128, 1-48.
8. Üşümezsoy, Ş. (1995). Kazdağ syntaxis: The onliqe converging and opposite verging thrust systems of the Paleotethyan arc trench lithologies. *International earth sciences colloqium on the Aegean region, Proceedings*, Vol. 1, 181-201.
9. Şengör, A. C., & Yılmaz, Y. (1981). Tethyan evolution of Turkey: a plate tectonic approach. *Tectonophysics*, 75(3-4), 181-241.
10. Şengör, A.M.C., Yılmaz, Y. & (Ketin), İ. (1982). Remnants of a Pre-late Jurassic Ocean in Northern Turkey, Fragments of Permian-Triassic Paleo-Tethys? Reply, *Geol. Soc. America Bull.*, 93, 932-936.
11. Kaya, M., Yalçın, C., & Kumral, M. (2022). Geological and geochemical signatures of the calcite quarry in the southeast of Biga (Çanakkale, Turkey). *Advanced Engineering Days (AED)*, 4, 89-92.



© Author(s) 2022. This work is distributed under <https://creativecommons.org/licenses/by-sa/4.0/>



Overview of neurodegenerative disease

Havva Türkben^{*1}, Furkan Ayaz^{1,2}

¹Mersin University, Biotechnology Department, Türkiye, havvaturkben5153@gmail.com

²Mersin University, Biotechnology Research and Application Center, Türkiye, furkanayaz@mersin.edu.tr

Cite this study: Türkben, H., & Furkan, A. (2022). Overview of neurodegenerative disease. Engineering Applications, 1 (2), 117-123

Keywords

Parkinson's Disease
ALS Disease
Neurodegenerative
Biomarker

Review Article

Received: 24.09.2022

Revised: 23.10.2022

Accepted: 04.11.2022

Published: 14.11.2022



Abstract

Neurodegenerative diseases are connected with the degeneration of neurons, together with they may be of genetic origin or develop due to environmental factors. These diseases affect certain features of neurons and result in the inability to fully fulfill or lose some functions in the person. The leading neurodegenerative diseases are Alzheimer's disease (AD), Parkinson's disease (PD), amyotrophic lateral sclerosis (ALS) disease. The epidemiology and pathogenesis of these and other neurodegenerative diseases have not yet been completely explained. Within the scope of this research, neurodegenerative diseases are closely examined, the treatments applied are evaluated, and the molecular changes in the formation and course of the disease are detailed.

1. Introduction

The term neurodegeneration is formed by the combination of the word's neuron meaning nerve cell and degeneration meaning loss of function [1].

Neurodegenerative diseases include the group of diseases that result in death, the mechanism of formation has not yet been fully elucidated and there is no definitive treatment. One of the main reasons why these diseases cannot be treated is that neurons lack the ability to divide or have very little ability to divide. However, recent studies show that it is possible to treat neurodegenerative diseases with stem cells [1].

Alzheimer's disease (AD) is one of the most common neurodegenerative diseases. This is followed by Parkinson's disease (PH) and amyotrophic lateral sclerosis (ALS), Huntington's disease, frontotemporal dementia, spinocerebellar ataxias, spinal muscular atrophy (SMA). As a result of these diseases, abnormal symptoms such as cognitive disorders, limitations in mobility, difficulties in speaking, breathing difficulties, memory loss are observed [1].

Basic molecular changes in the formation of neurodegenerative diseases; It includes many molecular changes such as regression and positive aggregation, accumulation of specific proteins in the cell, protein abnormalities in the cell, anatomical fragility of the 3D structure of proteins, neuronal abnormalities, apoptosis mechanism characterized as programmed cell death, inflammation, intracellular oxidative and proteomic stress. In addition to these, among the factors that increase the risk of developing neurodegenerative disease, hormone levels, caffeine-containing food use, infection status, age and gender are also counted. Especially with the increase in age, the risk of developing neurodegenerative diseases increases as well. However, the vast majority of these diseases are known by postmortem autopsy [1].

The basis of the grouping of neurodegenerative diseases under the common disease group is to consider the diseases mentioned one by one and to examine the formation processes of these diseases in determining their

pathogenesis. These diseases are grouped and named as neurodegenerative diseases, with the findings of genetic and molecular changes between diseases meeting at a certain point [2].

Studies on the treatment of neurodegenerative diseases, which have become more common in the last 40 years due to the increase in age in human populations, have gained momentum with modeling. The models used can be 3D as well as animal models. With the animal models created, it is aimed to illuminate the multifaceted structure of neurodegenerative disease or diseases. The created animal models simulate the nature of the disease. Transgenic mice are the most commonly used animal models [1].

Apart from modelling, treatment methods in neurodegenerative diseases are researched and developed with genome sequencing techniques and next generation sequencing technologies [1].

2. Parkinson's Disease

Parkinson's disease is the second most common neurodegenerative disease after Alzheimer's disease that causes neuromediator dysfunction affecting the central nervous system, peripheral nervous system and enteric nervous system. Parkinson's disease, which is known as movement disorder, is one of the slow progressing neurodegenerative diseases, which is generally seen in advanced ages. Until the disease is diagnosed, neuronal losses have greatly increased [3-4].

The etiology of the disease is not yet fully known. However, there are factors that increase the risk of Parkinson's disease [3-4].

2.1. Epidemiology of Parkinson's disease

Parkinson's disease is the second most common neurodegenerative disease that occurs in middle and advanced ages, progresses progressively and spreads over long periods such as 10-20 years [5]. It affects 1%-2% of people over the age of 65 and 4% of people over the age of 80. The incidence is higher in men than in women [5]. It is known that Europeans are more affected by Parkinson's disease than Asians [5].

2.2. Pathophysiology of Parkinson's disease

Parkinson's disease is associated with the accumulation of α -synuclein proteins in cytoplasmic inclusions called Lewy bodies in neurons and the loss of dopaminergic neurons and the loss of these losses in the substantia nigra from the basal ganglia [6].

The accumulation of α -synucleins in the Lewy body is widespread in the neocortical and cortical regions of the brain. Lewy bodies formed by the accumulation of α -synucleins damage the connections between neurons and stop neuronal transmission and neurotransmitter secretion [6-7].

It develops due to neuronal losses of substantia nigra pars compacta (Snp) cells in the brain stem that secrete dopamine. Dopamine is a neurotransmitter chemical and is involved in many important events that occur in the brain, such as metabolic activities, physiological movements, and neuronal transmission. The SNPC region of the brain contains approximately 800,000 cells, and approximately 60%-80% of these cells must be lost for a diagnosis of Parkinson's disease [8]. The rate of disease seen from the mentioned genetic and molecular factors is around 5% - 10%.

Mitochondrial dysfunction and increased oxidative stress due to increased mitochondrial dysfunction are also involved in the pathophysiology of Parkinson's disease. The increase in oxidative stress in the cell results in neuronal losses and is associated with Parkinson's disease. In addition, the ubiquitin-proteosomal system is also involved in the development of Parkinson's disease. As a result of all these molecular changes, misfolded proteins accumulate and pave the way for Parkinson's disease [9].

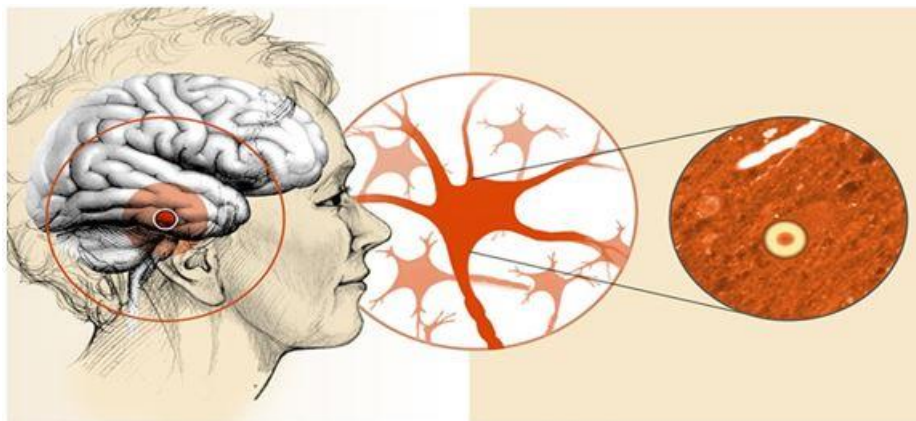


Figure 1. Close-up imaging of Lewy body accumulation in cytoplasmic inclusions in neurons

2.3. Clinical manifestations of Parkinson's disease

Depending on the pathophysiological findings associated with Parkinson's disease, stiffness in the joints, also called rigid limb, due to neuronal losses and lack of transmission between neurons, muscle tremors called resting tremor, muscle spasms called dyskinesia, slowed movements called bradykinesia, decreased voluntary movements called akinesia, It has many clinical symptoms such as difficulty in standing upright, posture disorder, excessive salivation called salivation, difficulty in swallowing called dysphagia, slowing of bowel movements called constipation and consequent constipation, inability to smell, depression, anxiety, sleep fragmentation [10].

2.4. Treatment of Parkinson's disease

There is no cure for Parkinson's disease yet, and existing treatments reduce the patient's symptoms. Medications used for treatment contain the active substance dopamine. In the drug treatment administered to the patient, the response to the active substance is measured [10].

2.5 Genes responsible for Parkinson's disease

Among the genes responsible for Parkinson's disease, PINK1, DJ-1, PRKN, SNCA, PLA2G6, ATP13A2 and FBOX7 are counted [11].

PINK1: This gene is also known as PARK 6. It is an exonic gene encoding protein kinase. It has mitochondrial activity and serine-kinase activity. Its effect in Parkinson's disease has been associated with causing mitochondrial activity disorder. It is the second most common gene mutation in the formation of early Parkinson's disease. These mutations include missense or nonsense mutations. The missense and nonsense mutations it creates are defined and named as p.Gln129fsX157, p.Pro196Leu, p.Gly309Asp, p.Trp437X, p.Gly440Glu, p.Gln456X [11].

DJ-1: This gene is also called PARK 7 and consists of 7 exons. It constitutes 1% to 2% of early Parkinson's disease. It is responsible for performing neuroprotective functions and antioxidant functions. As a result of the mutation of the DJ-1 gene, the protein forms conformational changes and goes into misfolding and degradation in the proteomic way. As a result, neuroprotective and antioxidant functions are lost and Parkinson's disease occurs [11].

PRKN: This gene is also called PARK2. It is the second largest gene found in the human genome. It expresses the parkin protein, which is 465 amino acids long. It is broad-spectrum, covering a large number of mutations. There are 887 parkin mutations identified. As a result of mutations in this gene and loss of protein function, neurons become vulnerable to cytotoxic effects, and Parkinson's disease occurs in this case [11].

LRRK2: This gene constitutes the most common mutations in the autosomal inherited form of Parkinson's disease. 50 different mutations are known. It is associated with the formation of Lewy bodies and neuronal losses with the mutations it creates [11].

SNCA: This gene is responsible for the expression of α -synuclein proteins. Lewy bodies and brain pathologies are seen as a result of mutations in this gene [11].

2.5. Environmental risk factors for Parkinson's disease

In the formation of Parkinson's disease, environmental factors as well as genetic factors have an effect on the formation of the disease. Pesticides used as pesticides are at the forefront of these factors. Pesticides are pesticides that are frequently used to combat weeds in agricultural areas. It has been observed that the risk of developing late-onset Parkinson's disease increases in people who use paraquat and maneb derivatives and their ingredients in the pesticide group used in agricultural areas [12].

Another environmental factor that increases the risk of developing the disease is the oxidative stress that occurs after exposure to heavy metals. Oxidative stress occurs as a result of the accumulation of heavy metals in the substantia nigra. This accumulation paves the way for Parkinson's disease. For example; It is known that lead, one of the heavy metals, negatively affects the release of the neurotransmitter dopamine. It causes an increase in lipid peroxidation, decreases antioxidant cell capacity, and as a result causes α -synuclein accumulation [13].

Another heavy metal is lead. It has been observed that the risk of developing Parkinson's disease is doubled by examining the bone structure after exposure to lead [13].

Another heavy metal is manganese. Although manganese does not act as directly as other heavy metals, it is effective in the formation of Parkinson's disease and the accumulation of α -synucleins. As a result of this accumulation, in addition to the symptoms of Parkinson's disease, patients have symptoms called manganism and seen after long-term exposure to manganese [13].

In addition to heavy metals, the concentration of iron ions in the brain should not be above or below certain levels, and the balance should be maintained. While iron deficiency causes disruption in motor functions, iron accumulation due to iron excess forms the basis of neurological disorders [13].

It is known that there are environmental factors that increase the risk of Parkinson's disease, as well as effects that reduce the disease. Among the mitigating effects are the use of cigarettes, alcohol or coffee. The nicotine substance in cigarettes is a neuroprotective substance on its own. It has been observed that nicotine, which is a neuroprotective substance, prevents dopaminergic neuronal toxicity by reducing it [14-15].

3. Amyotrophic Lateral Sclerosis (ALS) Disease

Amyotrophic lateral sclerosis is a progressive fatal neurodegenerative motor neuron disease associated with the degeneration of neurons in the brain and spinal cord. Looking at the name of the disease, the word amyotrophic means lack of muscle nutrition and characterizes the result of atrophy [16-17].

It results in the loss of neurons in the central nervous system, spinal cord, and brain stem. If the motor neurons damaged in ALS disease are composed of upper corticospinal motor neurons, they cause uncontrolled movements called muscle spasticity. If the damaged motor neurons are composed of lower motor neurons, it causes muscle weakness. As a result of the loss of these neurons, various symptoms such as weakness in the legs and muscles, muscle wasting, and swallowing dysfunction are observed. In the last stage of the disease, patients cannot have voluntary muscle movements, so there are cases of paralysis. In addition to these, up to 10% of patients develop dementia in addition to ALS. However, the dementia that occurs is not effective enough to cause the patient to lose cognitive functions [16-17].

None of the studies within the scope of the treatment of ALS disease are in the direction of prevention of the disease, but in the direction of reducing the symptoms of the disease. Drug treatments in use have antiglutamate properties. In addition, one of the treatments used is stem cell therapy. However, successful results of stem cell treatments applied and used have not been recorded [18].

3.1. The pathogenesis of ALS disease

A mutation in the gene encoding the antioxidant enzyme superoxide dismutase 1 (SOD1) plays a role in the pathogenesis of ALS disease. The mutated SOD1 causes conformational change in the enzyme, resulting in misfolding. In addition, ALS disease occurs as a result of incorrect or incomplete activity of the mitochondria organelle. As a result of changes in the structure of motor neurons, axonal or neuronal disruptions, free radical formation, glutamate excitotoxicity, and oxidative stress play an active role in the pathogenesis of ALS disease. [16-17].

3.2. Factors that cause ALS

As with other neurodegenerative factors, environmental and genetic factors play a role in the development of ALS. Environmental factors include many factors such as age, gender, exposure to electrical fields, pesticides, fertilizers, insecticides, formaldehydes, air pollution, alcohol use, smoking and exposure to heavy metals. Genetic factors that are effective in the development of ALS include factors such as familial gene mutations, viral infections, autoimmunity-induced reactions and glutamate excitotoxicity. Only 10% of ALS patients are inherited familial and genetically, while the remaining 90% develop sporadically. The age of onset of the disease varies between 50 and 75 [19].

3.3. Use of models in ALS disease

Models are used to understand the pathogenesis of ALS disease and the expression levels of proteins and genes involved in its pathogenesis, and to identify mutations that play a role in the formation of the disease. Although these models do not fully represent the disease in the human body, they are used in the development of new treatments, uncovering and examining unknown aspects of the disease. Models used in ALS disease can be animal models as well as cell models [20].

3.4. Cell models in ALS disease

It is used to determine the proteins that accumulate and aggregate during the mutation process of the motor neuron with the mutated SOD1 gene by cell models and to examine the toxic effects of these proteins. In the light of cell models, it is aimed to develop methods to treat the disease, including the methods of isolating toxic proteins from cells [20].

In addition, it is a model of applying the desired changes in the genetic structure of the cells taken from the ALS patient with stem cell models and creating induced pluripotent stem cells (iPSC) transplanted to the patient. The created iPSC models are used to predict the therapeutic effects of drugs to be administered as drug therapy in cells. One of the main reasons for the widespread use of this modeling is to transform the skin or blood cells of the person into induced pluripotent stem cells as therapeutic cells [20].

3.5. Worm (nematode) model in ALS disease

C. elegans, one of the worm species that does not have a complex structure, can reach 1 mm in adulthood and has 959 cells, is used. It has been observed that this species preserves its genes by preserving it much better than humans. Since they have a 3-week lifespan and 3-day life cycle, and their 302 neurons have been mapped, they allow healthy monitoring of motor neuron development and imaging under the microscope with fluorescent markers [20].

3.6. Fruit fly (drosophila) model in ALS disease

The fruit fly is very similar to the worm models used in ALS disease. It is preferred because of the presence of fly species with SOD1 gene mutation that causes ALS disease and the phenotypic characteristics of these fly species as a result of ALS disease. It enables the development of drug treatments that are thought to be effective after the phenotypic characteristics of fruit flies with ALS disease, which are described as rough eyes, are observed [20].

3.7. Zebrafish (danio rerio) model in ALS disease

It is preferred because the structure of motor neurons in zebrafish is similar to that of human motor neurons, as in the fruit fly. Zebrafish are a type of fish that can be easily grown in a laboratory environment and reproduce quickly. Likewise, the ability of zebrafish to insert the SOD1 gene, which is the most prominent gene mutation of ALS disease, has made its use in modeling more convenient [20].

3.8. Rodent (mouse) model of ALS disease

The most commonly used animal in the modeling of ALS disease is the mouse, the rodent species. It is used as an animal model thanks to its features such as having motor neurons similar to human motor neurons, having the SOD1 gene mutation, which is the ALS disease gene, having a suitable size for stem cell and gene therapy studies, rapid reproduction and easy breeding. At the same time, rodent-like creatures have a more complex nervous system compared to other living things, allowing for the testing of treatment methods to be developed [20].

3.9. Imaging Methods of Neurodegenerative Diseases

Brain imaging technologies are the leading biomarkers used in neurodegenerative diseases, which are used to diagnose neuronal activity or damage in the brain. These imaging techniques consist of different methods such as magnetic resonance (MRI), computed tomography (CT), functional magnetic resonance (fMRI), positron emission tomography (PET) and single positron emission computed tomography (SPECT). These imaging methods can be used in the diagnosis phase as well as in the follow-up of the course of the disease. In this way, neuroimaging methods have reproducibility [21].

4. Biomarker Use in Neurodegenerative Diseases

As a biomarker or biomarker can measure the biological processes that occur normally in people, it is a feature that includes pathogenic processes, biological processes that occur as a result of the person's encounter with the therapeutic agent and is accepted as the result of the responses of these processes. It is also accepted as an indicator of the biological process in which the symptoms of the suspected disease and the consequences of these symptoms are associated. The use of biomarkers in neurodegenerative diseases provides an opportunity for early diagnosis. It is used not only with the opportunity to make an early diagnosis, but also to determine and monitor the progression of the disease, and to determine the effectiveness of the treatments used as therapeutic agents.

There are some characteristics that an ideal biomarker should have. These features are;

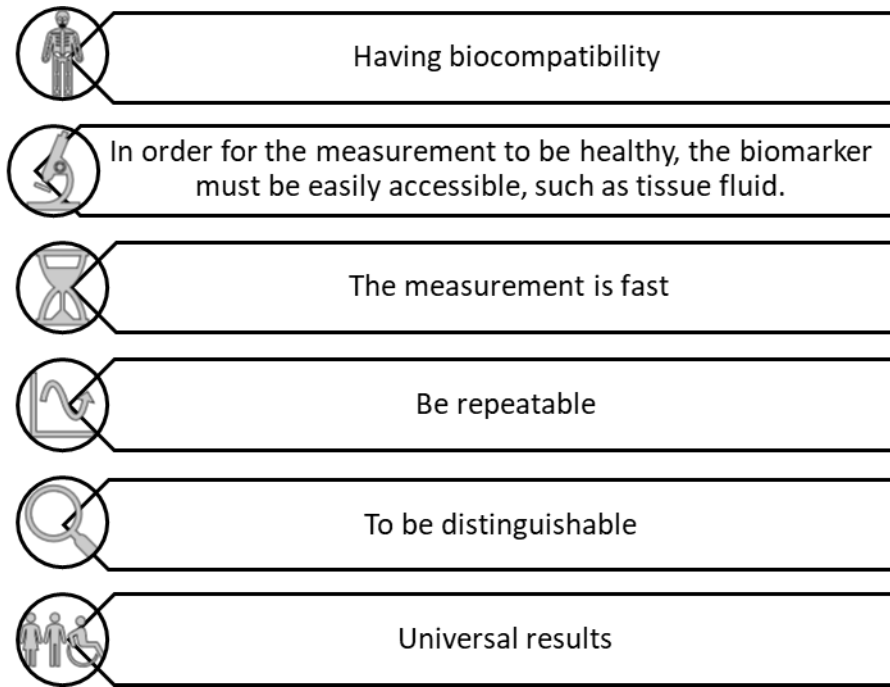


Figure 2. Characteristics of ideal biomarkers

5. Conclusion

Due to the lack of use of biomarkers, it becomes difficult to diagnose the asymptomatic period, which is called the period before the emergence of the disease in the individual. In addition, obstacles such as the widespread use of animal models and the high cost of experiments with animal models are among the factors that make it difficult to develop treatment methods for neurodegenerative diseases. In order to prevent these situations, the use of biomarkers and animal models should be expanded [21].

Acknowledgement

This study was partly presented at the 4th Advance Engineering Days [22].

Funding

This research received no external funding.

Author contributions:

Havva Türkben: Conceptualized, wrote, reviewed. **Furkan Ayaz:** Edited the final version

Conflicts of interest

The authors declare no conflicts of interest.

References

1. Checkoway, H., Lundin, J. I., & Kelada, S. N. (2011). Nörodejeneratif hastalıklar. IARC bilimsel yayınları, (163), 407-419.
2. Mayeux, R. (2003). Epidemiology of neurodegeneration. *Annual review of neuroscience*, 26, 81.
3. Poewe, W., Seppi, K., Tanner, CM, Halliday, G.M., Brundin, P., Volkman, J., ... & Lang, A. E. (2017). Parkinson's disease. *Nature studies Disease primaries*, 3 (1), 1-21.
4. Shimohama, S., Sawada, H., Kitamura, Y., & Taniguchi, T. (2003). Disease model: Parkinson's disease. *Trends in molecular medicine*, 9 (8), 360-365.
5. Çakmur, R. (2011). Parkinson's disease and its medical treatment. *Clinical Development*, 23(1), 53-61.

6. Vázquez-Vélez, G. E., & Zoghbi, H. Y. (2021). Parkinson's disease genetics and pathophysiology. *Annual Review of Neuroscience*, 44, 87-108.
7. Agid, Y. (1991). Parkinson's disease: pathophysiology. *The Lancet*, 337 (8753), 1321-1324
8. Moore, D. J., West, A. B., Dawson, V. L., & Dawson, T. M. (2005). Molecular pathophysiology of Parkinson's disease. *Annu. Rev. Neurosci.*, 28, 57-87.
9. Bergman, H., & Deuschl, G. (2002). Pathophysiology of Parkinson's disease: from clinical neurology to basic neuroscience and back. *Movement disorders: official journal of the Movement Disorder Society*, 17(S3), S28-S40.
10. Aslan, S. N., & Karahalil, B. (2019). Oksidatif stres ve Parkinson Hastalığı. *Journal of Faculty of Pharmacy of Ankara University*, 43(1), 94-116.
11. Kurman, Y. (2018). Parkinson's Disease and Associated Genes. *Düzce University Journal of Science and Technology*, 6(1), 231-239
12. Gatto, N. M., Rhodes, S. L., Manthripragada, A. D., Bronstein, J., Cockburn, M., Farrer, M., & Ritz, B. (2010). α -Synuclein gene may interact with environmental factors in increasing risk of Parkinson's disease. *Neuroepidemiology*, 35(3), 191-195.
13. Akbayır, E., Şen, M., Ay, U., Şenyar, S., Tüzün, E., Küçükali, C. İ. (2017). Etiopathogenesis of Parkinson's Disease. *Journal of Experimental Medicine*, 7(13).
14. Noyce, A. J., Bestwick, J. P., Silveira-Moriyama, L., Hawkes, C. H., Giovannoni, G., Lees, A. J., & Schrag, A. (2012). Meta-analysis of early nonmotor features and risk factors for Parkinson disease. *Annals of neurology*, 72(6), 893-901.
15. Carr, L. A., & Rowell, P. P. (1990). Attenuation of 1-methyl-4-phenyl-1, 2, 3, 6-tetrahydropyridine-induced neurotoxicity by tobacco smoke. *Neuropharmacology*, 29(3), 311-314.
16. Zarei, S., Carr, K., Reiley, L., Diaz, K., Guerra, O., Altamirano, P. F., ... & Chinea, A. (2015). A comprehensive review of amyotrophic lateral sclerosis. *Surgical neurology international*, 6.
17. Sharma, R., Hicks, S., Berna, C. M., Kennard, C., Talbot, K., & Turner, M. R. (2011). Oculomotor dysfunction in amyotrophic lateral sclerosis: a comprehensive review. *Archives of neurology*, 68(7), 857-861.
18. Şener, H. Ö., Parman, Y., Şengün, İ., Koç, F., & Oflazer, P. (2009). Stem Cell Applications in Amyotrophic Lateral Sclerosis. *Turkish Journal of Neurology*, 15(3), 105-108.
19. Masrori, P., & Van Damme, P. (2020). Amyotrophic lateral sclerosis: a clinical review. *European journal of neurology*, 27(10), 1918-1929.
20. Anonymous, 2022, Disease models, <https://www.als.org/research/research-we-fund/scientific-focus-areas/disease-models>. ALS association.
21. Bouwman, F. H., Frisoni, G. B., Johnson, S. C., Chen, X., Engelborghs, S., Ikeuchi, T., ... & Teunissen, C. (2022). Clinical application of CSF biomarkers for Alzheimer's disease: From rationale to ratios. *Alzheimer's & Dementia: Diagnosis, Assessment & Disease Monitoring*, 14(1), e12314.
22. Türkben, H., & Ayaz, F. (2022). Dendritic cells: Their functions in immunity and disease. *Advanced Engineering Days (AED)*, 4, 16-17.



© Author(s) 2022. This work is distributed under <https://creativecommons.org/licenses/by-sa/4.0/>



Direct pouring system design and optimization in steel castings

Mustafa Murat Zor*¹, Serdar Kesim¹, Buğra Erbakan¹, Ferhat Tülüce¹, Alper Yoloğlu¹, Kazım Çakır¹

¹ÇİMSATAŞ Çukurova Construction Machinery IND. TRADE. A.S. Mersin, Türkiye, [foundry@cimsatas.com](mailto:foundation@cimsatas.com)

Cite this study: Zor, M. M., Kesim, S., Erbakan, B., Tülüce, F., Yoloğlu, A., & Çakır, K. (2022). Direct pouring system design and optimization in steel castings. *Engineering Applications*, 1 (2), 124-131

Keywords

Steel casting
Direct pouring system
Modeling and simulation
Casting defects
Filtration

Research Article

Received: 26.09.2022
Revised: 23.10.2022
Accepted: 05.11.2022
Published: 14.11.2022



Abstract

The aim of this study is to establish a correlation between various version direct pouring systems for steel castings in industrial conditions. In the study, a computer-aided design solid modeling program was used in the design of the kalpur direct pouring system, non-filter bottom direct pouring system, and filtered direct pouring system for steel castings. The flow and solidification simulation of the kalpur direct pouring system and the non-filter bottom direct pouring system of the casting part was made in magma flow and solidification program. The study clearly shows that the kalpur direct pouring system has revealed that it plays a significant role in preventing non-metallic casting defects in steel castings, such as sand, gas, and slag. In addition, it has been revealed in the study that the non-filter bottom direct pouring system prevents non-metallic casting defects in steel castings such as the kalpur direct pouring system. Kalpur direct pouring system is recommended to be used in ferrous based castings by FOSECO, was used for the first time in the ÇİMSATAŞ foundry in the steel castings and the appropriate result was obtained.

1. Introduction

Non-metallic inclusions are important defect in steel casting process. Inclusion defects of steel castings are defects such as slag of oxide and other substances generated in the pouring ladle by the reaction, and sand of molds and cores that flake away and are included in the molten metal, flowing into casting parts and appearing on the surfaces of parts as non-metallic inclusions. In order to reach desirable quality casting part, well design pouring system is the first step. Dimensions of the pouring system need to be calculated according to casting part geometry because of each casting part has different shape and an incorrect design is the root cause of the casting defects onto casting parts, mostly. High casting quality depends on a reasonable pouring system design. Traditionally, the foundry design and method engineers highly employ their own experience and trial and error method to design the pouring system. But this design method is time consuming and hard to get an optimal design. Today, foundry design and method engineers are experimenting different optimization methods that optimize the pouring system, including size, shape and position by using flow and solidification programs [1-6].

In recent years, foundry metal filtration technology has been rising popularity in casting system for casting processes of many metals such as cast irons, steel and aluminum. Filtration technology is evolving as the demand for clean, quality castings with high yield, low scrap rates, and low process costs increases. The benefit of filters, especially reticulated foam filters, besides their turbulence-reducing effect, is to prevent non-metallic inclusions such as sand and slag from entering the casting part during pouring the liquid metal into the sand mold [7-10]. This study presents the results of filtered pouring system known as kalpur direct pouring system (developed by FOSECO) and the non-filter bottom direct pouring system (ÇİMSATAŞ casting practice) studies.

1.1. Kalpur direct pouring system

Kalpur direct pouring system developed by FOSECO for foundries is used in green sand moulding lines and resin moulding lines to obtain high part efficiency and clean casting parts. Kalpur direct pouring system includes many critical components within its own structure; exothermic feeder, ceramic foam filter, and collapsible breaker core etc. The main purpose of the kalpur direct pouring system is; reduced fettling cost, reduced non-metallic inclusions, lower turbulence related defects, improved directional solidification, good surface finish optimized yield, and increased space on the pattern plate. Parts molded with the kalpur direct pouring system can be poured with lip pouring ladle or bottom pouring ladle [10-13].

1.2. Non-filter bottom direct pouring system

Non-filter bottom direct pouring system is one of the casting practices of the ÇİMSATAŞ foundry. Non-filter bottom direct pouring system is used in resin moulding line in ÇİMSATAŞ foundry to obtain high part efficiency and clean casting parts. The basic components of the non-filter bottom direct pouring system designed by ÇİMSATAŞ are the exothermic feeder, pouring basin, and sand cap. The main purpose of the non-filter bottom direct pouring system is; reduced fettling cost, reduced non-metallic inclusions, lower turbulence related defects, improved directional solidification, good surface finish optimised yield, and increased space on the pattern plate. Parts molded with the kalpur direct pouring system can be poured only with bottom pouring ladle.

1.3. Filtered direct pouring system

In the steel casting process, the filtered direct pouring system is known as the casting practice based on placing a ceramic foam filter in a feeder. The basic components of filtered direct pouring system is feeder and ceramic foam filter. Filtered direct pouring system is used in resin moulding lines and green sand moulding lines. Main purposes of the filtered direct pouring system are; reduced non-metallic inclusions, lower turbulence related defects, improved directional solidification, good surface finish, optimized yield, and increased space on the pattern plate. Parts molded with filtered direct pouring system can be poured with bottom pouring ladle or lip pouring ladle [13-14].

2. Material and Method

In this study, it is aimed to develop direct pouring systems for steel castings by using a computer-aided solid modeling program. The direct pouring system designs of the bearing casting part are based on the modulus and geometry of the casting part. In the study, the material of the part was determined according to the EN 10293 standard and material of the casting part was selected G20Mn6N. The part with three different direct filling systems was molded in the flaskless resin moulding system and cast in the ÇİMSATAŞ foundry. The nominal chemical composition of the casting part was selected as shown in Table 1 and the image of the bearing casting part is shown in Figure 1.

Table 1. Chemical composition of the bearing casting part

Content	% C	% Mn	% Si	% P	% S	% Cr	% Ni	% Mo	% V
	0,199	1,593	0,432	0,014	0,007	0,191	0,065	0,035	0,013
Content	% Cu	% B	% Ti	% Sn	% Al	% Zr	% Nb	% Pb	% Sb
	0,071	0,00018	0,001	0,003	0,048	0,002	0,008	0,001	0,000
Content	% Fe	% CEQ	% Zn	% Ce	% Bi	% W	% As	% Co	% N
	97,264	0,528	0,002	0,001	0,000	0,000	0,007	0,008	0,008

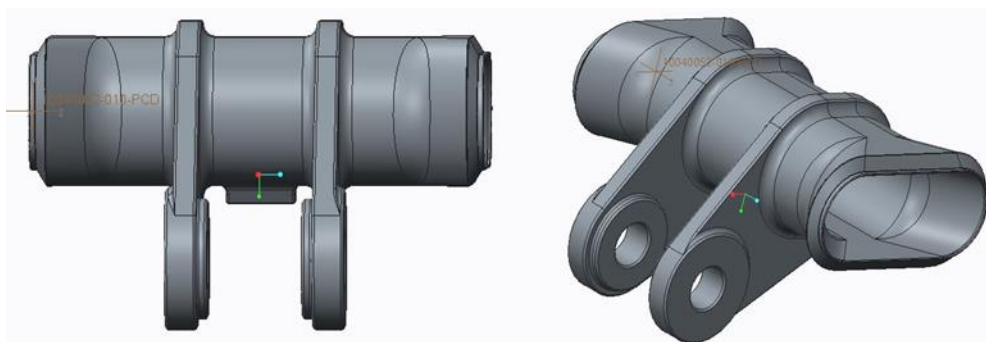


Figure 1. Schematic representation of the bearing casting part

In the first direct pouring system study, filtered direct pouring system was designed by placing a dimension of Stelex Pro $\text{Ø}150 \times 30$ mm 10 PPI graphite-based filter was placed inside the BGK6 exothermic feeder in the cope side of the part solid data. Then, the flow and solidification simulation of the part was made at 1600°C by choosing lip pouring ladle. According to simulation results, filtered direct pouring system was assembled to the casting part model. Images of the simulation results of the casting part are shown in Figure 2, and filtered direct pouring system is shown in Figure 3.

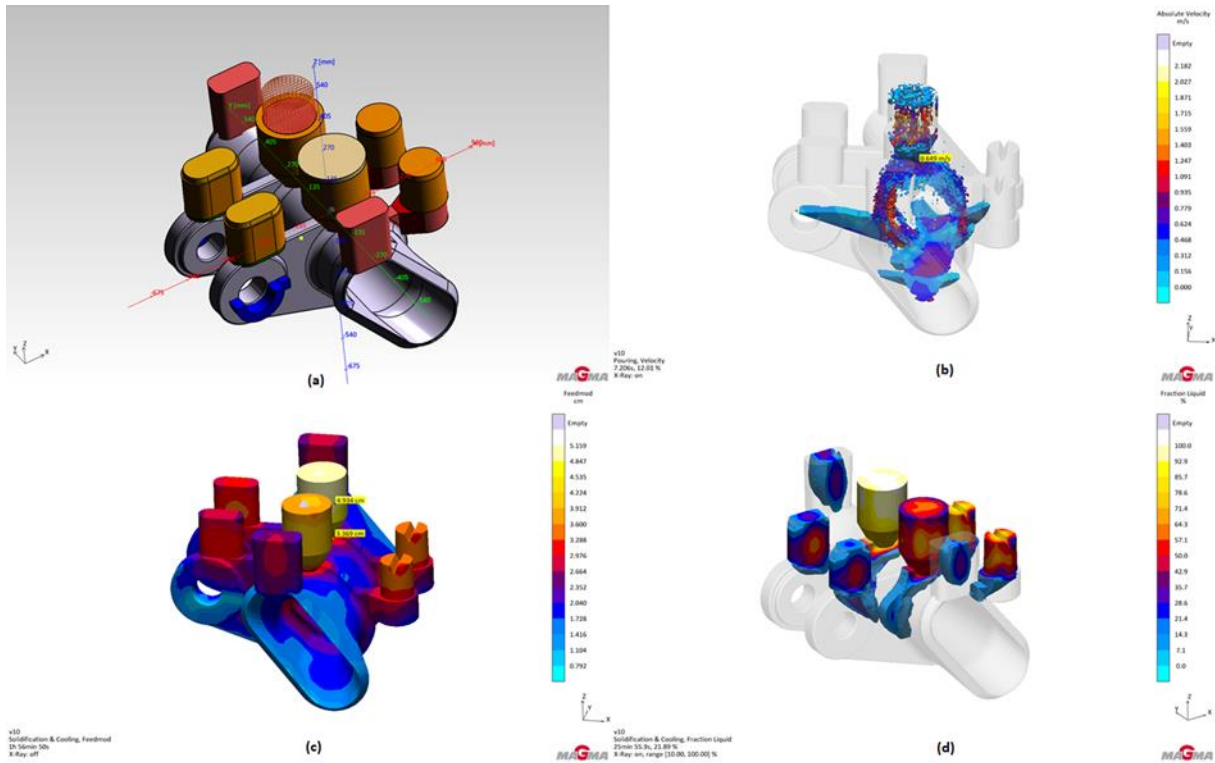


Figure 2. a); The image of the casting part geometry, (b); The image of the metal flow and filling simulation of the casting part, (c); The image of the feeding mod of the casting part, (d); The image of the friction liquid mod of the casting part



Figure 3. Schematic representation of the filtered direct pouring system

After simulation results, one part was molded in the flaskless resin moulding system in the ÇİMSATAŞ foundry and the casting was carried out with a lip pouring ladle at 1600 °C and 38 second. Total weight of the casting part is 590 kg. Image of poured part with the filtered direct pouring system is shown in Figure 4.



Figure 4. The image of poured casting part with the filtered direct pouring system

The part that was poured with the filtered direct pouring system was examined and then a design change was made in the part. In the casting part design, Stelex Pro Ø150x30 mm 10 PPI graphite-based filter was placed inside the Kalminex ZTAE PPE 18/20 exothermic feeder and the filling point of the casting part was revised as kalpur direct pouring system. Kalpur direct pouring system was placed at the lowest point of the cope side in the casting part solid data and flow and solidification simulation was made at 1600 °C by choosing bottom pouring ladle. According to simulation results, kalpur direct pouring system was assembled to the casting part model. Images of the simulation results of the casting part are shown in Figure 5, and kalpur direct pouring system is shown in Figure 6.

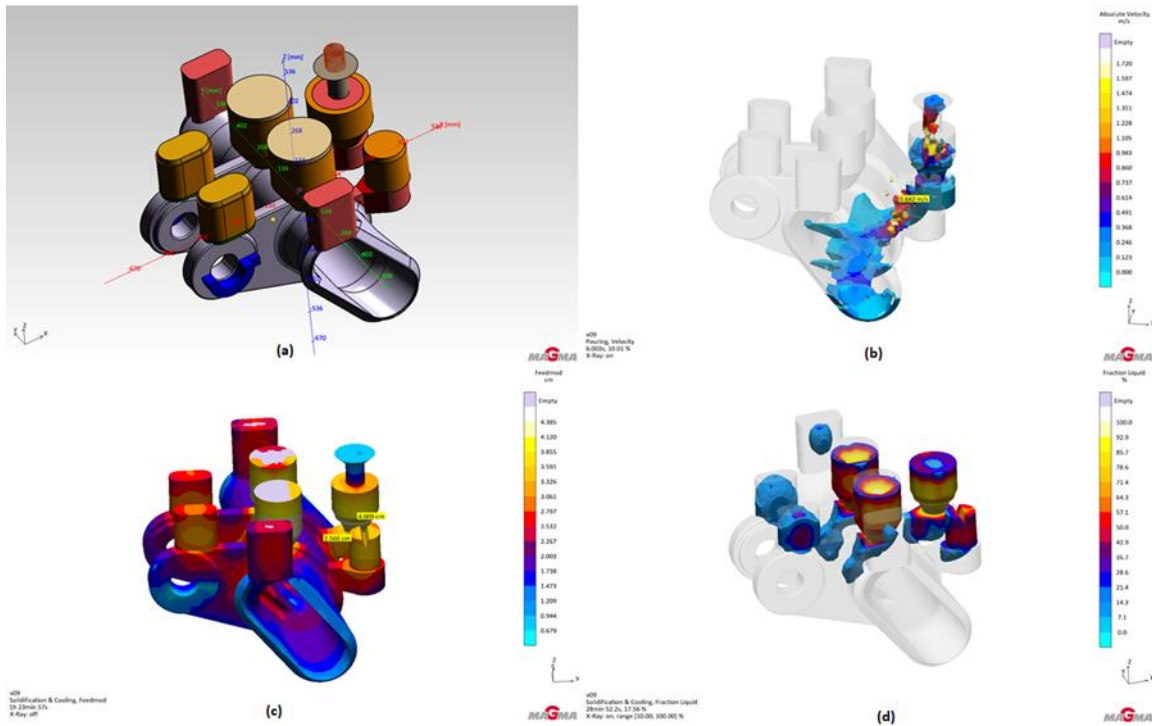


Figure 5. (a); The image of the casting part geometry, **(b);** The image of the metal flow and filling simulation of the casting part, **(c);** The image of the feeding mod of the casting part, **(d);** The image of the friction liquid mod of the casting part



Figure 6. The Image of the kalpur direct pouring system

After simulation results, one part was molded in the flaskless resin moulding system in the ÇİMSATAŞ foundry and the casting was carried out with bottom pouring ladle at 1609 °C and 32 second. Total weight of the casting part is 613 kg. Image of poured part with the kalpur direct pouring system is shown in [Figure 7](#).



Figure 7. The image of poured casting part with the kalpur direct pouring system

After examining the poured part with the Kalpur direct casting system, the part design was revised as non-filter bottom direct pouring system. In the casting part design, Stelex Pro Ø150x30 mm 10 PPI graphite-based filter was not placed inside Kalminex ZTAE PPE 18/20 exothermic feeder as the casting practice of the ÇİMSATAŞ foundry. The filling point of the casting part was chosen as the same region as the kalpur direct pouring system. Flow and solidification simulation of the casting part was made at 1600 °C by choosing bottom pouring ladle. According to simulation results, non-filter bottom direct pouring system was assembled to the casting part model. Images of the simulation results of the casting part are shown in [Figure 8](#), and non-filter bottom direct pouring system is shown [Figure 9](#).

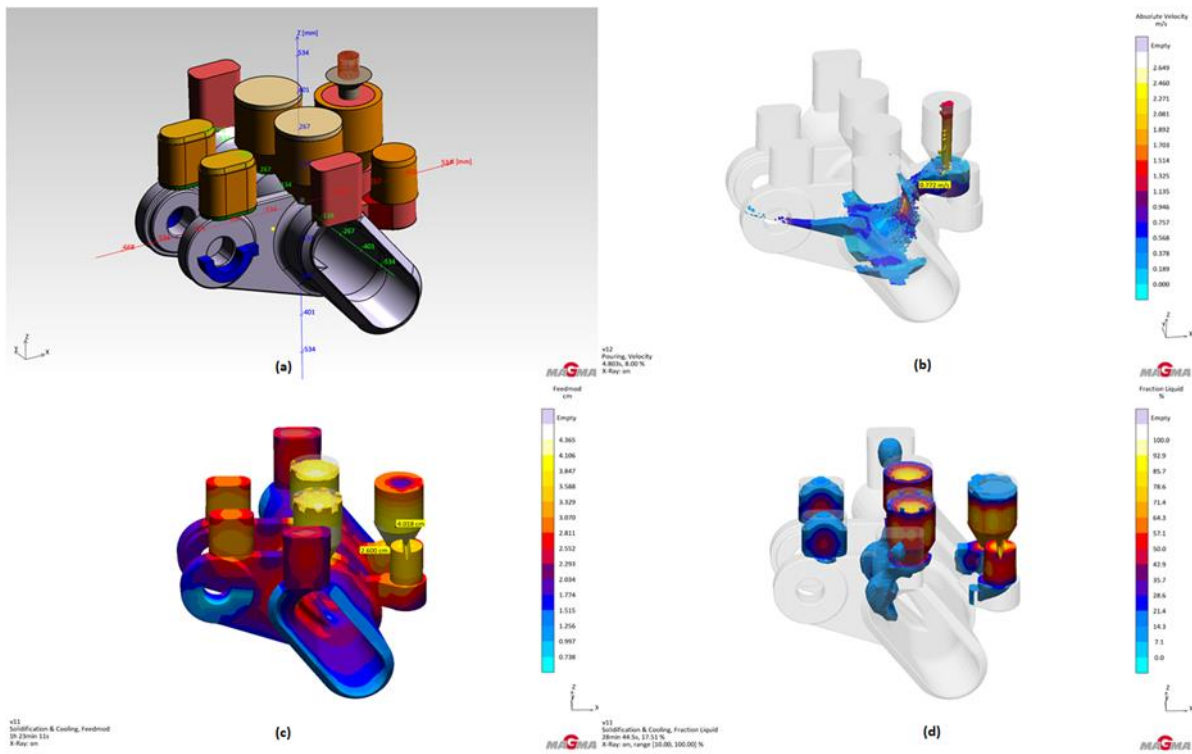


Figure 8. (a); The image of the casting part geometry, **(b);** The image of the metal flow and filling simulation of the casting part, **(c);** The image of the feeding mod of the casting part, **(d);** The image of the friction liquid mod of the casting part



Figure 9. The image of the non-filter bottom direct pouring system

After simulation results, one part was molded in the flaskless resin moulding system in the ÇİMSATAŞ foundry and the casting was carried out with bottom pouring ladle at 1582 °C and 20 second. Total weight of the casting part is 613 kg. Image of poured part with the non-filter direct pouring system is shown in Figure 10.



Figure 10. The image of poured casting part with the non-filter bottom direct pouring system

3. Results and Discussion

In this study, casting parts were designed according to the simulation results with different direct pouring system versions in steel castings. The findings were obtained from the simulation and casting results of the parts.

- It is found that the simulation results highly represent the actual casting results.
- Cold shut defects were detected as well as non-metallic inclusions on the surface of the part poured with the filtered direct pouring system. And filling time of the casting part is 38 second.
- Poured with kalpur direct pouring system and non-filter bottom direct pouring system, the gross weight of the casting parts has increased from 590 kg to 613 kg. In total, gross weight of the casting parts have increased by 23 kg.
- It has been revealed that pouring design of the casting part and the selection of the pouring region is very important for the surface quality of the casting part.
- With the kalpur direct pouring system, a remarkable improvement has occurred on the surface quality of the casting part.
- With the non-filter bottom direct pouring system, the need for Stelex Pro $\text{\O}150 \times 30$ mm filter used in the moulding of the part has been eliminated. It has been observed that clean parts can be poured with this system by using bottom pouring ladle too.
- While the filling time of the poured part with the kalpur direct pouring system is 32 seconds, the filling time of the poured part with the non-filter bottom direct pouring system is 20 seconds.
- It has been observed that the surface qualities of the poured parts are close to each other with the kalpur direct pouring system and the non-filter bottom direct pouring system.
- It has been observed that the surface qualities of the poured part are worst with filtered direct pouring system.

4. Conclusion

Although non-filter bottom direct pouring system for steel castings minimizes the escape of non-metallic inclusions from ladle into the casting part during sand mould filling, the use of ceramic foam filter inside the non-filter bottom direct pouring systems are very important for the scrap rate of the foundries.

With the design of the different version of the direct pouring systems in the ÇİMSATAŞ foundry, the surface quality of the casting part has improved positively by design of the kalpur direct pouring system and non-filter bottom direct pouring system. Ceramic foam filters are cost-effective and efficient way to reduce casting defects. The improvement in the casting part surfaces which get obtained by using direct pouring system was reduced the rework needed (such as cosmetic welding, grinding, etc.).

The results of the study show that the kalpur direct pouring system and non-filter bottom direct pouring system have best given positive and reliable results in the steel casting process.

Acknowledgement

We would like to thank ÇİMSATAŞ General Manager Mr. Fatih ERDOĞAN, ÇİMSATAŞ Production Group Manager Mr. Necmettin ACAR, ÇİMSATAŞ Foundry Finishing Engineer Mr. Mert DEMİRDÖĞEN, ÇİMSATAŞ Foundry Production Engineer Mr. Vedat UZ, ÇİMSATAŞ Foundry Production Foreman Mr. Sabahattin KAYA, ÇİMSATAŞ Foundry Finishing Foreman Mr. Erdal YALÇIN, ÇİMSATAŞ Foundry Finishing Foreman Mr. Halil Deniz ÇOBAN, ÇİMSATAŞ Foundry Model Shop Foreman Mr. Ahmet AVCI, FOSECO Simulation Engineer Mr. Volkan EVNİ, and FOSECO Sales Engineer Mr. Halis ARTUT.

This study was partly presented at the 4th Advanced Engineering Days [15].

Funding

This research received no external funding.

Author contributions

Mustafa Murat Zor: Conceptualization, Methodology, Software, Data curation, Writing-Original draft preparation, Software, **Serdar Kesim:** Validation. **Buğra Erbakan:** Visualization. **Ferhat Tülüçe:** Validation, Editing, **Alper Yoloğlu:** Data curation, Editing, **Kazım Çakır:** Editing

Conflicts of interest

The authors declare no conflicts of interest.

References

1. Campbell, J. (2015). *Complete casting handbook: metal casting processes, metallurgy, techniques and design*. Butterworth-Heinemann.
2. Campell, J. (2004). *Casting Practice The 10 Rule of Castings*, 1st ed., Butterworth-Heinemann, Oxford
3. Campell, J. (2012). Stop Pouring, Start Casting, *International Journal of Metal Casting Research*, 6(3), 7-18
4. Melendez, A. J., Carlson, K. D., & Beckermann, C. (2010). Modelling of reoxidation inclusion formation in steel sand casting. *International Journal of Cast Metals Research*, 23(5), 278-288.
5. Renukananda, K. H., & Ravi, B. (2016). Multi-gate systems in casting process: comparative study of liquid metal and water flow. *Materials and Manufacturing Processes*, 31(8), 1091-1101.
6. Brown, J. (Ed.). (2000). *Foseco ferrous foundryman's handbook*. Butterworth-Heinemann.
7. Modaresi, A., Safikhani, A., Noohi, A. M. S., Hamidnezhad, N., & Maki, S. M. (2017). Gating system design and simulation of gray iron casting to eliminate oxide layers caused by turbulence. *International Journal of Metalcasting*, 11(2), 328-339.
8. Janiszewski, K., & Kudliński, Z. (2006). The Influence of Non-Metallic Inclusions Physical State on Effectiveness of the Steel Filtration Process. *steel research international*, 77(3), 169-176.
9. Foseco Foundry International, (1999). SEDEX, the Ceramic Foundry Filter with Foam Structure. Staffordshire, England.
10. Hsu, F. Y., Jolly, M. R., & Campbell, J. (2009). A multiple-gate runner system for gravity casting. *Journal of Materials Processing Technology*, 209(17), 5736-5750.
11. Janiszewski, K. (2013). The slenderness ratio of the filter used in the process of liquid steel filtration as the additional parameter of the filter form. *steel research international*, 84(3), 288-296.
12. Ogawa, K., Kanou, S., & Kashihara, S. (2006). *Fewer Sand Inclusion Defects by CAE* (Vol. 52, No. 158, pp. 1-7). Komatsu Technical Report.
13. Hrabina, D. (2014). Effective Filtration of Steel Castings, 7th International Ankiros Foundry Congress, 11-13 September, Istanbul, Turkey
14. Jezierski, J., Dojka, R., & Jenerka K. (2017). Optimizing Gating System for Steel Castings, 5th International Conference on Modern Manufacturing Technologies in Industrial Engineering, 2017, 14-17
15. Zor, M. M., Kesim, S., Erbakan, B., Tülüçe, F., Yoloğlu, A., & Çakır, K. Ç. (2022). Direct pouring system design and optimization in steel castings. *Advanced Engineering Days (AED)*, 4, 111-115.



© Author(s) 2022. This work is distributed under <https://creativecommons.org/licenses/by-sa/4.0/>



Components used in the vulcanization of rubber

Ahmet Güngör*¹ 

¹Sabancı University, Materials Science and Nano Engineering, Türkiye, ahmet.gungor@sabanciuniv.edu

Cite this study: Güngör, A., (2022). Components used in the vulcanization of rubber. Engineering Applications, 1 (2), 132-136

Keywords

Rubber
Filler
Carbon black
Vulcanization
Compound

Review Article

Received: 27.09.2022
Revised: 26.10.2022
Accepted: 06.11.2022
Published: 14.11.2022



Abstract

Elastomers, which are rubber-based materials, are among the important raw materials used in the industry today, as they have a wide area of use in many sectors such as textile, food, livestock, armature, construction, etc., especially in the automotive industry. The business world, which is developing day by day with the advancement of technology, is rapidly consuming the raw materials we have, and unfortunately, our resources are gradually decreasing due to the fact that most of these raw materials are not recycled. For these reasons, it is of great importance to know the material used very well and to analyze its static, dynamic, thermal, physical, chemical, etc. properties according to their usage areas. In this study, the materials used during the preparation and vulcanization of rubber-based materials, which have a wide area of use in many sectors such as automotive, textile, food, livestock, armature, construction, and their intended use will be emphasized.

1. Introduction

The rubber compound is a recipe consisting of rubber polymers and other additional materials for the rubber to exhibit the desired properties in the industry. The successful functioning of rubber products depends on choosing the right polymers and mixing the rubber chemicals and fillers in the appropriate ratio. The mixture of materials selected for this purpose and providing proportional integrity with each other is called rubber recipe or rubber formula [1].

In the rubber mixture, a recipe is prepared so that the sum of the elastomer or elastomers is 100. All materials except elastomer are put on the prescription as "phr", which is defined as "parts per hundred of rubber" [2]. A rubber compound usually contains 40-50% by weight of the rubber polymer. The typical content of a mixture is given in Table 1 [1].

Table 1. Typical rubber composition

Amount of material (phr)	Quantity (phr)
Rubber	100
Fillers	20-100
Plasticizers	5-30
Vulcanization Agent	5-10
Accelerators	0-30
Activators	1-5
Antioxidants	1-3

The first usable rubber formulation was prepared by Charles Goodyear with NR rubber with cooking a sulfur [3]. In order to develop a rubber mixture, a material that can determine the necessary properties for the dough, knowledge of chemical mixture preparation, and experience in this regard are required [3].

A typical rubber mixture; rubber polymer, cooking materials that provide cross-linking, fillers used to reinforce and/or cheapen the mixture, plasticizers that give the dough softness in the processing process and then give it the desired flexibility and low temperature flexibility, protect the material from deterioration both during processing and during the use of the piece [4]. Stabilizers are added to the mixture according to the need and amount. The main purpose of rubber additives; to improve the properties of the material to be worked [4].

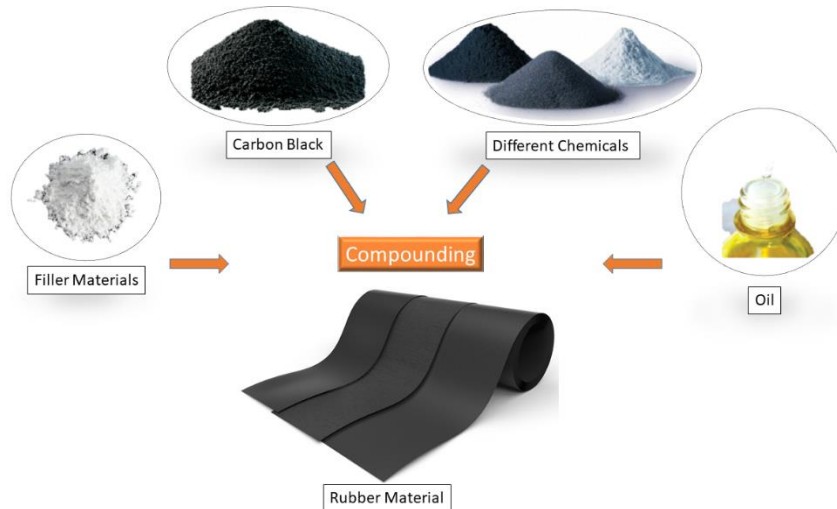


Figure 1. The scheme of rubber compounding

Added additives interact with the elastomer physically or chemically. Industrial applications will be limited as the mechanical and thermal properties of rubbers cannot be adequately provided without suitable fillers and additives [5].

While preparing a rubber mixture, it is expected to gain the following properties;

- ✓ In the environment where it will work as a finished product; mechanical, chemical, thermal, electrical, etc. to have the desired characteristics.
- ✓ Compliance with the processes, molds and machines to which the mixture will be applied during preparation, and vulcanization.
- ✓ The cost of the prepared mixture is competitive.

The additives that make up the rubber mixture are given, respectively [5].

1.1 Filler Materials

Filler materials are included in the rubber mixture for the aim of reinforcing the rubber, increasing its usability and improving its character, coloring the rubber, and making it economical. They can be organic or inorganic in nature. Fillers can be divided into two groups like black and white fillers. Black fillers are carbon blacks. White fillers are fillers such as calcium carbonate, silica, clay, talc, zinc oxide [6].

Black fillers give the rubber a strength that is incomparable with white fillers. The white fillers used in addition to the black fillers, on the other hand, give the rubber homogeneous mixing and lubrication properties thanks to the weak polar bonds between it and the rubber. In other words, the black fillers used in rubber improve the properties of the rubber, while the white fillers are mostly used to cheapen the formulation and improve the processing properties of the rubber [2].

Carbon black is an amorphous carbon in a semi-graphite structure, which, when mixed with rubber, increases the tensile strength, modulus, abrasion resistance and tear strength of rubber. Carbon black is obtained as a result of the thermal cracking of liquid and gaseous hydrocarbons [7]. Properties that determine the quality of carbon black as a reinforcing agent; grain size or surface area, structure and surface activity. In general, each of the carbon black properties affects the workability and the cured product. If the grain size is small, an increase in hardness, abrasion resistance, breaking strength and electrical conductivity, and a decrease in elasticity are observed in the products after vulcanization [8]. As the grain size increases, the surface activity decreases and the strengthening effect decreases. That is, the breaking force, tear, and abrasion resistance are reduced [9].

White fillers, on the other hand, are used in rubber technology to improve the physical or mechanical properties of the rubber mixture and to reduce the cost. These properties can be achieved by blending mineral fillers with carbon black or using light-colored products, alone or in combination with other fillers [10].

1.2. Plasticizers

Plasticizers are macromolecules with short-chain lengths compatible with the main polymer structure. It does not make chemical bonds with the polymer but settles between the macromolecular. Those that do not adapt well can migrate to the surface over time [11].

Plasticizers reduce the hardness and swelling properties of rubber, improves its low temperature flexibility by decreasing its glass transition temperature (T_g), and increases its resistance to the flame by increasing its electrical conductivity from its physical properties. At the same time, reducing the viscosity of the mixture, before curing; provides convenience in mixing and extrusion processes by ensuring the fluidity of the mixture. Thus, energy savings are provided in the processes. In addition, they facilitate the mixing in the formation of rubber dough and ensure that the added substances are mixed homogeneously [12].

1.3. Antioxidants

Aging causes changes in physical and mechanical properties. The greater the unsaturation rate in the polymer, the greater the susceptibility to aging [13]. Because they are sensitive to double bonds, oxygen, ozone and other reactive substances. Oxygen causes the polymer bonds to break down. In addition, they continue to react with sulfur and cause hardening. Continuation of polymerization or intermolecular cross-linking in synthetic rubbers can lead to hardening and brittleness [14]. High temperature can lead to various deteriorations even in oxygen-free environments, such as; thermal breakdown of crosslinks, intermolecular and intramolecular crosslinking or displacement of crosslinks. Sunlight increases the effect of oxygen and forms a film of oxidized rubber. This layer consists of grooves that join each other in random directions [15].

1.4. Vulcanization Agents

The aim of using vulcanizing agents is to create a network chain structure by providing cross-linking between polymer chains. Sulfur is used for the unsaturated polymer group, while peroxide is used for the saturated polymer group [16]. The most known and frequently used crosslinking agent is sulfur [16]. There are two types of sulfur use, normal and insoluble. Normal sulfur has an octet ring structure. Since it increases the solubility with temperature, it can cause pre-vulcanization in mixture storages before curing. Since it has the possibility of free circulation within the structure, its homogeneous distribution in the mixture may deteriorate over time. Insoluble sulfur, on the other hand, is amorphous and does not dissolve during storage, so there is no pre-vulcanization problem and a homogeneous distribution can be achieved in the mixture [17].

It is also widely used in peroxide and phenol-formaldehyde resins. Peroxide forms direct bonds to carbon chains forming carbon-carbon bonds. These bonds take more energy to break, which often results in higher service temperatures and lower permanent deformation in finished products. Some polymers can only be cross-linked with peroxides. Peroxide is faster but more expensive than the sulfur crosslinking agent. It is a special process in cross-linking with high radiation energy [18].

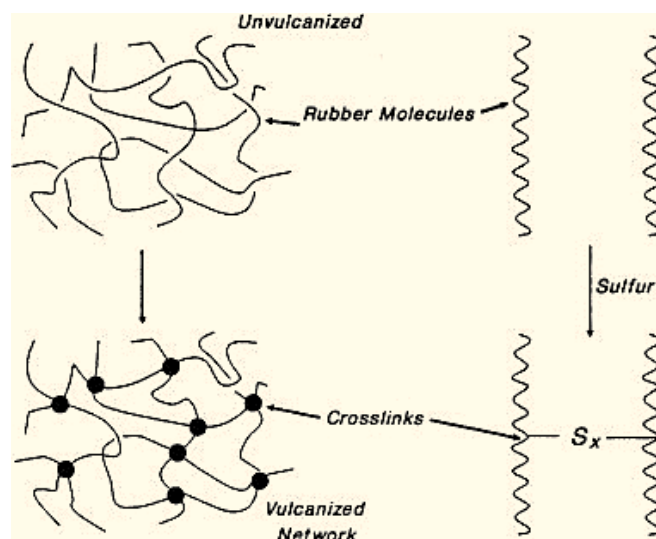


Figure 2. The formation of vulcanized rubber [19]

1.5. Accelerators and Activators

When using sulfur without accelerator in vulcanization, the crosslinking reaction rate will be slow. When sulfur and accelerator are used together, cooking occurs in a short time and economically. The resistance of the product to aging increases [20]. With the vulcanization method using the accelerator, the heat resistance, fatigue resistance, dynamic properties and aging properties of the rubber product are improved. Organic accelerators are used more as accelerators than inorganic accelerators. With the use of an accelerator, the crosslinking reaction is accelerated. Vulcanization is more economical [21,22].

Accelerators that accelerate vulcanization need organic substances. Activators are used to show the most efficient effect of accelerators. Metal oxide, fatty acids are examples of activators. Stearic acid can be used as an accelerator and softener activator in rubber. The activities of activators differ according to their types. One of the most important activators is zinc oxide. Stearic acid increases the solubility of zinc oxide in rubber [23,24].

2. Conclusion

Rubber, the use of which dates back many years, comes into our mix as a material that is needed more and more with the developing technology and especially the increasing automotive industry. In the world and in our country, rubber is used in many materials that make our daily life easier, both as a main and by-product. Increasing production potential, which is shaped according to consumer demand, is also becoming the focus of attention of investors in the chemical industry.

As mentioned in the study, there is an ongoing need for rubber for centuries and efforts to meet this need. It is important to know the preparation process and the used compositions of rubber, which is actively used in many fields today. It is extremely important to choose the components and their ratios according to the type of rubber used or to prepare a recipe for the area to be used. In this context, the preparation of rubber dough and knowing its vulcanization parameters increase its importance in terms of the production of products for the rubber industry.

Funding

This research received no external funding.

Conflicts of interest

The authors declare no conflicts of interest.

References

1. Vayyaprontavida Kaliyathan, A., Varghese, K. M., Nair, A. S., & Thomas, S. (2020). Rubber-rubber blends: A critical review. *Progress in Rubber, Plastics and Recycling Technology*, 36(3), 196-242.
2. Zhang, Y., Ge, S., Tang, B., Koga, T., Rafailovich, M. H., Sokolov, J. C., ... & Nguyen, D. (2001). Effect of carbon black and silica fillers in elastomer blends. *Macromolecules*, 34(20), 7056-7065.
3. Greene, J. P. (2021). Elastomers and Rubbers, in: Automot. Plast. Compos., William Andrew Publishing, 127-147.
4. Rodgers, B. (2020). Tire Engineering, Academic Press.
5. Ibrahim, A., & Dahlan, M. (1998). Thermoplastic natural rubber blends. *Progress in Polymer Science*, 23(4), 665-706.
6. Leblanc, J. L. (2002). Rubber-filler interactions and rheological properties in filled compounds. *Progress in polymer science*, 27(4), 627-687.
7. Plagge, J., & Lang, A. (2021). Filler-polymer interaction investigated using graphitized carbon blacks: Another attempt to explain reinforcement. *Polymer*, 218, 123513.
8. Khodabakhshi, S., Fulvio, P. F., & Andreoli, E. (2020). Carbon black reborn: Structure and chemistry for renewable energy harnessing. *Carbon*, 162, 604-649.
9. Fan, Y., Fowler, G. D., & Zhao, M. (2020). The past, present and future of carbon black as a rubber reinforcing filler-A review. *Journal of Cleaner Production*, 247, 119115.
10. Saad, A. L. G., & Younan, A. F. (1995). Rheological, mechanical and electrical properties of natural rubber-white filler mixtures reinforced with nylon 6 short fibers. *Polymer Degradation and Stability*, 50(2), 133-140.
11. Koltzenburg, S., M. Maskos, O. & Nuyken, (2017). Polymer chemistry, Springer Berlin Heidelberg.



12. Callister, W. D., & Rethwisch, D. G. (2018). *Materials science and engineering: an introduction* (Vol. 9, pp. 96-98). New York: Wiley.
13. Xie, H., Li, H., Lai, X., Wu, W., & Zeng, X. (2015). Synthesis of A Star-Shaped Macromolecular Antioxidant Based on β -Cyclodextrin and its Antioxidative Properties in Natural Rubber. *Macromolecular Materials and Engineering*, 300(9), 893-900.
14. Huangfu, S., Jin, G., Sun, Q., Li, L., Yu, P., Wang, R., & Zhang, L. (2021). The use of crude carbon dots as novel antioxidants for natural rubber. *Polymer Degradation and Stability*, 186, 109506.
15. Wu, W., Zeng, X., Li, H., Lai, X., & Xie, H. (2015). Synthesis and antioxidative properties in natural rubber of novel macromolecular hindered phenol antioxidants containing thioether and urethane groups. *Polymer Degradation and Stability*, 111, 232-238.
16. Akiba, M. A., & Hashim, A. S. (1997). Vulcanization and crosslinking in elastomers. *Progress in polymer science*, 22(3), 475-521.
17. Saputra, R., Walvekar, R., Khalid, M., Mubarak, N. M., & Sillanpää, M. (2021). Current progress in waste tire rubber devulcanization. *Chemosphere*, 265, 129033.
18. Wang M.-J., & Morris, M., (2021). Rubber Reinforcement Related to Tire Performance, Rubber Reinf. with Part. Fill., 394-507.
19. Ikeda, Y. (2014). Understanding network control by vulcanization for sulfur cross-linked natural rubber (NR). In *Chemistry, Manufacture and Applications of Natural Rubber* (pp. 119-134). Woodhead Publishing.
20. Coran, A. Y. (1965). Vulcanization. Part VII. Kinetics of sulfur vulcanization of natural rubber in presence of delayed-action accelerators. *Rubber Chemistry and Technology*, 38(1), 1-14.
21. Nieuwenhuizen, P. J. (2001). Zinc accelerator complexes.: Versatile homogeneous catalysts in sulfur vulcanization. *Applied Catalysis A: General*, 207(1-2), 55-68.
22. Zhong, B., Jia, Z., Luo, Y., & Jia, D. (2015). A method to improve the mechanical performance of styrene-butadiene rubber via vulcanization accelerator modified silica. *Composites Science and Technology*, 117, 46-53.
23. Ducháček, V., Kuta, A., & Příbyl, P. (1993). Efficiency of metal activators of accelerated sulfur vulcanization. *Journal of applied polymer science*, 47(4), 743-746.
24. Mostoni, S., Milana, P., Di Credico, B., D'Arienzo, M., & Scotti, R. (2019). Zinc-based curing activators: new trends for reducing zinc content in rubber vulcanization process. *Catalysts*, 9(8), 664.



© Author(s) 2022. This work is distributed under <https://creativecommons.org/licenses/by-sa/4.0/>



Development of individualized education system with artificial intelligence Fuzzy logic method

Hüseyin Fırat Kayıran ^{*1}, Ufuk Şahmeran ²

¹ARDSI, Mersin Provincial Coordination Unit, Mersin, Türkiye, huseyinfirat kayiran@tkdk.gov.tr

²Uskudar American Academy, Istanbul, Türkiye, usahmeran23@my.uaa.k12.tr

Cite this study: Kayıran, H. F., & Şahmeran, U. (2022). Development of individualized education system with artificial intelligence Fuzzy logic method. *Engineering Applications*, 1 (2), 137-144

Keywords

Artificial intelligence
Fuzzy logic
Algorithms
Mathematical modelling

Research Article

Received: 27.09.2022

Revised: 27.10.2022

Accepted: 06.11.2022

Published: 14.11.2022



Abstract

Within the scope of this study, an education system has been developed with mushroom management. Fuzzy logic systems considering the intellectual structure of people it is a collection of improved systems. Taking a 1 or 0 approach to any event instead, it is approached with certain degrees of membership. With Mamdani management, shapes AND OR institutions emerge to cover each different situation. In general; the questions they have shown before are intended to show difficult questions to difficult students with a fast and high accuracy rate, reducing the difficulty of the problem when they go to higher times and low accuracy rates. Graphs have been created for inputs and outputs. The degrees of openness of the inputs and outputs were calculated. Fuzzy logic can be used in different approaches.

1. Introduction

The Fuzzy Logic System can be considered as one of the computational Intelligent (CI) methods that are very complex. In the literature, it is used to represent nonlinear systems and problems that cannot be solved mathematically [1-2]. Artificial intelligence is very important nowadays. Coordinated studies in health, law and other departments, especially in the field of artificial intelligence and mechanics, are academicians by continuing. The topics discussed around artificial intelligence, the components are artificial neural networks, expert systems, fuzzy logic, genetic algorithms. There are many disciplines that adopt artificial intelligence. Some of them are computer engineering, philosophy, cognitive science, electronic sciences [3]. By giving importance to the study of intelligence automation with computers, the foundations of artificial intelligence were laid in the 1950s and 1960s, when the definition of intelligence and artificial intelligence was discussed, artificial intelligence gained usability in every field in the society we live in [4-5]. Artificial intelligence is the process by which the human brain, non-organic systems (computer, program, robot, etc.) Based on its functions. In short, artificial intelligence is a set of systems that think like a human, perceive like a human, interpret like a human, analyze like a human and make decisions like a human after all these stages. Scientists have defined artificial intelligence differently. For example, artificial intelligence is the science of computer programs that simulate intelligent behavior, and artificial intelligence is the science of converting things into machines that require intelligence when done by humans [6-7]. When the literature is scanned, it is possible to come across different studies with artificial intelligence and sub-branches. For example, in a study conducted; Student academic performance estimation was made by artificial intelligence using machine learning algorithms of students. At the end of the study; the decision tree algorithm gives the best accuracy rate with a maximum depth value of 2 for 649 student data. The random forest algorithm gives the best accuracy with 649 student data. The logistic regression algorithm was found to give the best accuracy with 395 student data [8]. In different studies, the importance of the development of artificial intelligence

in the field of food, epidemics and pandemics and its applicability in the field of health have been investigated. The literature findings were shared in the results section [9-11]. Intelligent tutoring systems (ITS) are also becoming more and more important today. ITS are used to stimulate one-to-one personal tutoring. ITS are generally used in large scale distance teaching situations, where there are hundreds of students and one-to-one teaching is impossible. ITS can choose a student's learning route and the content to teach them based on learner models, algorithms, and neural networks [12]. Research on ITS has two basic aims: to develop and test models regarding the cognitive processes involved in instruction, as well as to deliver complex instructional guidance on a one-to-one basis that is better than that obtained with traditional computer-aided programs and close to that of a skilled human tutor [13]. A study observed a huge and statistically significant increase in the learning outcomes with higher course completion rates and learning 2 to 2.5 times higher than students in other platforms and control groups [14]. Our study will be a new perspective to ITS by using fuzzy logic theorem.

2. Fuzzy Logic

In 1965, Fuzzy logic was mentioned in the work by Lotfi Askar Zadeh [15]. The concepts of fuzzy logic and fuzzy sets were first introduced in 1965 by Lotfi A. It is set out in an article published by Zadeh. Later, in his notes published in 1973, Zadeh proposed the idea that fuzzy set theory has a structure that can be modeled on the human decision-making system with the best approximation [16]. In classical logic, the limitations are certain, an element is either a member of a set or it is not. There is a logic of 0 and 1 in classical sets. In fuzzy logic, on the other hand, there is partial membership. In this way, it can operate in vague and approximate situations similar to human logic. Fuzzy logic is currently used in many fields such as the automotive industry, electronic control systems, and home electronics. Especially with the use of electrical appliances, energy has been saved and such tools have been smartened up [17]. An example fuzzy logic diagram is shown in Figure 1.

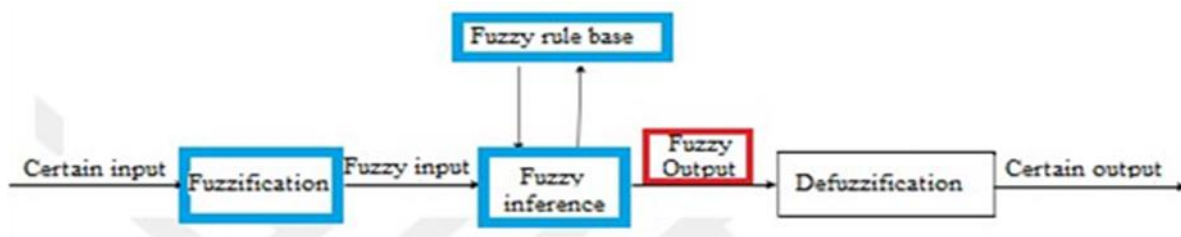


Figure 1. Operation of the fuzzy system fuzzy logic system [18]

3. Material and Method

The Mamdani approach can be considered as a very compatible thought structure with man [19]. The difficulty level of each problem in the study will be calculated by fuzzy logic. Two different inputs will be subjected to the rules and the difficulty level of the problem will give the output. Mamdani inference will be used in the study. When the student starts using the system, he will be shown 10 leveling questions, which are shown to everyone. These questions will be selected by educators and will consist of different difficulties. It is very important to have selective questions. According to the percentage of wrong / right that arise as a result of these questions and the time spent per question on these questions, the questions will begin to be shown to him according to his academic level. With each question it solves, the time and accuracy will be updated according to previous calculations. In this way, it is aimed to gradually increase the student's learning level by increasing the difficulty level. Two different inputs will be subjected to rules and will output the difficulty level of the problem. Mamdani inference will be used in the study. Figure 2 shows the graph of the general formula used in fuzzy logic calculations.

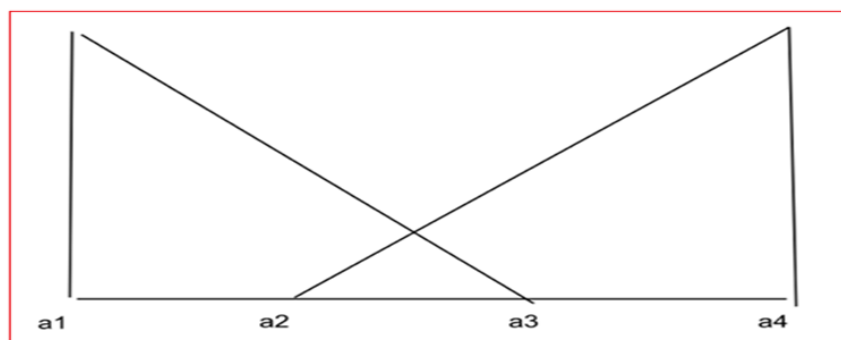


Figure 2. General formula used in fuzzy logic calculations

The formulas used in the study are listed below;

$$0 \quad x < a1 \quad (1)$$

$$\frac{x-a1}{a3-a1} \quad a1 \leq x \leq a2 \quad (2)$$

$$1 \quad x > a4 \quad (3)$$

Inputs are very important in fuzzy logic; the inputs determine the result of the functions. The inputs to be used in this study and their output are as follows:

Inputs: Average time to solve questions (x) and the accuracy rate (y) in the questions solved

Output: Difficulty level of the new questions (z)

x, y and z are time to solve the question, accuracy rate and difficulty of the question.

- Three explanatory variables are defined for the duration fuzzy set X: A1, A2 and A3 (low, medium and high)
- Two explanatory variables are defined for the accuracy rate fuzzy set Y: B1 and B2: (more and less)
- Three explanatory variables are defined for the difficulty fuzzy set Z: C1, C2 and C3: (low, normal and high)

The difficulty level of each problem in the study will be calculated by fuzzy logic. Two different inputs will be subjected to the rules and the difficulty level of the problem will give the output. Mamdani inference will be used in the study. When the student starts using the system, he will be shown 10 leveling questions, which are shown to everyone. These questions will be selected by educators and will consist of different difficulties. It is very important to have selective questions. According to the percentage of wrong / right that arise as a result of these questions and the time spent per question on these questions, the questions will begin to be shown to him according to his academic level. With each question it solves, the time and accuracy will be updated according to previous calculations. In this way, it is aimed to gradually increase the student's learning level by increasing the difficulty level. Fuzzy logic works according to certain rules. These rules use AND and OR functions. If the AND function is used, both conditions must be true. In the OR function, only one of the two conditions is true to give the output. The rules we use for Mamdani inference in this study are as follows:

IF x = A3 OR y = B1 THEN z = C1 IF time very OR low accuracy THEN difficulty low

IF x = A2 AND y = B2 THEN z = C2

IF x = A1 AND B2 THEN z = C3

Fuzzy operations work within the context of these rules. However, even if the verbal expression is as above, of course, these operations should have a numerical representation, only in this way we can make a calculation and obtain a numerical value. Using this numerical value, the difficulty level of the problem will be determined. Graphs are used to achieve this in fuzzy logic. Each rule written above has a separate graph. The membership degree of a value is calculated from the graphs and the numerical value of the output is calculated by using these rules above.

4. Results

The inputs were defined as the time to solve the questions and the accuracy rate of the questions. In the question solving time graph, the Y-axis shows the membership status, while the X-axis gives the time to solve the question in seconds. The graph of the students' question solving speed is given in [Figure 3](#).

In [Table 1](#), the degree of turbidity of the students' problem-solving speed is given.

In the accuracy rate graph, the Y axis shows the membership status, while the X axis gives the accuracy rate in percentage. In [Figure 4](#), a graph of the accuracy rate was given for the questions solved by the students.

[Figure 4](#) will be used to calculate the membership values in the table below. The membership values will be given out of hundred (like 70 instead of 0.7) for the case of simplicity. In [Table 2](#), the degree of fuzziness of the accuracy rate in the questions solved by the students.

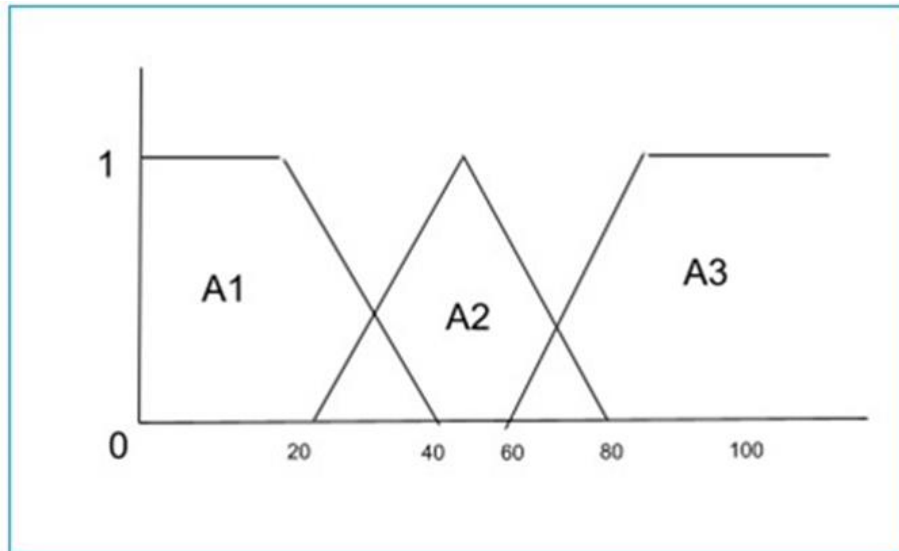


Figure 3. Students' question solving speed graph

Table1. The fuzziness degree of students' problem-solving speed

Time to solve the question (seconds)	Low(A1)	Medium(A2)	High(A3)
0	100	0	0
5	100	0	0
10	100	0	0
15	100	0	0
20	100	0	0
25	75	16.6	0
30	50	33.3	0
35	25	50	0
40	0	66.6	0
45	0	83.3	0
50	0	100	0
55	0	83.3	0
60	0	66.6	0
65	0	50	25
70	0	33.3	50
75	0	16.6	75
80	0	0	100
85	0	0	100
90	0	0	100
95	0	0	100
100	0	0	100

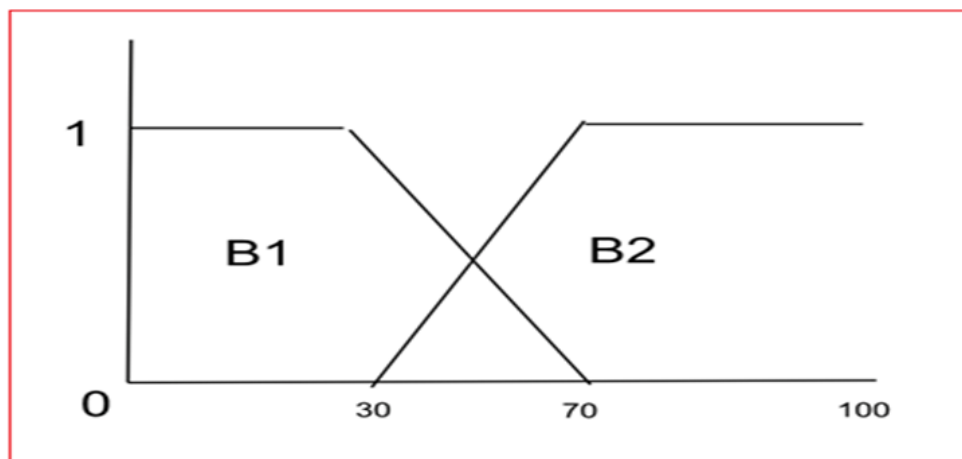


Figure 4. Accuracy rate graph in the questions solved by the students

Table 2. The fuzziness degree of the accuracy rate in the questions solved by the students

Correctness Rate	Low(B1)	High(B2)
0	100	0
5	100	0
10	100	0
15	100	0
20	100	0
25	100	0
30	100	0
35	87.5	12.5
40	75	25
45	62.5	37.5
50	50	50
55	37.5	62.5
60	25	75
65	12.5	87.5
70	0	100
75	0	100
80	0	100
85	0	100
90	0	100
95	0	100
100	0	100

The output is the difficulty level of the problem. In the difficulty level graph, the vertical axis shows the membership status, while the horizontal axis gives the difficulty level in percent. In Figure 5, the difficulty level graph of the questions given by the application as output is given.

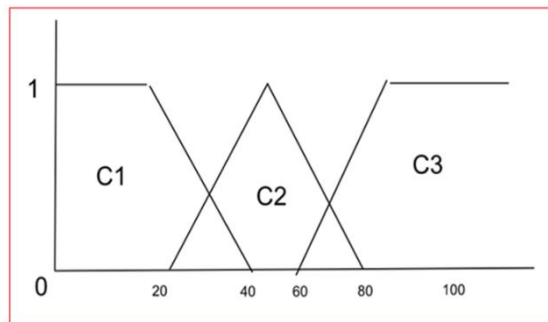


Figure 5. Difficulty level graph of the questions that the application gives as output

The Y axis shows the membership status, and the x axis shows the percentage of difficulty of questions.

Table 3. The degree of fuzziness of the questions that the application gives as output

The percentage of difficulty	Low (C1)	Medium (C2)	Hard (C3)
0	100	0	0
5	100	0	0
10	100	0	0
15	100	0	0
20	100	0	0
25	75	16,6	0
30	50	33.3	0
35	25	50	0
40	0	66.6	0
45	0	83.3	0
50	0	100	0
55	0	83.3	0
60	0	66.6	0
65	0	50	25
70	0	33.3	50
75	0	16.6	75
80	0	0	100
85	0	0	100
90	0	0	100
95	0	0	100
100	0	0	100

The corresponding membership status is looked from the right three columns, and the output is the percentage of difficulty that is obtained from the left column. The process will be explained by example cases. Example cases are given below.

Example Cases

Example 1: The average time per question of a student is 30 seconds and the accuracy rate is 80%. Looking at the question solving speed table, 30 seconds are seen as A1:50 and A2: 33.3. The higher one A1: 50 is accepted. The 80% accuracy rate corresponds to B2:100 when looking at the table. This situation obeys the rule IF $x = A1 \text{ AND } B2 \text{ THEN } z = C3$
Output C3:50 (AND function takes the minimum).
Looking at the value of 50 from the C3 table, questions from the question pool with 70% difficulty will be displayed.

Example 2: The average time per question of a student is 60 seconds and the accuracy rate is 65%. Looking at the question solving speed table, 60 seconds are seen as A1: 0 and A2: 66.6. The higher one, A2: 66.6 is accepted. 65% accuracy rate corresponds to B2:100 when looking at the accuracy rate able. This situation obeys the rule IF $x = A2 \text{ AND } B2 \text{ THEN } z = C2$
Output C2:66.6 (AND function takes the minimum).
Looking at the value of 66.6 from the C2 table, questions from the question pool with 60% difficulty will be displayed.

Example 3: The average time per question of a student is 75 seconds and the accuracy rate is 60%. Looking at the question solving speed table, 60 seconds are seen as A2: 16.6 and A3: 75. The higher one A3: 75 is accepted. The 60% accuracy rate corresponds to B2:100 when looking at the table. This situation obeys the rule IF $x = A3 \text{ OR } y = B1 \text{ THEN } z = C1$
Output C1: 100 (OR function takes the maximum).
Looking at the value of 100 from the C1 table, questions from the question pool with question difficulty between 0% and 20% will be displayed.

Example 4: The average time per question of a student is 25 seconds and the accuracy rate is 45%. Looking at the question solving speed table, 25 seconds are seen as A1: 75 and A2: 16.6. The higher one A1: 75 is accepted. The accuracy rate for 45% corresponds to B1: 62.5 and B2: 37.5 when looking at the table. The higher B1: 62.5 is accepted. This situation obeys the rule IF $x = A3 \text{ OR } y = B1 \text{ THEN } z = C1$
The output is C1: 75 (the OR function takes the maximum).
Looking at the value of 75 from the C1 table, questions from the question pool with a question difficulty of 25% will be displayed.

Example 5: The average time per question of a student is 60 seconds and the accuracy rate is 45%. Looking at the question solving speed table, 60 seconds is seen as A2: 66.6. The accuracy rate for 45% corresponds to B1: 62.5 and B2: 37.5 when looking at the table. The higher one B1: 62.5 is accepted. This situation obeys the rule IF $x = A3 \text{ OR } y = B1 \text{ THEN } z = C1$
Output C1: 66.6 (OR function takes the maximum).
Looking at the value of 66.6 from the C1 table, questions from the question pool with a question difficulty between 25% and 30% will be displayed.

Example 6: The average time per question of a student is 75 seconds and the accuracy rate is 35%. Looking at the question solving speed table, 25 seconds are seen as A2: 16.6 and A3: 75. The higher one A3: 75 is accepted. Looking at the table, the accuracy rate for 35% corresponds to B1:87.5 and B2: 12.5. The higher B1: 87.5 is accepted. This situation obeys the rule IF $x = A3 \text{ OR } y = B1 \text{ THEN } z = C1$
Output C1: 87.5 (OR function takes the maximum).
Looking at the value of 87.5 from the C1 table, questions from the question pool with a question difficulty of between 20% and 25% will be displayed.

5. Conclusion

The aim of this study is to create an individualized education system by applying the principle of fuzzy logic so that students can get maximum efficiency and add a new perspective to individual tutoring systems (ITS) by the use of fuzzy logic. The results obtained by the Mamdani method turned out to be feasible. At the end of the study, it was determined that the two important factors indicating that he is academically successful and that he has learned the subject completely are the accuracy rate in the questions and the time to solve the questions. Rules were created with fuzzy logic and these rules were poured into graphs and output was provided. The principle of operation of this program is illustrated by example cases. It has been determined that the program works as requested. With this study, it is believed that it can be used in classrooms, especially for students preparing for high school and university exams. It will also be useful in distance online learning environments, especially since it allows students to study on their own to a certain extent. Even though it may not completely eliminate the need for a real tutor, it will be useful for students who don't have access to tutoring all the time.

Acknowledgement

This study was partly presented at the 4th Advanced Engineering Days [20].

Funding

This research received no external funding.

Author contributions

Hüseyin Fırat Kayıran: Methodology, Validation, Editing. **Ufuk Şahmeran:** Visualization, Writing.

Conflicts of interest

The authors declare no conflicts of interest.

References

1. Eberhart, R. C. (1998, November). Overview of computational intelligence [and biomedical engineering applications]. In *Proceedings of the 20th Annual International Conference of the IEEE Engineering in Medicine and Biology Society. Vol. 20 Biomedical Engineering Towards the Year 2000 and Beyond (Cat. No. 98CH36286)* (Vol. 3, pp. 1125-1129). IEEE.
2. Zadeh, L. A. (1973). Outline of a new approach to the analysis of complex systems and decision processes. *IEEE Transactions on systems, Man, and Cybernetics*, (1), 28-44.
3. Pirim, A. G. H. (2006). YAPAY ZEKA. Yaşar Üniversitesi E-Dergisi, 1 (1), 81-93.
4. Luger, F. G. & William, A. (1993). Stubblefield, Artificial Intelligence: Structures and Strategies for Complex Problem Solving, 2nd ed. Harlow, England: Addison-Wesley.
5. Nilsson, N. J. (2009). *The quest for artificial intelligence*. Cambridge University Press.
6. Minsky, M. (1960). Steps towards artificial intelligence. Lexington, Lincoln Laboratory.
7. Brooks, R. A., (1991). Artificial intelligence without representation. Elsevier, 139-159.
8. Bastem, H. N., (2021). Prediction of student academic performance using artificial intelligence via machine learning algorithms, Çankaya University Enstitüsü of Sciences, Computer Engineering, Master's thesis.
9. Kayıran, H. F. (2022). Investigation of the applicability of artificial intelligence and machine learning in the field of health. *Advanced Engineering Days (AED)*, 3, 16-19.
10. Kayıran, H. F. (2020). Use of Artificial Intelligence in Food Engineering. In *4th International Mersin Symposium, Mersin*.
11. Kayıran, H. F., Gökalp, H. (2020). Epidemiology Artificial Intelligence (Robots) and Law. In *4th International Mersin Symposium, Mersin*.
12. Zawacki-Richter, O., Marín, V. I., Bond, M., & Gouverneur, F. (2019). Systematic review of research on artificial intelligence applications in higher education—where are the educators?. *International Journal of Educational Technology in Higher Education*, 16(1), 1-27.
13. Sedlmeier, P. (2001). *Intelligent Tutoring Systems*. ScienceDirect, Pergamon.
14. St-Hilaire, F., Vu, D. D., Frau, A., Burns, N., Faraji, F., Potochny, J., ... & Kochmar, E. (2022). A New Era: Intelligent Tutoring Systems Will Transform Online Learning for Millions. arXiv preprint arXiv:2203.03724.

15. Zadeh, L. A. (1965). Fuzzy sets. *Information and control*, 8(3), 338-353.
16. Güray, P., (2019). Control with Fuzzy Logic. guraysonugur.aku.edu.tr/wpcontent/uploads/sites/11/2019/03/BMK-Ders-2.pdf.
17. Drinker & Boiler (2007). Modeling the dishwasher with fuzzy logic. *Engineer and Machine*, 48(565), 3-8.
18. Yellow, M., Murat, Y., & Kirabali, M., (2005). Fuzzy Modeling Approach and Applications. *Journal of Scientific Reports-A*.
19. Chai, Y., Jia, L., & Zhang, Z. (2009). Mamdani model based adaptive neural fuzzy inference system and its application. *International Journal of Computer and Information Engineering*, 3(3), 663-670.
20. Kayıran, H. F., & Şahmeran, U. (2022). Development of individualized education system with artificial intelligence fuzzy logic method. *Advanced Engineering Days (AED)*, 4, 103-105.



© Author(s) 2022. This work is distributed under <https://creativecommons.org/licenses/by-sa/4.0/>



Provenance, petrographic and geochemical signatures of sandstones in Çalarasın Formation: A unit of ophiolitic melange in eastern of Kargı District

Cihan Yalçın ¹, Nurullah Hanilçi ², Mustafa Kumral ³, Mustafa Kaya ³

¹Ministry of Industry and Technology, General Directorate of Industrial Zones, Ankara, Türkiye, cihan.yalcin@sanayi.gov.tr

²İstanbul University-Cerrahpaşa, Geological Engineering, İstanbul, Türkiye, nhanilci@gmail.com

³İstanbul Technical University, Geological Engineering, İstanbul, Türkiye, kumral@itu.edu.tr; kayamusta@itu.edu.tr

Cite this study: Yalçın, C., Hanilçi, N., Kumral, M., & Kaya, M. (2022). Provenance, petrographic and geochemical signatures of sandstones in Çalarasın Formation: A unit of ophiolitic melange in eastern of Kargı District. *Engineering Applications*, 1 (2), 145-156

Keywords

Provenance
Geochemical
Sandstone
Çalarasın formation
Central Pontide

Research Article

Received: 28.09.2022

Revised: 28.10.2022

Accepted: 06.11.2022

Published: 14.11.2022



Abstract

Tectonic slices of different origins are observed in the eastern of Kargı (Çorum) district. These slices' metamorphic units and lithologies of ophiolitic melange are observed with tectonic contact. The Çalarasın formation is observed at the upper levels of the ophiolitic mélangé, which extends to the east of Kargı (Çorum) in the Central Pontides. The formation is composed of thin-bedded siltstone intercalated sandstone-shale and mudstone alternations. The sandstones of the formation include quartz, plagioclase, calcite, biotite, chlorite, and volcanic rock particles. The sandstones were analyzed for geochemical properties and provenance traces, respectively. According to these analyzes, SiO₂ % is found between 26.46-71.78%, Al₂O₃% 5.22-10.86, Fe₂O₃% 2.89-7.11 and CaO% 6.13-36.02 respectively. When trace elements are evaluated, Sc content ranges from 76.13-201.03 ppm, and Y content ranges from 9.54-55.11 ppm. Sandstones are rich in large ion lithophile elements (LIL; Ba, Th, U) and poor in high-field strength elements (HFS; Nb, Ti, Zr). Positive anomalies in terms of Pb and Y and negative ones in terms of Eu and P are observed in rocks. The sandstones are poor in terms of REE. The amount of HREE is substantially richer than the amount of LREE. Sandstones were normalized according to PAAS, and a distribution inversely proportional to the primitive values emerged. Ce/Ce* anomaly displays that the same oxygen environment has existed in the environment for a long time, but this situation has changed in the transition zone. Major oxide values suggest that the environment is arid and semi-arid media. It was determined that the sandstones were fed from the intermediate and mafic magmatic sources and tectonically represented the active continental margin and the island arc area.

1. Introduction

By acknowledging the geochemistry of sedimentary rocks, significant data can be obtained about the rocks' tectonic location, geochemical composition, origin, and source area [1-5]. In supplement, environmental interpretations can be represented by acknowledging petrographic characters. In these surveys, sandstones in sedimentary succession are usually preferred.

In the studies to figure out the tectonic origins of the basins, the current states of the most mobile and immobile elements are evaluated [6]. This is expressed by the values of both major oxides and trace elements. In particular, trace elements show the characteristics of the major source (tectonic environments and source-rock compositions) during weathering and transportation [2, 4, 7]. Rare earth elements are also used to characterize the source and tectonic environment of the sedimentation [8-11]. As a result of all these evaluations, interpretations are made corresponding to the geochemical data of the sedimentary rock. For example, elemental ratios such as La/Sc, La/Co, and Th/Sc are preferred for separating mafic and felsic source rocks [12]. It is noted that trace elements such as La and Th are more concentrated in felsic igneous rocks, while Co, Sc and Cr have

higher concentrations in mafic rocks [10-11, 13]. All accepted elemental analysis results are evaluated closely, and a sedimentary rock's origin and tectonic environment are interpreted.

Pontides were established as part of the Alpine-Himalayan belt by Ketin [14], and Okay et al. [15] separated it into Istanbul, Strandja, and Sakarya zones, respectively. The Pontides are geographically distributed as western, central, and eastern Pontides. Yilmaz et al. [16] stated that the Pontides are the orogenic belt related to the opening and closing of the Tethys Ocean in the northernmost part of Turkey. As a result of this tectonic movement, a submarine turbidite basin was formed in the Central Pontides during the Early Cretaceous [17].

The Central Pontides consist of metamorphic, magmatic, and sedimentary rock groups in the Late Paleozoic-Early Cenozoic age range along the 'suture zones' formed by the closure of the Paleo-Tethys and Neotethys oceans [18-25]. Ustaömer and Robertson [26] stated that the metamorphic rocks in the area they call the Domuzdağ-Saraycıkdağı complex in the region have undergone metamorphism in the blueschist facies and the regressive greenschist facies.

East of Kargı (Gökçedoğan), located in the Central Pontides, specific tectonostratigraphic sequences dwelling in lower and upper tectonic slices [27]. These slices are Pelitözü, Gölköy, and ophiolitic melange slices, respectively [28-29]. In the upper levels of the ophiolitic mélangé, the Çalarasın formation consists of sedimentary rocks. This paper highlights the provenance diagnosis and geotectonic environment interpretations of the sandstones of the Çalarasın formation by revealing the petrographic and geochemical studies.

2. Material and Method

Thin sections and geochemical analyzes of 7 samples collected from sandstones in the Çalarasın formation were performed in ITU-JAL. Geochemical analyzes consist of major oxide (Table 1), trace element (Table 2), and rare earth element values (Table 3). The analysis results obtained were evaluated in different diagrams. In addition, REE results were normalized according to PAAS (Table 4) and compared in the spider diagram. The analysis results in question are given in Table 1. In addition, the ratios and anomalies of critical elements for the diagnosis of geotectonic environment and provenance were determined.

2.1. Geological framework

The study area is located in a district where the Middle Jurassic and Cretaceous accretionary prism is still called the Central Pontides Supercomplex [30-32]. To the east of Kargı is the Middle Jurassic accretionary complex, which has the Kirazbaşı complex consisting of ophiolitic mélangé, and the Domuzdağ complex, whose metamorphic conditions change towards the north [33-34].

Autochthonous and allochthonous rock groups are observed together in the study area (Figure 1). Kunduz metamorphics are observed at the base of the region. This metamorphic unit is overlain by Permian aged Çamdağ and Jura-Cretaceous aged İnaltı formation with tectonic contact. In addition, in a large part of the study area, the lithologies of the Ophiolitic Melange overlie the Kunduz metamorphics with a tectonic contact. With these thrust contacts, tectonic slices were formed in the region [29]. On these slices, Beşpınar, Yedikır, and Ilgaz formations and Quaternary alluviums are observed with angular unconformity (Figure 1).

2.2. Ophiolitic melange

The Ophiolitic Melange of the Kirazbaşı complex consists of dunite and serpentinite at the base, spilitic lava, metadiabase, metabasalt, radiolarite, chert, mudstone, and pelagic limestones [33, 34] on the gabbro. At the top levels of the succession, there is the Çalarasın formation [35], which consists of alternating siltstone, sandstone, shale, and mudstone, respectively (Figure 2).

In addition, conglomerate-gravelly sandstone layers without lateral continuity are also observed in this unit. In the steep topography, whitish-grey, cream-colored medium-thick bedded limestone olistoliths of varying sizes are seen at different unit levels.

The sandstones observed in the vicinity of the Çalarasın district are brownish, reddish grey on the weathered surface, bright black in areas where the fresh fracture surface is altered, and brown and grey in localities where alteration is observed, unstable, medium-hard, fossil-free, poorly sorted and ungraded.

2.3. Petrography

In the thin section review of the sandstones in Beşpınar, it is recognized that there are many volcanic rock fragments in the rock. There are mainly quartz, plagioclase, calcite, and rock particles. Grains are medium well, rounded, poorly sorted, and ungraded. Quartz exists as monocrystalline. Calcite is in the matrix, and secondary quartz and iron oxide minerals are emplaced in its fractures and cracks. It was observed to be fed from volcanic rocks during the deposition (Figure 3).

Corresponding to Folk [36], the rock was determined as lithic arenite because the quartz content is less than 90%, the rock particle is more than feldspar, and the matrix ratio is less than 15%.

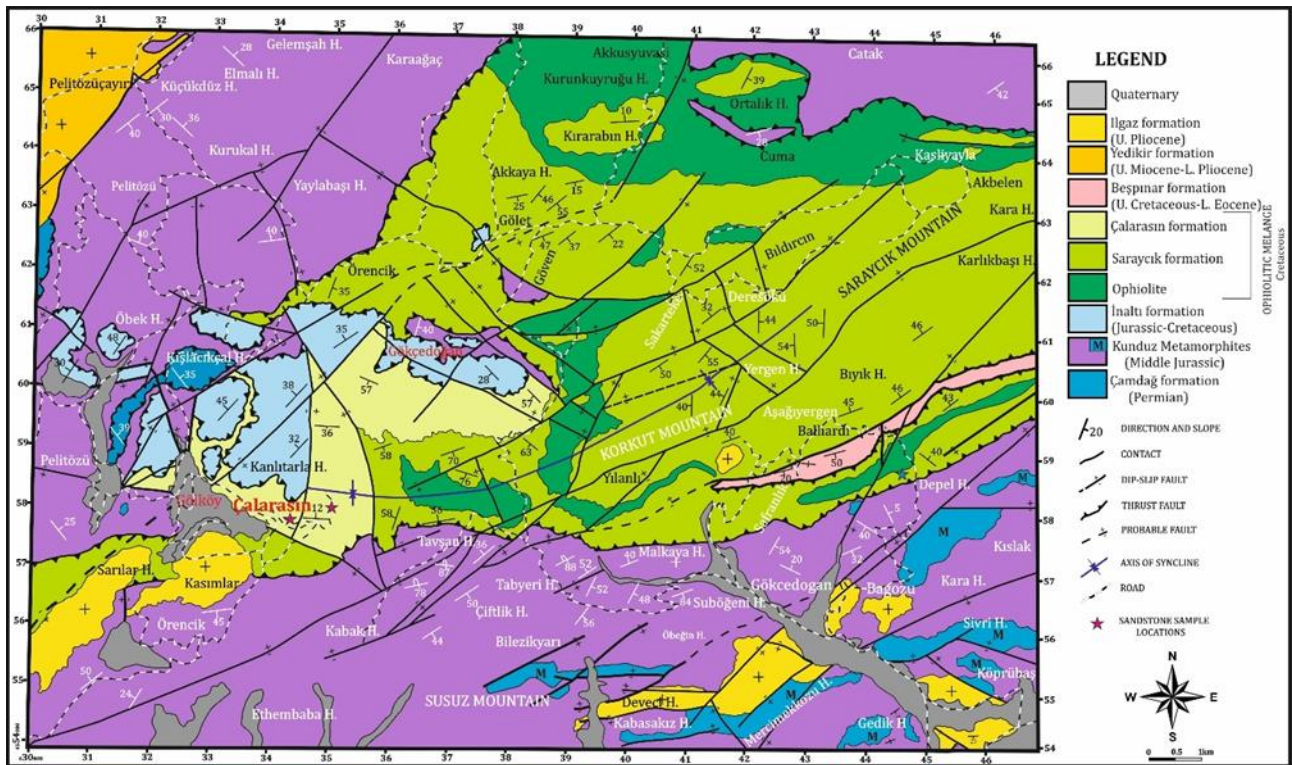


Figure 1. Geological map of the study area (Modified from Yalçın et al., [29])



Figure 2. General view of the Çalarasin formation (South to North View)

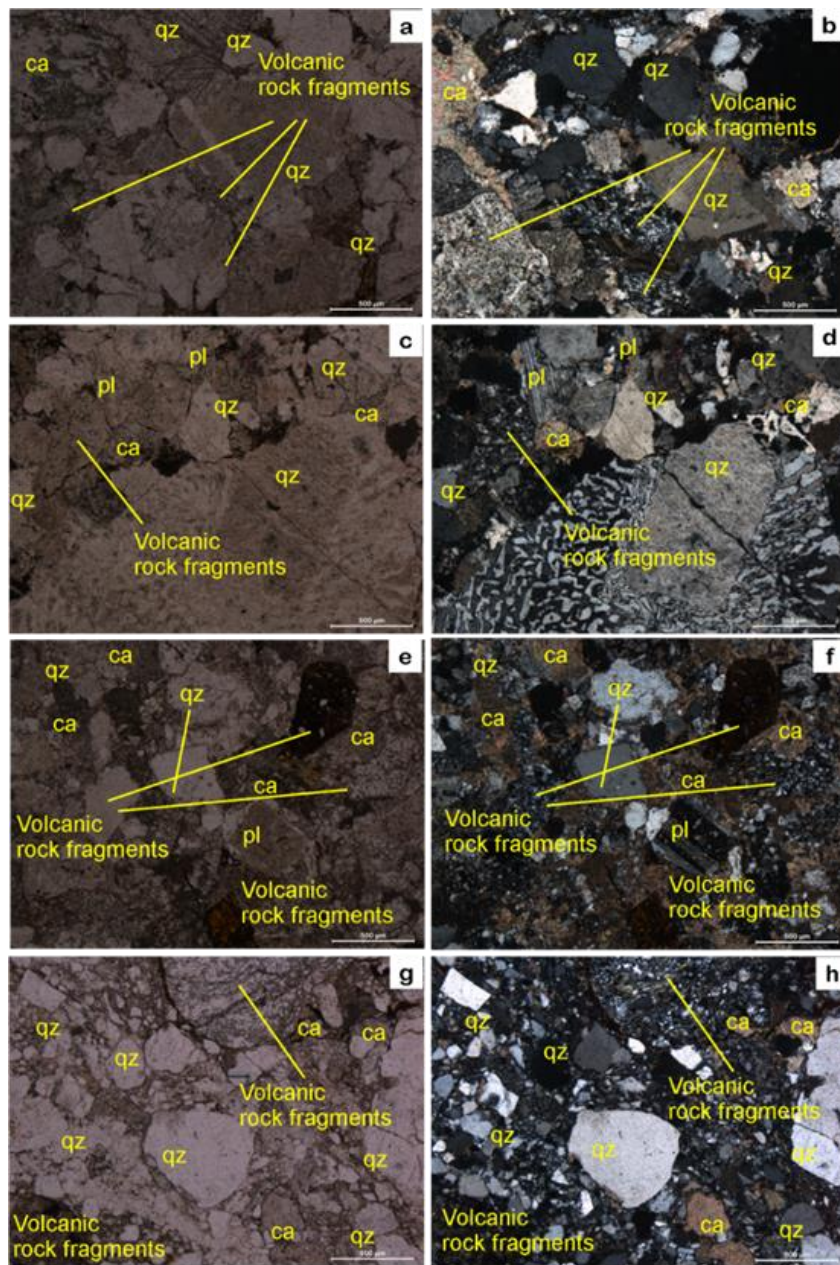


Figure 3. Polarizing microscope images of the sandstones of the Çalarasin formation Abbreviations: ca: calcite; qz: quartz; pl: plagioclase)

Table 1. Major oxides (%wt) concentrations of the sandstones

ROCK	Sandstone	Sandstone	Sandstone	Sandstone	Sandstone	Sandstone	Sandstone
SAMPLE	KGD-9	KGD-10	KGD-12	KGD-13	KGD-14	KGD-15	KGD-20
Latitude (°N)	34.630	34.600	34.606	34.630	34.630	34.630	34.606
Longitude (°E)	58.020	57.990	57.990	58.020	58.020	58.020	57.970
Major Oxides (%)							
SiO ₂	71,78	52,72	62,91	26,46	69,02	56,34	62,86
Al ₂ O ₃	9,22	6,45	10,18	6,71	5,22	7,10	10,86
Fe ₂ O ₃	2,89	3,13	5,55	1,77	3,55	3,45	7,11
MgO	1,09	0,89	1,86	0,76	0,77	1,15	2,67
CaO	6,13	20,43	9,55	36,02	13,22	18,52	6,80
Na ₂ O	3,28	1,54	2,68	0,69	0,55	2,12	2,76
K ₂ O	0,60	0,70	0,75	1,18	0,76	0,56	0,90
TiO ₂	0,27	0,26	0,35	0,32	0,30	0,22	0,59
P ₂ O ₅	0,09	0,10	0,10	0,06	0,09	0,05	0,08
MnO	0,05	0,37	0,09	0,07	0,05	0,24	0,11
Cr ₂ O ₃	0,00	0,00	0,00	0,01	0,01	0,00	0,00
LOI	4,41	13,2	5,82	25,76	6,34	10,05	5,03
Total	99,82	99,78	99,84	99,81	99,98	99,81	99,76

Table 2. Trace element concentrations (ppm) of the sandstones

ROCK	Sandstone	Sandstone	Sandstone	Sandstone	Sandstone	Sandstone	Sandstone
SAMPLE	KGD-9	KGD-10	KGD-12	KGD-13	KGD-14	KGD-15	KGD-20
Trace elements							
Sc	201,03	149,44	167,43	76,13	198,97	115,85	131,56
Y	55,11	11,76	11,47	15,83	10,01	14,16	9,54
Th	0,73	9,26	2,48	6,03	3,01	2,48	2,22
Li	23,88	38,81	35,14	11,65	27,72	27,40	40,02
Be	1,57	0,89	0,85	1,90	1,09	1,52	1,31
Co	39,98	13,49	15,60	30,59	12,25	18,18	15,39
Ni	61,88	61,27	27,48	35,99	18,85	36,41	51,95
Cu	69,70	0,00	0,00	0,00	0,00	0,00	0,00
Zn	369,21	0,00	0,00	0,00	0,00	0,00	0,00
Ga	22,50	20,06	14,66	11,97	7,78	11,77	24,71
As	39,93	42,54	37,15	42,72	32,58	32,89	33,02
Se	16,15	38,02	4,41	18,96	0,00	10,46	0,00
Rb	16,38	21,70	18,69	46,46	20,66	16,13	17,17
Sr	298,92	246,47	101,17	237,35	148,96	224,09	97,19
Ag	8,71	3,26	0,76	0,81	0,51	0,49	0,85
Cd	0,51	0,18	0,00	0,46	0,03	0,09	0,00
In	0,42	0,60	0,20	0,15	0,07	0,00	0,08
Cs	2,03	0,85	0,57	2,37	0,71	0,35	0,41
Ba	134,32	461,23	199,42	137,94	89,08	171,43	541,86
Tl	0,24	0,03	0,08	0,26	0,04	0,05	0,03
Pb	37,88	0,00	0,00	120,80	0,23	13,49	28,00
U	0,00	1,36	0,58	2,79	0,79	0,64	0,68
Au	0,09	0,02	0,04	0,06	0,03	0,03	0,02
Hf	8,57	1,29	0,99	0,23	0,81	0,81	1,17
Ir	0,07	0,01	0,03	0,01	0,01	0,02	0,02
Pd	1,09	2,61	1,83	0,57	1,84	1,47	2,29
Pt	0,12	0,02	0,02	0,00	0,01	0,04	0,02
Rh	0,07	0,05	0,03	0,05	0,04	0,05	0,04
Ru	0,06	0,23	0,18	0,15	0,21	0,23	0,22
Sb	0,50	3,14	0,86	2,07	0,86	2,90	3,58
Sn	1,73	1,16	1,07	1,52	1,03	0,92	1,14
Te	0,01	0,07	0,12	0,04	0,05	0,06	0,09

3. Geochemistry

As a result of the analysis, the %SiO₂ changes of the sandstones in the Çalarasın formation are between 26.46-71.78. It is recognized that the example with low SiO₂ content is carbonate-rich carbonate sandstone. In petrographic studies, it has been determined that sandstones are usually carbonate cemented and rich in volcanic rock particles. Al₂O₃ values range between 5.22-10.86%, Fe₂O₃ values between 2.89-7.11%, and CaO values between 6.13-36.02%. There is no significant difference in the samples regarding Na₂O, K₂O, P₂O₅, TiO₂, and MnO, respectively. When trace elements are evaluated, it is seen that the Ba, Sc, and Sr ratios of the samples are high. It is seen that the Ba content reaches up to 541.86 ppm. Sc content varies between 76.13-201.03 ppm, and Sr content ranges between 97.19-298.92 ppm.

According to the chondrite normalized trace element spider diagram of the sandstones [37], it is observed that there is enrichment with large ion lithophile elements (LILE; Ba, Th, U) (Figure 4). Elements with high-field strength elements (HFSE; Nb, Ti, Zr) show depletion. Positive Pb and Y anomalies are observed in the rocks. A negative anomaly is observed in terms of Eu and P. The enrichment in Th indicates that heavy minerals containing Th are situated in the volcanic rock particle.

A Rare Earth Element (REE) spider diagram [38] normalized to the Chondrite of sandstones was prepared (Figure 5). At the same time, the values normalized according to PAAS are shown in the same diagram. According to the diagram, enrichment by Light Rare Earth Elements (LREE; La, Ce, Pr, Nd) and a horizontal and near-

horizontal distribution was observed for Heavy Rare Earth Elements (HREE; Er, Tm, Yb, Lu) for sandstones. There is a negative anomaly in terms of Eu content. However, the values normalized according to PAAS show an inverse proportional distribution compared to the normalized values (Figure 5).

Table 3. REE concentrations (ppm) and some ratios of the sandstones

ROCK	Sandstone	Sandstone	Sandstone	Sandstone	Sandstone	Sandstone	Sandstone
SAMPLE	KGD-9	KGD-10	KGD-12	KGD-13	KGD-14	KGD-15	KGD-20
Rare Earth Elements							
La	6,81	10,56	7,42	11,69	8,05	8,11	5,61
Ce	20,59	21,24	15,32	22,89	16,30	15,24	11,92
Pr	3,50	2,34	1,85	2,89	2,11	1,78	1,46
Nd	18,88	9,23	7,43	11,03	8,63	7,18	5,99
Sm	6,44	2,47	2,06	2,33	2,12	1,85	1,92
Eu	2,15	0,83	0,60	0,51	0,57	0,52	0,68
Gd	9,72	3,14	2,73	2,81	2,85	2,62	2,20
Tb	1,62	0,38	0,36	0,37	0,35	0,36	0,30
Dy	10,71	2,11	2,10	2,30	1,87	2,30	1,75
Ho	2,26	0,42	0,45	0,50	0,38	0,50	0,38
Er	6,79	1,14	1,27	1,59	1,00	1,50	1,11
Tm	0,97	0,16	0,19	0,23	0,13	0,22	0,16
Yb	6,14	1,03	1,23	1,54	0,82	1,44	1,08
Lu	0,92	0,16	0,20	0,24	0,12	0,22	0,18
Σ REE	97,49	55,23	43,22	60,90	45,30	43,84	34,74
Σ LREE	58,36	46,67	34,70	51,33	37,78	34,67	27,58
Σ HREE	39,13	8,56	8,53	9,58	7,52	9,17	7,15
Ce/Ce*	0,31	0,74	0,65	0,76	0,64	0,70	0,59
Eu/Eu*	1,26	1,40	1,19	0,93	1,08	1,11	1,55
Th/Sc	0,00	0,06	0,01	0,08	0,02	0,02	0,02
La/Sc	0,10	1,25	0,58	0,78	0,21	0,80	2,14
La/Co	0,30	7,31	2,65	3,65	1,18	2,98	10,94
Th/Co	4,31	7,43	6,06	5,66	7,54	5,27	5,85
Ba/Sc	0,33	0,20	0,22	0,20	0,21	0,25	0,20
Ba/Co	0,93	1,17	1,03	0,95	1,19	0,94	1,02

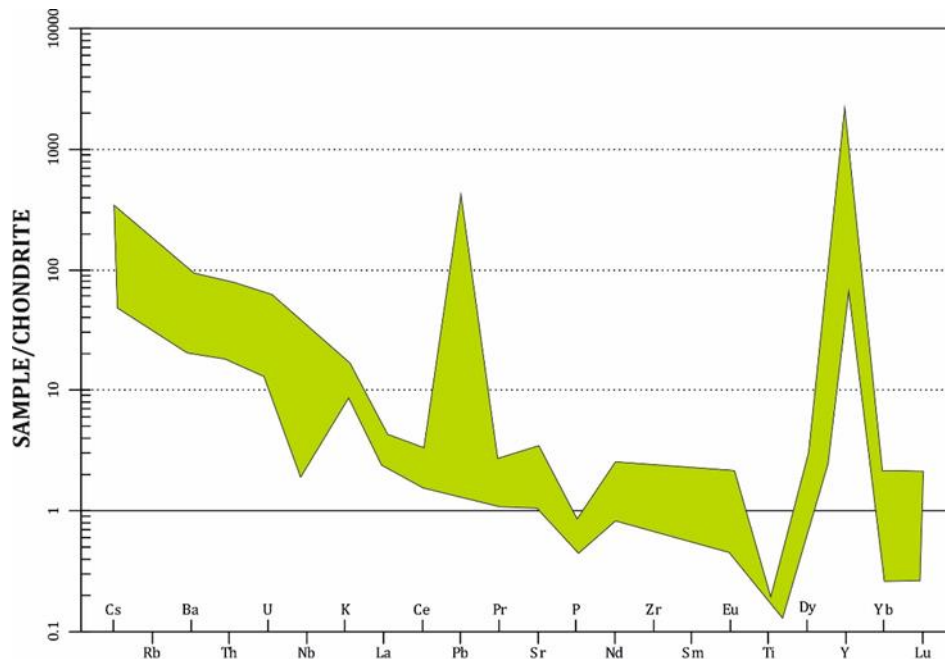


Figure 4. Spider diagram of chondrite-normalized trace and REE elements

Table 4. PAAS normalized REE concentrations (ppm) of the sandstones

ROCK	Sandstone	Sandstone	Sandstone	Sandstone	Sandstone	Sandstone	Sandstone
SAMPLE	KGD-9	KGD-10	KGD-12	KGD-13	KGD-14	KGD-15	KGD-20
La	0,178	0,276	0,194	0,306	0,211	0,212	0,147
Ce	0,259	0,267	0,192	0,288	0,205	0,192	0,150
Pr	0,396	0,265	0,210	0,327	0,239	0,201	0,166
Nd	0,557	0,272	0,219	0,325	0,255	0,212	0,177
Sm	1,161	0,445	0,372	0,420	0,382	0,333	0,346
Eu	1,987	0,773	0,560	0,472	0,529	0,485	0,633
Gd	2,085	0,674	0,585	0,603	0,612	0,562	0,472
Tb	2,098	0,495	0,461	0,473	0,449	0,468	0,386
Dy	2,287	0,452	0,449	0,492	0,400	0,492	0,374
Ho	2,276	0,426	0,454	0,501	0,382	0,502	0,380
Er	2,384	0,401	0,447	0,558	0,352	0,527	0,388
Tm	2,395	0,404	0,472	0,576	0,333	0,538	0,396
Yb	2,176	0,365	0,437	0,546	0,290	0,512	0,383
Lu	2,135	0,373	0,451	0,553	0,270	0,513	0,413

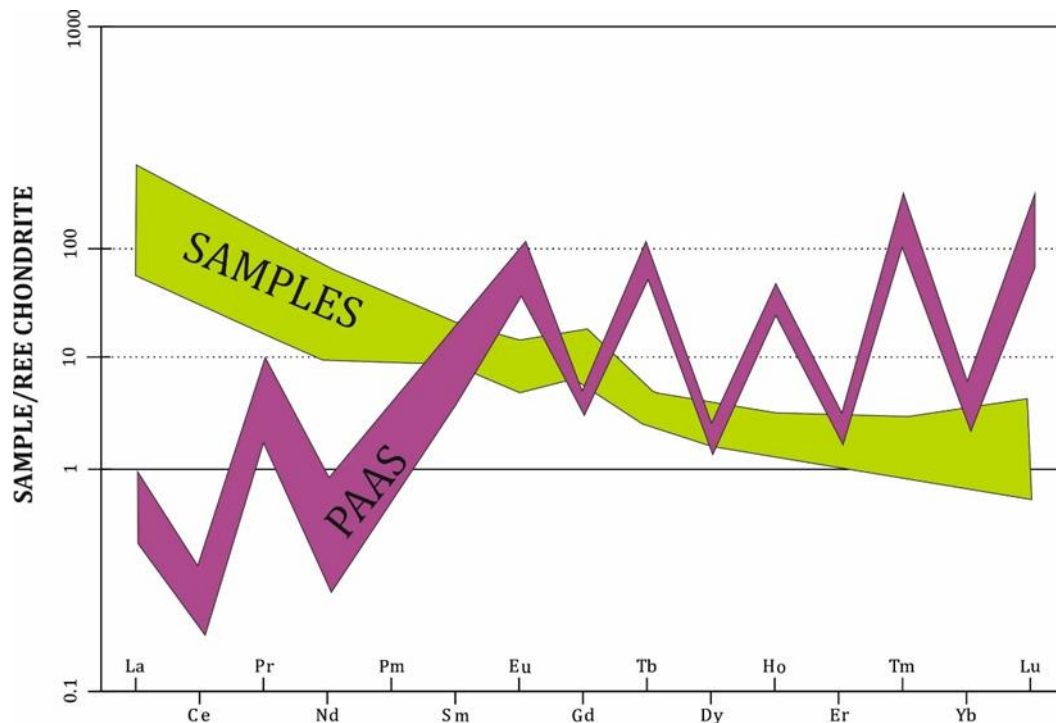


Figure 5. Spider diagram of chondrite and PAAS normalized REE elements

Ce anomaly is a parameter used to determine the redox conditions of the environment [39]. Ce is found in trivalent terrestrial sedimentary and igneous rocks [40]. In addition, different cations of Ce are found in seawater in anoxic or suboxic environments [41]. According to these Ce values, the environment can be interpreted. A diagram was prepared to reveal the Ce anomalies of the sandstone (Figure 6). According to this diagram, it can be said that although the amount of oxygen in the deposition environment remains the same for a long time, there is some change in the transition zone.

4. Provenance

To reveal the provenance traces of the sandstones, the diagram was prepared using the main oxide values [42]. According to the prepared diagram, it was determined that the sandstones were fed from intermediate and mafic magmatic sources (Figure 7).

To determine the geotectonic environment of the sandstones, a change diagram based on the first and second differentiation functions proposed by Bhatia [1] was prepared (Figure 8). According to the prepared diagram, 3 of the samples fall in the passive margin area, 3 in the continental arc area, and 1 in the island arc area.

According to the diagram of Suttner and Dutta [43], which was prepared according to the major oxide values, the rocks were formed in semi-arid and arid environment conditions (Figure 9). 1 sample reflects the humid environmental conditions.

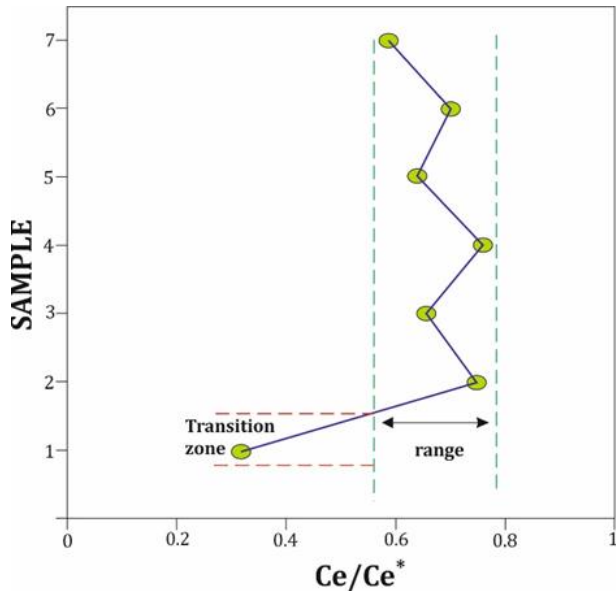


Figure 6. Ce anomaly variations of sandstones

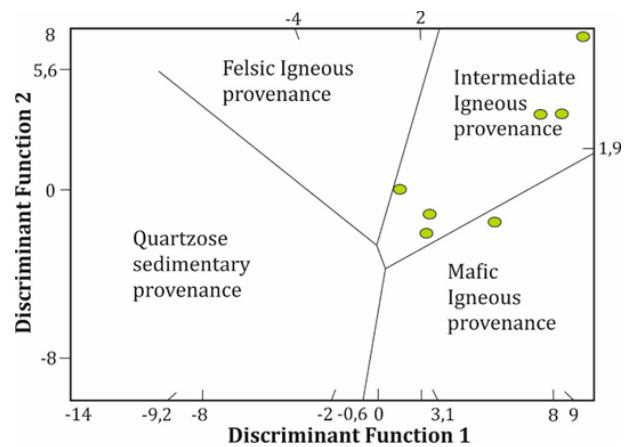


Figure 7. Geotectonic discrimination diagram for the provenance of sandstones by major elements [42]

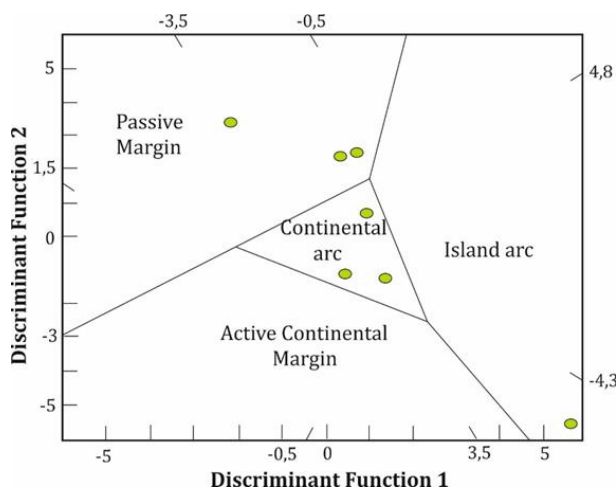


Figure 8. F1-F2 discriminant function diagram of sandstones [1]

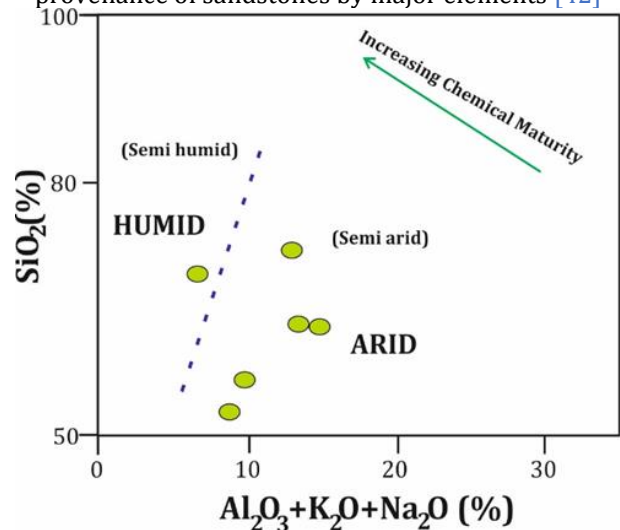


Figure 9. Chemical maturity of sandstone [43]

For sandstones, most of the samples examined in the $(\text{Fe}_2\text{O}_3+\text{MgO})-\text{TiO}_2$ diagram [1] are distributed outside the defined areas (Figure 10a). Only one specimen is located in the active continental margin area. In the $(\text{Fe}_2\text{O}_3+\text{MgO})-(\text{Al}_2\text{O}_3/\text{SiO}_2)$ diagram [1], many samples fall into the active continental margin area (Figure 10b). In the La/Th variation diagram developed by Bhatia and Crook [2], the samples fall into the island arc area (Figure 10c), and in the Th-Co-Zr/10 diagram (Figure 10d), the samples fall into the island arc area.

Th and Sc are important and useful elements in provenance interpretations [8]. In addition, Eu anomalies have a critical role in the diagnosis of provenance. For this reason, Eu anomaly and compositional variations [44] of magmatic origin rocks were evaluated together in the Th/Sc diagram [45] (Figure 11). It has been determined that some of the sandstones exhibit a similar distribution to the basaltic composition and some present different characteristics. In addition, strategically important La/Sc, La/Co, Th/Co, Ba/Sc, Ba/Co, and Th/Sc ratios were determined and correlated according to the compositional variations of granitic and volcanic rocks [44]. These data show that the sandstones are fed from basaltic composition, but some are from rocks of different characteristics.

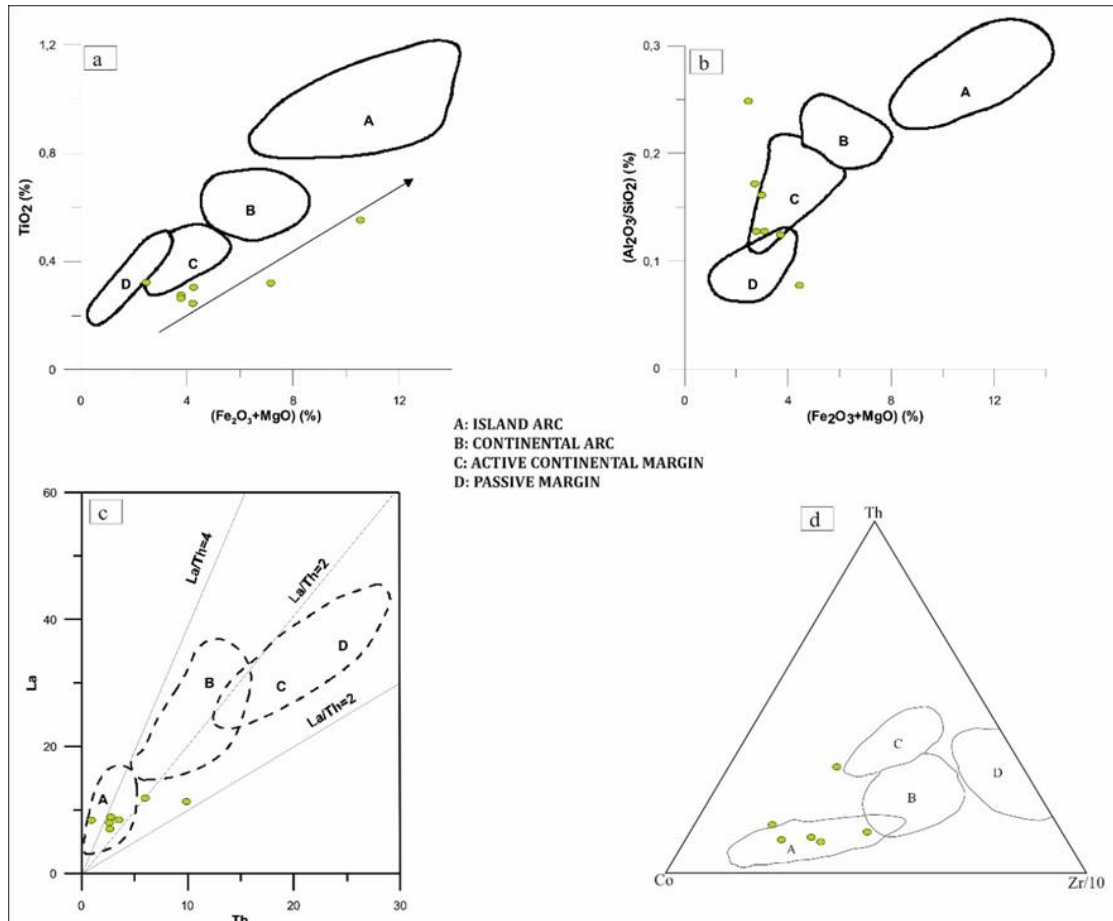


Figure 10. Geotectonic diagrams of sandstones

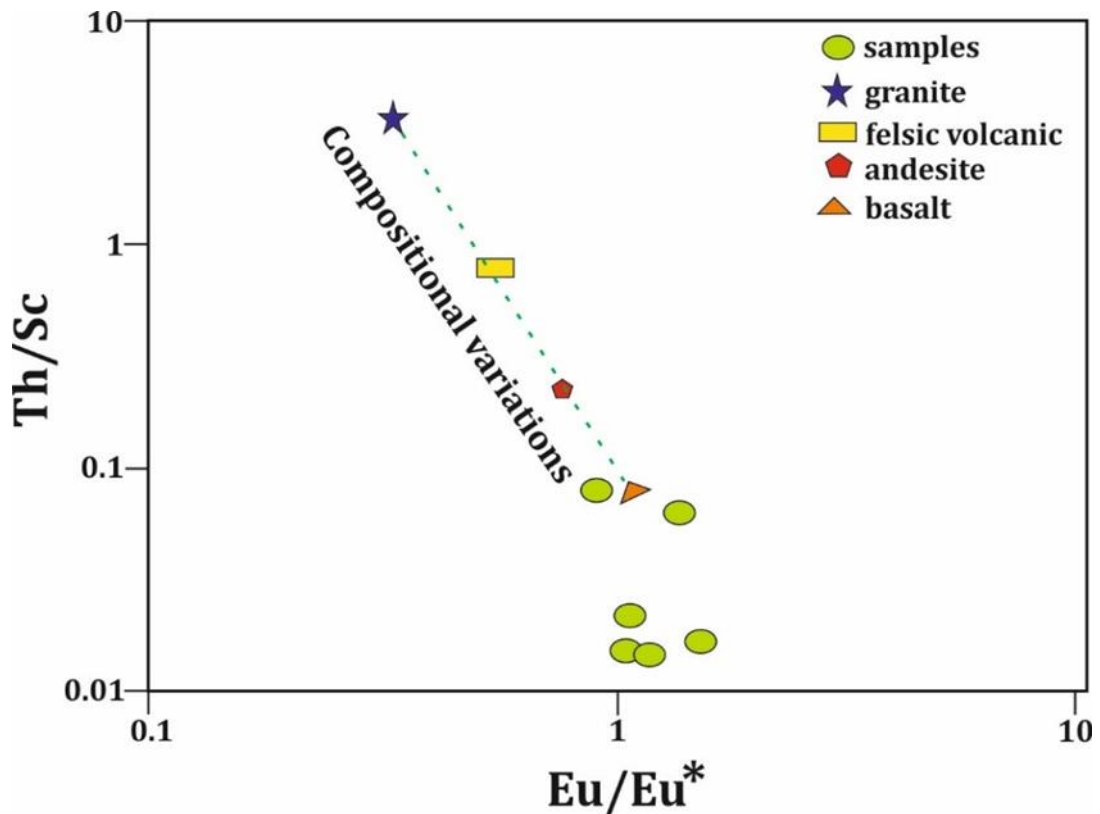


Figure 11. Chemical Eu/Eu^* - Th/Sc binary diagram [46]

5. Conclusion

The petrographic and geochemical properties of the sandstones, which are located in a very complex area and represent the upper levels of the lithologies belonging to the ophiolitic melange, have been revealed. As a result of the study, it was determined that the sandstones defined as lithic arenite were fed from intermediate and mafic magmatic sources and concentrated in the tectonically active continental area and island arc area.

When sandstones poor in REE are normalized according to PAAS, a distribution inversely proportional to the primary situation emerges. Ce anomaly shows that the same oxygen environment has existed in the environment for a long time, but this situation has changed somewhat in the transition zone.

In the $\text{SiO}_2\text{-Al}_2\text{O}_3\text{+Na}_2\text{O+K}_2\text{O}$ diagram, it was determined that the environment was arid and semi-arid. The amount of HREE is considerably higher than the amount of LREE. La/Sc, La/Co, Th/Co, Ba/Sc, Ba/Co, and Th/Sc ratios, which have critical roles in provenance studies, were determined and compared with the compositions of granitic and volcanic rocks. According to these results, it has been determined that the sandstones reflect a unique characteristic. Isotope studies should be done for more detailed interpretations.

Acknowledgement

This study is part of a Ph.D. thesis prepared in the Graduate School of Science and Engineering of İstanbul University and supported by TUBITAK project no: 113Y536. This study was partly presented at the 4th Advanced engineering Days [47] on 21 September 2022.

Funding

This research received no external funding.

Author contributions:

Cihan Yalçın: Writing-Reviewing and Editing, Geology, Methodology, Geochemistry. **Nurullah Hanilçi:** Editing, Geochemistry. **Mustafa Kumral:** Petrography, **Mustafa Kaya:** Petrography, XRF/ICP-MS

Conflicts of interest

The authors declare no conflicts of interest.

References

1. Bhatia, M. R. (1983). Plate tectonics and geochemical composition of sandstones. *The Journal of Geology*, 91(6), 611-627.
2. Bhatia, M. R., & Crook, K. A. (1986). Trace element characteristics of graywackes and tectonic setting discrimination of sedimentary basins. *Contributions to mineralogy and petrology*, 92(2), 181-193.
3. Roser, B. P., & Korsch, R. J. (1988). Provenance signatures of sandstone-mudstone suites determined using discriminant function analysis of major-element data. *Chemical geology*, 67(1-2), 119-139.
4. McLennan, S. M. (2018). Rare earth elements in sedimentary rocks: influence of provenance and sedimentary processes. In *Geochemistry and mineralogy of rare earth elements* (pp. 169-200).
5. Armstrong-Altrin, J. S., & Verma, S. P. (2005). Critical evaluation of six tectonic setting discrimination diagrams using geochemical data of Neogene sediments from known tectonic settings. *Sedimentary Geology*, 177(1-2), 115-129.
6. Armstrong-Altrin, J. S., Lee, Y. I., Verma, S. P., & Ramasamy, S. (2004). Geochemistry of sandstones from the Upper Miocene Kudankulam Formation, southern India: implications for provenance, weathering, and tectonic setting. *Journal of sedimentary Research*, 74(2), 285-297.
7. Condie, K. C., Boryta, M. D., Liu, J., & Qian, X. (1992). The origin of khondalites: geochemical evidence from the Archean to early Proterozoic granulite belt in the North China craton. *Precambrian Research*, 59(3-4), 207-223.
8. Taylor, S. R., & McLennan, S. M. (1985). The continental crust: its composition and evolution: an examination of the geological record preserved in sedimentary rocks. Oxford, U.K., Blackwell, 328 pages.
9. Wronkiewicz, D. J. (1989). Geochemistry and provenance of sediments from the Pongola Supergroup, South Africa: evidence for a 3.0-Ga-old continental craton. *Geochimica et Cosmochimica Acta*, 53(7), 1537-1549.
10. Wronkiewicz, D. J., & Condie, K. C. (1987). Geochemistry of Archean shales from the Witwatersrand Supergroup, South Africa: source-area weathering and provenance. *Geochimica et Cosmochimica Acta*, 51(9), 2401-2416.

11. Wronkiewicz, D. J., & Condie, K. C. (1990). Geochemistry and mineralogy of sediments from the Ventersdorp and Transvaal Supergroups, South Africa: cratonic evolution during the early Proterozoic. *Geochimica et Cosmochimica Acta*, 54(2), 343-354.
12. Tijani, M. N., Nton, M. E., & Kitagawa, R. (2010). Textural and geochemical characteristics of the Ajali Sandstone, Anambra Basin, SE Nigeria: implication for its provenance. *Comptes Rendus Geoscience*, 342(2), 136-150.
13. Ronov, A. B., Balashov, Y. A., Girin, Y. P., Bratishko, R. K., & Kazakov, G. A. (1974). Regularities of rare-earth element distribution in the sedimentary shell and in the crust of the earth. *Sedimentology*, 21(2), 171-193.
14. Ketin, İ. (1966). Tectonic units of Anatolia (Asia minor). *Bulletin of the Mineral Research and Exploration*, 66(66), 24-34.
15. Okay, A. I., Celal Sengor, A. M., & Görür, N. (1994). Kinematic history of the opening of the Black Sea and its effect on the surrounding regions. *Geology*, 22(3), 267-270.
16. Yılmaz, Y., Tüysüz, O., Yigitbas, E., Genç, S.C. & Şengör, A.M.C., (1997). Geology and tectonic evolution of the Pontides, in Robinson, A.G. (ed). Regional and Petroleum Geology of the Black Sea and Surrounding Region, vol. 68. Bulletin of American Association Petroleum Geology, pp. 183-226.
17. Akdoğan, R., Okay, A. I., Sunal, G., Tari, G., Meinhold, G., & Kylander-Clark, A. R. (2017). Provenance of a large Lower Cretaceous turbidite submarine fan complex on the active Laurasian margin: Central Pontides, northern Turkey. *Journal of Asian Earth Sciences*, 134, 309-329. <https://doi.org/10.1016/j.jseaes.2016.11.028>.
18. Robertson, A. H. (2002). Overview of the genesis and emplacement of Mesozoic ophiolites in the Eastern Mediterranean Tethyan region. *Lithos*, 65(1-2), 1-67.
19. Robertson, A. H., & Ustaömer, T. (2004). Tectonic evolution of the Intra-Pontide suture zone in the Armutlu Peninsula, NW Turkey. *Tectonophysics*, 381(1-4), 175-209.
20. Robertson, A. H., Ustaömer, T., Parlak, O., Ünlügöç, U. C., Taşlı, K., & Inan, N. (2006). The Berit transect of the Tauride thrust belt, S Turkey: Late Cretaceous–Early Cenozoic accretionary/collisional processes related to closure of the Southern Neotethys. *Journal of Asian Earth Sciences*, 27(1), 108-145.
21. Okay, A. I., Tüysüz, O., Satır, M., Ozkan-Altiner, S., Altiner, D., Sherlock, S., & Eren, R. H. (2006). Cretaceous and Triassic subduction-accretion, high-pressure–low-temperature metamorphism, and continental growth in the Central Pontides, Turkey. *Geological Society of America Bulletin*, 118(9-10), 1247-1269.
22. Okay, A. I., Sunal, G., Sherlock, S., Alt ner, D., Tüysüz, O., Kylander-Clark, A. R., & Aygül, M. (2013). Early Cretaceous sedimentation and orogeny on the active margin of Eurasia: Southern Central Pontides, Turkey. *Tectonics*, 32(5), 1247-1271.
23. Okay, A. I., & Nikishin, A. M. (2015). Tectonic evolution of the southern margin of Laurasia in the Black Sea region. *International Geology Review*, 57(5-8), 1051-1076.
24. Aygül, M., Okay, A. I., Oberhaensli, R., Schmidt, A., & Sudo, M. (2015). Late Cretaceous infant intra-oceanic arc volcanism, the Central Pontides, Turkey: petrogenetic and tectonic implications. *Journal of Asian Earth Sciences*, 111, 312-327. <https://doi.org/10.1016/j.jseaes.2015.07.005>.
25. Aygül, M., Okay, A. I., Oberhänsli, R., & Sudo, M. (2016). Pre-collisional accretionary growth of the southern Laurasian active margin, Central Pontides, Turkey. *Tectonophysics*, 671, 218-234.
26. Ustaömer, T., & Robertson, A. H. (1999). Geochemical evidence used to test alternative plate tectonic models for pre-Upper Jurassic (Palaeotethyan) units in the Central Pontides, N Turkey. *Geological Journal*, 34(1-2), 25-53.
27. Uğuz, M.F. & Sevin, M. (2009). 1/100.000 Ölçekli Türkiye Jeoloji Haritaları, No.115, Jeoloji Etütleri Daire Başkanlığı, Maden Tetkik ve Arama Genel Müdürlüğü, Ankara.
28. Yalçın, C. (2018). Geology and formation of the Gökçedoğan (Kargı-Çorum) Cu ± Zn mineralization. PhD Thesis, İstanbul University, Institute of Graduate Studies in Science and Engineering, 301.
29. Yalçın, C., Haniçlı, N., Kumral, M., & Kaya, M. (2022). Formation and Tectonic Evolution of Structural Slices in Eastern Kargı Massif (Çorum, Turkey). *Bulletin of the Mineral Research and Exploration*. Doi: 10.19111/bulletinofmre.1067604.
30. Marroni, M., Frassi, C., Göncüoğlu, M. C., Di Vincenzo, G., Pandolfi, L., Rebay, G., ... & Ottria, G. (2014). Late Jurassic amphibolite-facies metamorphism in the Intra-Pontide Suture Zone (Turkey): an eastward extension of the Vardar Ocean from the Balkans into Anatolia?. *Journal of the Geological Society*, 171(5), 605-608.
31. Okay, A. I., Sunal, G., Sherlock, S., Alt ner, D., Tüysüz, O., Kylander-Clark, A. R., & Aygül, M. (2013). Early Cretaceous sedimentation and orogeny on the active margin of Eurasia: Southern Central Pontides, Turkey. *Tectonics*, 32(5), 1247-1271.
32. Okay, A. I., & Nikishin, A. M. (2015). Tectonic evolution of the southern margin of Laurasia in the Black Sea region. *International Geology Review*, 57(5-8), 1051-1076.
33. Aygül, M., Okay, A. I., Oberhänsli, R., & Sudo, M. (2016). Pre-collisional accretionary growth of the southern Laurasian active margin, Central Pontides, Turkey. *Tectonophysics*, 671, 218-234.
34. Günay, K., Dönmez, C., Oyan, V., Yıldırım, N., Çiftçi, E., Yıldız, H., & Özküçük, S. (2018). Geology and geochemistry of sediment-hosted Hanönü massive sulfide deposit (Kastamonu–Turkey). *Ore Geology Reviews*, 101, 652-674.
35. Yılmaz, Y. & Tüysüz, O. (1984). Kastamonu-Boyabat-Vezirköprü-Tosya arasındaki bölgenin jeolojisi (Ilgaz-Kargı masiflerinin etüdü), Maden Tetkik ve Arama Raporu, Maden Tetkik ve Arama Yayınları, Ankara.

36. Folk, R. L. (1962). Spectral subdivision of limestone types in classification of carbonate rocks, W.E. Ham. (ed), AAPG Bull., 1, 62-82.
37. Sun, S. S., & McDonough, W.F., (1989). Chemical and isotopic systematics of oceanic basalts: implications for mantle composition and processes, Geological Society, London, Special Publications, 42, 313-345.
38. Boynton, W. V. (1984). Cosmochemistry of the rare earth elements: meteorite studies. In *Developments in geochemistry* (Vol. 2, pp. 63-114). Elsevier.
39. Elderfield, H., & Greaves, M. J. (1982). The rare earth elements in seawater. *Nature*, 296(5854), 214-219. <https://doi.org/10.1038/296214a0>.
40. Piper, D. Z. (1974). Rare earth elements in the sedimentary cycle: a summary. *Chemical geology*, 14(4), 285-304. [https://doi.org/10.1016/0009-2541\(74\)90066-7](https://doi.org/10.1016/0009-2541(74)90066-7).
41. German, C.R., & Elderfield, H. (1989). Rare earth elements in Saanich Inlet, British Columbia, a seasonally anoxic basin. *Geochimica et Cosmochimica Acta*, 53 (10), 2561-2571. [https://doi.org/10.1016/0016-7037\(89\)90128-2](https://doi.org/10.1016/0016-7037(89)90128-2).
42. Roser, B. P., & Korsch, R. J. (1988). Provenance signatures of sandstone-mudstone suites determined using discriminant function analysis of major-element data. *Chemical geology*, 67(1-2), 119-139.
43. Suttner, L. J., & Dutta, P. K. (1986). Alluvial sandstone composition and paleoclimate; I, Framework mineralogy. *Journal of Sedimentary Research*, 56(3), 329-345.
44. Condie, K. C. (1993). Chemical composition and evolution of the upper continental crust: contrasting results from surface samples and shales. *Chemical geology*, 104(1-4), 1-37.
45. Cullers, R. L. (1995). The controls on the major- and trace-element evolution of shales, siltstones and sandstones of Ordovician to Tertiary age in the Wet Mountains region, Colorado, USA. *Chemical Geology*, 123(1-4), 107-131.
46. Cullers, R. L., & Podkovyrov, V. N. (2002). The source and origin of terrigenous sedimentary rocks in the Mesoproterozoic Uj group, southeastern Russia. *Precambrian Research*, 117(3-4), 157-183. [http://dx.doi.org/10.1016/S0301-9268\(02\)00079-7](http://dx.doi.org/10.1016/S0301-9268(02)00079-7).
47. Yalçın, C., Hanilçi, N., Kumral, M., & Kaya, M. (2022). Petrographic and geochemical characterization of sandstones in upper level of ophiolitic melange in Central Pontides. *Advanced Engineering Days (AED)*, 4, 96-99.



© Author(s) 2022. This work is distributed under <https://creativecommons.org/licenses/by-sa/4.0/>



Investigation of the effects of using steel cross and reinforced concrete shears earthquake performance in building

Muhammed Mustafa Eser ^{*1}, Hüsnü Can ²

¹KTO Karatay University, Department of Civil Engineering, Türkiye muhammed.mustafa.eser@ogrenci.karatay.edu.tr

²Gazi University, Department of Civil Engineering, Türkiye, husnucan@gazi.edu.tr

Cite this study: Eser, M. M., & Can, H. (2022). Investigation of the effects of using steel cross and reinforced concrete shears earthquake performance in building. *Engineering Applications*, 1 (2), 157-162

Keywords

Reinforced concrete
Steel cross
Earthquake
Time history analysis
Finite element method

Research Article

Received: 29.09.2022
Revised: 30.10.2022
Accepted: 06.11.2022
Published: 14.11.2022



Abstract

Türkiye mostly on the seismic belt and it causes serious loss of life and property. To prevent this, quake proof structures should be developed and more research should be studied. While reinforced concrete shear walls are common in earthquake resistant buildings in Türkiye, steel usage has not spread. Reinforced concrete structures, which are well-known in project design and application used frequently. Steel structures have been used typically world-wide since the old years while different and innovative methods have been developed and new studies are continuing. Within the area of research, three different system models were designed including a reinforced concrete system without shear walls, a reinforced concrete system with a shear wall on the outermost axis and a reinforced concrete system with a steel cross on the outermost axis then examined. The analyzes are modeled in the SAP2000 program which is internationally accepted and frequently used in academic studies and it will be designed according to the Turkish Building Earthquake Code (TBDY-2018). Modeled buildings were analyzed using the equivalent earthquake load and time history calculation method.

1. Introduction

68% of all earthquakes in the world are in the Pacific belt, 21% are in the Mediterranean-Himalayan belt and the remaining 11% are in other continents. Turkey is located in the Mediterranean – Himalayan belt from these belts [1]. World earthquake map is shown in Figure 1. It is a fact that we will suffer great loss of life and property due to frequent earthquakes in the future, just as there have been many devastating earthquakes in our country in the past. According to the Turkey Earthquake Hazard Map, it is known that 92% of our country is in earthquake zones, 98% of our population lives under earthquake risk, and 98% of large industrial centers and 93% of our dams are located in earthquake zones. In the last 58 years, 58,202 citizens have lost their lives, 122,096 people have been injured, and approximately 411,465 buildings have been destroyed or severely damaged by earthquakes. As a result, it can be said that an average of 1.003 citizens die and 7,094 buildings are destroyed every year due to earthquakes [2].

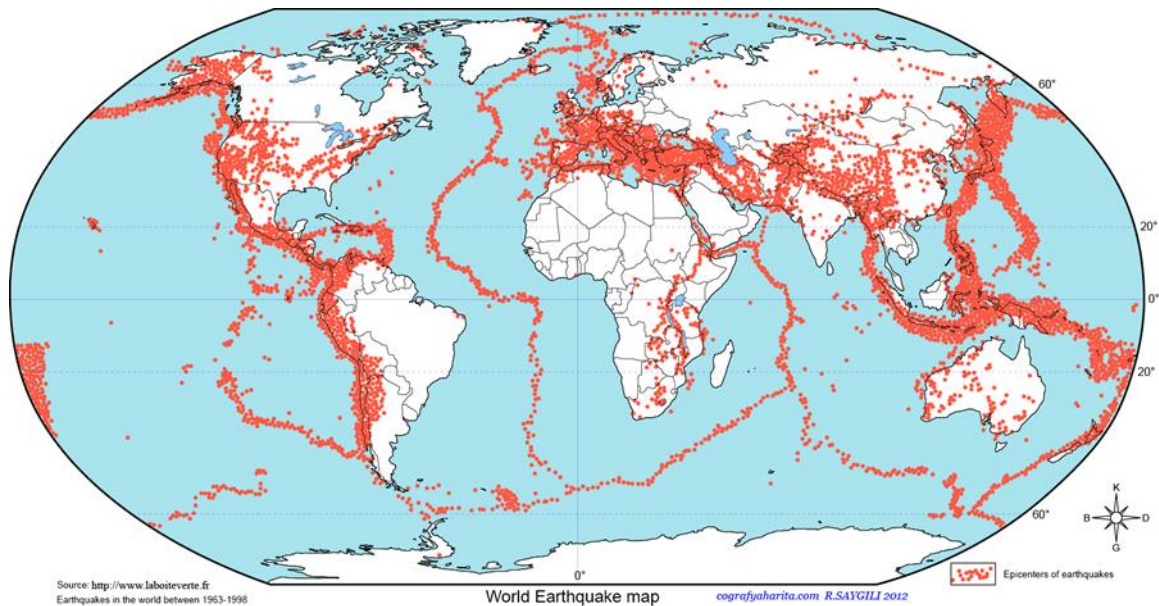


Figure 1. World Earthquake Map [3]

In the rapidly developing world, while the needs of humanity are increasing, new designs and models have been sought. Our choice of materials and design methods that we can use when designing buildings is quite wide and increasing. This increase offers new options while solving space and volume in architecture. This provides architectural diversity. Since it is important that the building models to be designed are constructable, the development of construction techniques leads to new designs.

In the buildings built in our country, importance is given to aesthetics and architecture as well as to the economic and robustness of the building. Since our country is in an earthquake zone, one of the most important forces affecting our buildings is earthquake. Earthquake is a reality for our country and we engineers need to do various researches and studies for this. In this study, it is aimed to compare the performances of reinforced concrete (RC) shears used in large areas in our country and steel cross against earthquakes. In addition, it is aimed to expand the scope of the study and to find detailed results for wider data by taking the placement of both reinforced concrete shears and steel cross to be used instead of shear walls in different places

Reinforced concrete shear wall structures are used very frequently in our country and in the world. In addition, different studies have been carried out on reinforced concrete. Steel plate structures have been widely used in the United States, Canada and Japan since the 1970s, and these structures have not suffered serious damage as a result of earthquakes [4]. Common strengthening methods are based on two basic approaches. The first of these is to strengthen the structure by adding steel diagonal elements or shear walls, and the other is to increase the strength of structural elements such as column beams in reinforced concrete structures or to increase the performance of the structure by strengthening the column-beam junctions [5]. In similar studies, it has been observed that the reinforcement area decreases in reinforced concrete sections when steel cross is used. In addition, when calculating the approximate costs of the structures, he concluded that the cost is 3.09% more economical if steel cross is used [6].

2. Material and Method

In order to ensure that the reinforced concrete buildings, which are used extensively in our country, are reliably strong, some regulations are used while static calculations are made. TBDY-2018 is the regulation that should be taken as a basis in order to determine earthquake forces and to build resistant structures in Turkey [7]. Earthquake forces can be determined by dynamic analysis, taking into account ground accelerations and the mass, stiffness and damping properties of the structure [8]. Earthquake forces cannot be taken as a constant load for every structure and situation because they are not a certain force. Many approaches and methods have been developed on the subject.

Two of the three most commonly used methods were used in this study. The methods that are considered to be used are the equivalent earthquake load method and the calculation method in the time history. Equivalent earthquake load method is based on the first mode of the building and it is accepted that the earthquake forces acting on the floors are proportional to the floor mass and the height of the floor from the foundation. Since the mass of the building is taken into account in the calculation of the vibration period and the distribution of the earthquake load, this method can be considered as a dynamic method based on the first degree of freedom of the building [9]. The purpose of the calculation method in the time history is to integrate the equation of motion of the

system step by step, taking into account the nonlinear behavior of the carrier system. During the analysis, the displacement, plastic deformation and internal forces occurring in the system at each time increment and the maximum values of these magnitudes corresponding to the earthquake demand are calculated [10]. In this method, according to (TBDY-2018), at least 11 earthquake records should be used and the two perpendicular horizontal components of these acceleration records should be simultaneously acted on in the direction of the X and Y principal axes of the carrier system. In addition, a maximum of three acceleration records from the same earthquake should be used [7-11]. 11 different earthquake records were selected to analyze with the calculation method in the time history. These records were taken from the Earth motion database of the Pacific Earthquake Engineering Research Center (PEER) and scaled [12].

3. Modeling of The Structure

Our structure has been designed in accordance with the TBDY-2018 regulation, considering that C30/37 class concrete, B420C class reinforcement and S355 class steel cross are used. The foundation is not included in the calculations and the columns at the ground level are defined as built-in. Calculations and analyzes have gained worldwide reliability and the widely used Structural Analysis Program (SAP2000) is used [13]. The location where the building is thought to be was chosen in Eyüp district of Istanbul province and is shown in Figure 2. Ground class is determined as ZB.



Figure 2. The location where the designed building is thought to be [2]

Our building is designed to stand without collapse under the effects of earthquakes. The cross-sectional dimensions of the building are given in Table 1.

Table 1. Cross-sectional dimensions of the structure

Material	Section
Column	50x50 cm
Beam	50x30 cm
Shear wall	30 cm
Slab thickness	15 cm
Steel cross	HE120A

The structure is designed in a symmetrical square form in order to understand the analysis results more efficiently in terms of x and y. The floor heights are 3 meters equally on each floor and the column openings are 5 meters.

In Model 1, there are only reinforced concrete column and beam elements in the structure. Three-dimensional finite element model of the structure and two-dimensional structural system plans is shown in Figure 3.

In Model 2, there are reinforced concrete columns, beams and shear wall elements in the building. Three-dimensional finite element model of the structure and two-dimensional structural system plans is shown in Figure 4.

In Model 3, there are reinforced concrete columns, beams and steel cross members in the structure. Three-dimensional finite element model of the structure and two-dimensional structural system plans is shown in Figure 5.

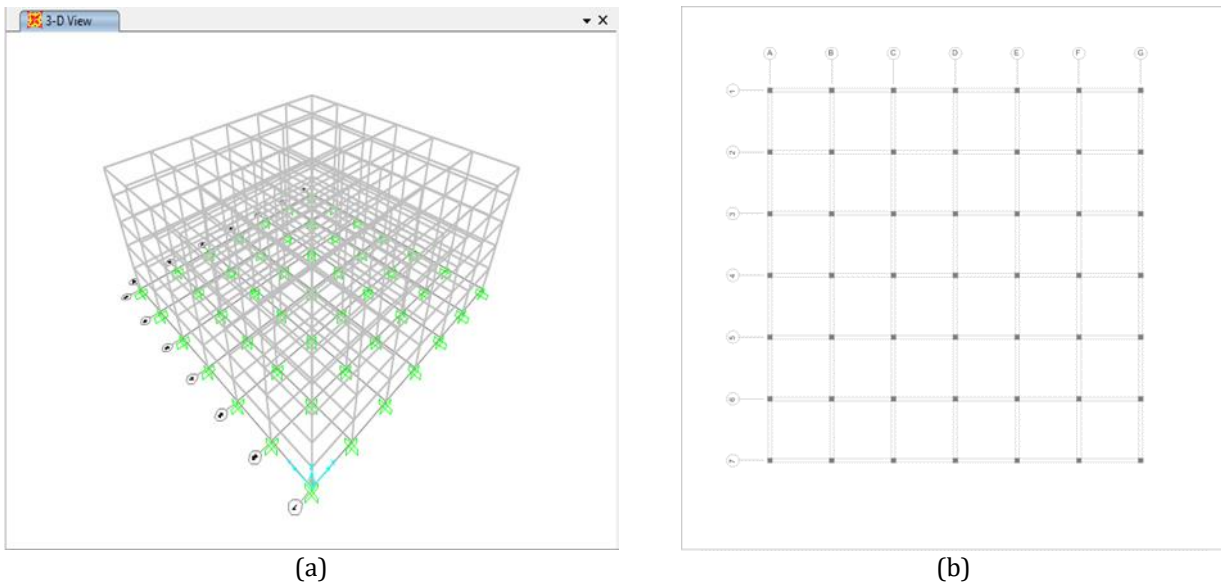


Figure 3. Model 1's (a) three-dimensional finite element model and (b) two-dimensional carrier system plan

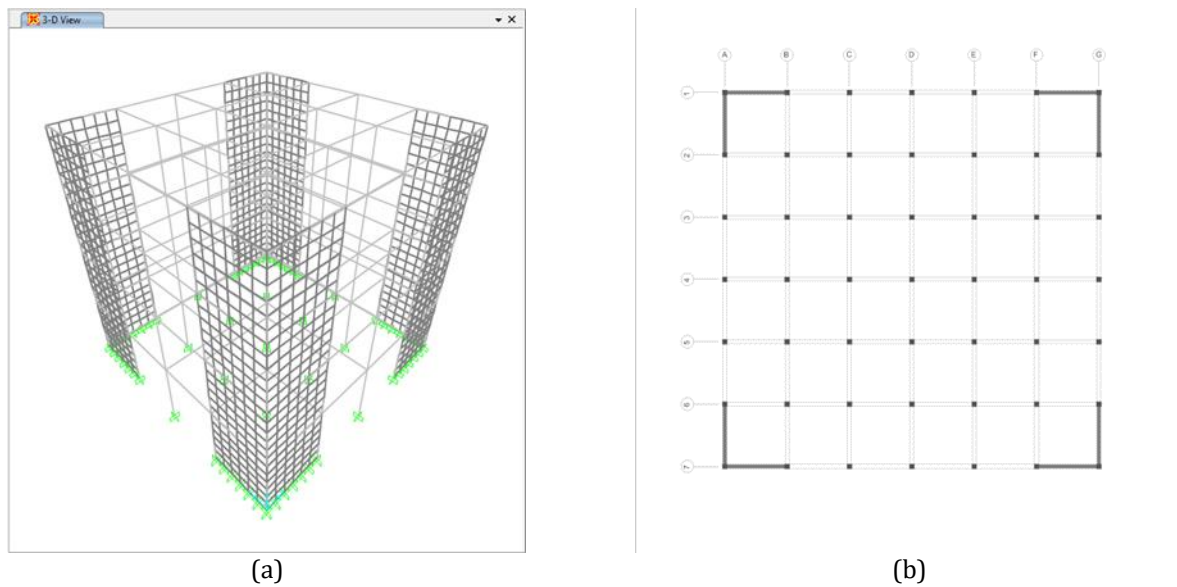


Figure 4. Model 2's (a) three-dimensional finite element model and (b) two-dimensional carrier system plan

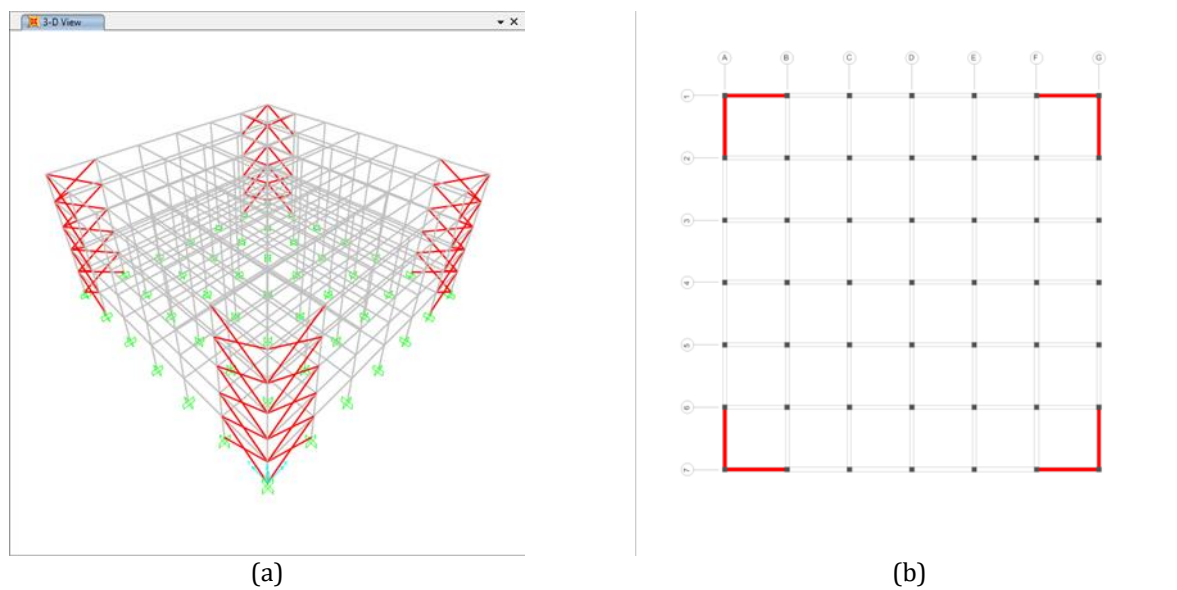


Figure 5. Model 3's (a) three-dimensional finite element model and (b) two-dimensional carrier system plan

4. Results

The period values obtained as a result of the analysis of our structure is shown in Figure 6. Since the first two modes of our structure are symmetrical, the first modes are equal in the x and y directions, and the third mode is torsion.

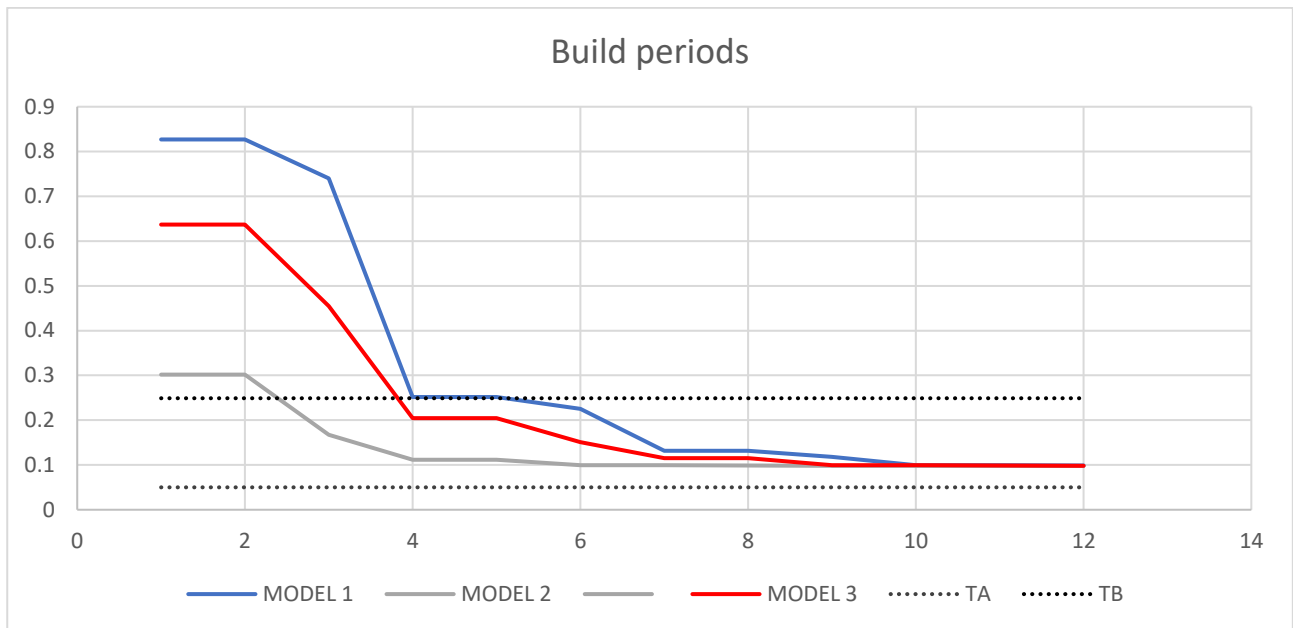


Figure 6. Modes of analyzed systems

Base shear forces determined as a result of 11 different earthquake records of the building are given in Table 2. In the model, in which steel cross elements are used instead of reinforced concrete walls, decreases in base shear walls forces are observed.

Table 2. Base shear forces determined as a result of 11 different earthquake records of the building

Models	Fx + (kN)	Fx - (kN)	Fy + (kN)	Fy - (kN)
Model 1	734.98	703.56	1030.9	1263.65
Model 2	4164.33	4153.07	4397.34	4520.31
Model 3	1724.63	1802.44	1826.72	1930.43

As a result of 11 different earthquake recordings of the building, the section effects affecting the corner column at the ground level are given in Table 3.

Table 3. Section effects of the building determined as a result of 11 different earthquake records

Models	P + (kN)	P - (kN)	V2 + (kN)	V2 - (kN)	V3 + (kN)	V3 - (kN)	M2 + (kNm)	M2 - (kNm)	M3 + (kNm)	M3 - (kNm)
Model 1	937.49	937.49	15.82	16.62	28.06	22.48	62.02	49.93	32.23	33.20
Model 2	937.50	937.51	14.69	14.99	15.23	15.12	31.98	31.81	30.64	31.21
Model 3	937.50	937.50	29.52	27.98	31.60	29.39	64.48	60.76	61.98	57.68

5. Conclusion and Discussion

As a result of the limited research and analysis, the reinforced concrete system model without shear walls, the system model with reinforced concrete shear wall, and the system models in which steel cross are used instead of shear walls in reinforced concrete structures have been examined. The analyzes made give us many parameters and provide data that can lead to many researches. As a result of the data obtained from the analyzes, it is seen that there are situations where steel can better meet the earthquake effects in structures in systems where steel cross is used instead of shear wall in reinforced concrete buildings. By developing these models and similar models, the structures can be strengthened against earthquakes by using steel elements in reinforced concrete structures. As a result, more earthquake resistant buildings can be constructed. The results obtained in this study are not yet completely finished and will be developed.

Acknowledgement

This study was partly presented at the 4th Advance Engineering Days [14]. We would like to thank Res. Asst. Fezayil Sunca for sharing his knowledge in building design and analysis.

Funding

This research received no external funding.

Author contributions

Muhammed Mustafa Eser: Investigation, Visualization, Analysis, Writing **Hüsnü Can:** Examination Writing- Reviewing and Editing.

Conflicts of interest

The authors declare no conflicts of interest.

References

1. Ketin, N. (2005). Genel Jeoloji Yerbilimine giriş. ISBN: 9789757463092
2. AFAD (2018). Turkish Earthquake Code for Buildings. The Disaster and Emergency Management Authority of Turkey, Ankara, Turkey.
3. Saygılı, R (2012). World Earthquake map, www.cografyaharita.com/dunya_jeoloji_haritalari.html
4. Kıymaz, G., & Coşkun, E. (2001). Steel plate shear structures, <https://docplayer.biz.tr/12451175-Celik-levha-perdeli-yapilar.html>.
5. Yön, B., & Sayın, E. (2011). Comparison of Reinforcing with Reinforced Concrete Shear Walls and Steel Bracings, 6th International Advanced Technologies Symposium. Elazığ, Türkiye. (237-242)
6. Naimi, S. (2019). Reinforcement of Reinforced Concrete structures with steel cross members. AURUM Journal of Engineering system and Architecture 3(2), 191-204.
7. TBDY. (2018). Turkey Building Earthquake Code. Official Newspaper. T.C. Ministry of Environment, Urbanisation and Climate Change
8. Özuygur, A., R. (2020). ACI 318 TS 500 Karşılaştırmalı Betonarme. ISBN: 9786254023705
9. Uçar, T., & Merter, O. (2012). A Study on Linear Elastic Methods Used for Seismic Analysis Buildings. Ordu University Journal of Science and Tecnology, 2(2), 15-31.
10. Sunca, F. (2016). Investigating Seismic Performance of The Semi-rigid Connected Prefabricated Structures. Master Thesis, Karadeniz Technical University The Graduate School of Natural and Applied Sciences Civil Engineering Graduate Program, Trabzon.
11. Sunca, G., Ç., K. (2019). Determining Seismic Performances of Reinforced Concrete Structures with Infill Walls for Different Ratio and Configuration. Master Thesis, Gümüşhane University the Graduate School of Natural and Applied Sciences the Graduate School of Natural and Applied Sciences, Gümüşhane.
12. PEER. (2014). Pacific Earthquake Engineering Research Center (PEER) Ground Motion Database.
13. SAP2000. (2015). Integrated Finite Element Analysis and Design of Structures, Computers and Structures Inc., Berkeley, California, USA.
14. Eser, M. M., & Can, H. (2022). Investigation of the effects of using steel cross and reinforced concrete shears earthquake performance in buildings. *Advanced Engineering Days (AED)*, 4, 74-77.



© Author(s) 2022. This work is distributed under <https://creativecommons.org/licenses/by-sa/4.0/>



Overview of multiple sclerosis (MS) and systemic lupus erythematosus (SLE)

Ceren Canatar ^{*1}, Furkan Ayaz ²

¹Mersin University, Biotechnology Department, Türkiye, cerencanatar07@gmail.com

²Mersin University, Biotechnology Research and Application Center, Türkiye, furkanayaz@mersin.edu.tr

Cite this study: Canatar, C., & Ayaz, F. (2022). Overview of multiple sclerosis (MS) and systemic lupus erythematosus (SLE). *Engineering Applications*, 1 (2), 163-169

Keywords

Immune response
Treatment
Autoimmune diseases
Multiple sclerosis (MS)
Systemic lupus
Erythematosus (SLE)

Review Article

Received: 29.09.2022

Revised: 30.10.2022

Accepted: 07.11.2022

Published: 14.11.2022



Abstract

Autoimmune diseases occur as a result of the immune response of the living organism against its own antigens. Some factors may have an effect on the formation of the autoimmune diseases that adversely affect some tissues, organs and systems. In general, the goals of the treatment approaches that should be applied for some autoimmune diseases are to alleviate the symptoms encountered in the development of the disease and to increase the vital functions of the organs and tissues that are affected by the inflammation. Multiple sclerosis (MS) and systemic lupus erythematosus (SLE) diseases are among some common autoimmune diseases. In this review study we will be focusing on both of these diseases.

1. Introduction

The organism's protection against foreign and harmful substances is possible with the immune response. The defense against foreign and harmful substances entering the living organism is carried out by the cells and molecules of the immune system. This protective response created by the organism is described as the immune response [1].

Antigens are molecules that are foreign to the system of the living organism and take part in the production of the immune response. As a result of the immune response, antibody molecules are formed. These antibodies specific to the antigen can bind to neutralize its activities or to eliminate the pathogens associated with the antigens. Antigens show binding with antibodies specific to them. The realization of binding between antigens and antibodies occurs through epitopes, which are also called determinant groups [1-3].

Under normal conditions, the organism does not produce an immune response against its autoantigens, that is, its own structures, and does not start an immune reaction, and this event is characterized as immune tolerance. However, the organism can create an immune response against its own antigens under the influence of some factors, and this leads to the emergence of autoimmune diseases. These factors occur as a result of changes in the chemical or physical properties of the organism's own antigens or immune system cells. In other words, autoimmune diseases occur as a result of impaired immune tolerance [1,4].

There are some factors that trigger the formation of the autoimmune diseases. These factors can be listed as hormonal, immunological, environmental as well as genetic ones [5].

Autoimmune diseases can cause dysfunction and damage to the tissues, as well as adversely affect the body's systems and certain organs [6].

2. MS Disease

Multiple sclerosis (MS) disease affects the central nervous system; it is a chronic, autoimmune and neurological disease characterized by the inflammation. In MS disease, which causes significant cognitive or physical problems, axon, oligodendrocyte and myelin sheath are damaged [7-9].

The axons of the neurons are surrounded by the myelin sheath. In MS disease, the myelin sheath is perceived by some immune system cells as a foreign substance against the body, and during the disease development, the immune system damages the myelin sheath [10].

MS disease is mostly seen in young adults (between 20 and 40 years of age), although it may rarely start at the age of 50 and above, or in childhood. The incidence of MS disease is higher in women than in men [11,12].

2.1. Symptoms of MS Disease

Different parts of the central nervous system can be affected in MS. This results in differences in signs and symptoms among sick individuals. Some of the symptoms seen in MS disease include; speech problems, depression, vision problems, difficulty walking, cognitive impairment, swallowing problems, fatigue, tingling and numbness, attention deficit and respiratory problems [8,9].

Fatigue Problem: Fatigue is among the common symptoms that occur in individuals with MS and prevent them from performing daily activities. Although the cause of the fatigue problem has not been clearly clarified, it is thought that some factors (such as depression, spasticity) affect this situation. Approximately 70% to 95% of individuals with MS have symptoms of fatigue [7, 13-15].

Cognitive Problems: One of the symptoms seen in individuals with MS disease and affecting the quality of life of the individual is cognitive problems. Forgetfulness is one of the cognitive problems seen in MS patients [14].

Speech Problems: Speech problems that occur in individuals with MS disease can be seen together with swallowing problems. Some changes in speech speed and hoarseness are among the speech problems of the patients [14,15].

Walking Problems: Walking problems can be seen in different stages of the MS disease. This situation has a negative effect on the daily activities of the patients [7].

2.2. Risk Factors Affecting the MS Disease

The reason for the development of MS disease remains unclear, but some factors are thought to trigger this condition. In general, among these factors; some autoimmune mechanisms, genetic predisposition, environmental factors, gender and age factor can be counted [8,16].

Deficiency of some vitamins such as B12 and D can be listed among the environmental risk factors that can trigger the development of both MS and some neurological diseases. Epstein-Barr virus (EBV) infection may also be among the environmental risk factors that can trigger the development of the MS disease. The incidence of MS disease is higher in individuals exposed to EBV infection in childhood, adolescence or later, compared to the other individuals who were not exposed to this virus [9,17].

The genetic predisposition factor, which is thought to have an effect on MS disease, is gaining importance day by day. The incidence of MS is higher in first-degree relatives compared to the general population, and in monozygotic twins compared to dizygotic twins. This supports that there is a relationship between genetic factors and the development of MS disease [18].

It is stated that there is a relationship between some human leukocyte antigen (HLA) molecules and MS disease. In other words, it is suggested that HLA molecules play a role among the factors that affect MS development [9,18].

It has been determined that the factors of gender and age also have an effect on the development of MS. The incidence of MS disease is higher in young adults compared to older individuals, and in females compared to the males [8].

Smoking, obesity, radiation, some chemical wastes, race and climatic conditions are among the factors that may directly or indirectly affect the development of MS disease [9,17,19].

2.3. Diagnosis of MS Disease

Demonstrating lesions in the central nervous system becomes the principle of the diagnosis of MS disease. Being able to make an early diagnosis of the disease is very important in terms of choosing the necessary treatment method to be preferred. There is no single diagnostic test for MS disease. Magnetic resonance imaging (MRI) and cerebrospinal fluid analysis help in the diagnosis of the disease. In addition, it is very important to learn about the nutritional habits of individuals, some diseases, if any, and the drugs they use in the diagnosis of MS disease [7-9, 12].

In addition to MRI and cerebrospinal fluid analysis; some other tests such as neurocognitive tests, evoked potentials, blood tests, urodynamic tests, electrophysiology and biopsy are among the tests that help in the diagnosis of MS [7,20].

2.4. Pathophysiology of MS Disease

It has been determined that the immune system is involved in the destruction of both nerve cells and the myelin sheath. In MS; Plaques occur with the loss of axons, inflammation and demyelination. In other words, cells that play a role in the immune system cause damage to the myelin sheath, and thus plaque formation occurs as a result of this situation. Some cells have been identified in the plaques that occur in the MS patients' central nervous system. Among some of the identified cells; B lymphocytes, T lymphocytes, plasma cells, macrophages, microglia cells are included in the development of the disease [8,21-23].

In the pathogenesis of MS, the blood-brain barrier is damaged. As a result of this damage, the permeability of the barrier is impaired. Damage and deterioration of the blood-brain barrier occurs as a result of the formation of lesions in the part of the brain and spinal cord that is described as white matter or white matter [24,25].

MS disease is thought to be mediated by T cells. CD4+ T cells have been detected in both the cerebrospinal fluid and blood of individuals with MS. However, the role of CD4+ T cells in the pathophysiology of the disease has not been clearly defined. In addition, it is known that CD8+ T cells can also be found in the MS lesions and thus play a role in the pathogenesis of MS [9,24].

It is known that Th1 and Th17 cells play a role in the pathogenesis of MS disease. Th1 and Th17 cells differentiate from CD4+ T cells. Some pro-inflammatory cytokines are secreted by Th1 and Th17 cells. Th1 and Th17 cells increase the inflammation that lead into the pathogenesis of MS [26,27].

It is known that B cells, which are involved in the antibody formation, also play a role in the pathogenesis of MS disease. In addition, B cells also have some roles such as producing some cytokines and activating T cells to further contribute the disease development. In this context, B cells may also have an effect on the course of MS disease. The presence of oligoclonal bands in the cerebrospinal fluid and the detection of B cells in MS lesions are among the findings showing that B cells are also involved in the pathogenesis of the MS disease [26-28].

B cells are involved in the secretion of some pro-inflammatory cytokines. This may cause loss of function in neuronal cells. TNF- α , IL-6, IL-12 and IFN- γ are among some of the secreted pro-inflammatory cytokines. B cells can also have positive effects on the central nervous system. These positive effects occur thanks to some anti-inflammatory cytokines they secrete [28].

2.5. Some Treatment Methods in MS Disease

The methods used for the treatment of MS disease are applied for specific purposes. Some of the aims of the applied methods are; increasing physical abilities, relieving symptoms, reducing the frequency and duration of attacks. Currently there is no real treatment method to overcome the disease [20].

2.5.1. Attack Treatment in MS Disease

It is very important to treat the attacks at a level that can increase the quality of life of the patients. These attacks limit their activities and cause functional losses. Reducing the duration of the attacks is among the goals of the attack treatment applied in the MS disease [7,25].

Corticosteroids are frequently used in the treatment of attacks of MS disease. Steroids used in this context have anti-inflammatory effects [25,29].

Plasmapheresis administration; it is among the preferred treatment options in cases where corticosteroid treatment is not sufficient and the expected outcome of the corticosteroid treatment is not obtained [29].

2.5.2. Interferon Beta (IFN - β) Treatment in MS Disease

The disease-modifying nature of IFN- β and its immunomodulatory effects make it possible to use this agent in the treatment of the MS disease [12,27,29].

IFN- β has some effects on the MS disease. These effects can be listed as: it reduces the secretion of the pro-inflammatory cytokines and increases the secretion of the anti-inflammatory cytokines, and regulates the activity of the regulatory T cells [7,8,26].

Thanks to some immunological effects of the IFN- β , a decrease in inflammation in the central nervous system and a slowdown in the progression of disability are observed. However, there may be some side effects of IFN- β therapy. These side effects are; appearance of some reactions on the skin, muscle pain, headache, depression, liver problems, fever, itching, anemia, and fatigue [7,12,26,27].

2.5.3. Glatiramer Acetate Treatment in MS Disease

Another treatment approach for MS disease is glatiramer acetate (GA) treatment. In individuals with MS, treatment with glatiramer acetate, an immunomodulatory agent, reduces the recurrence rate and the symptoms that occur. Glatiramer acetate has a mechanism of action that is different from the IFN- β agent and has not been elucidated in details [8,12,27].

Glatiramer acetate treatment may also cause some mild and serious side effects in individuals with MS. Some of the side effects include; some temporary conditions include fever, respiratory problems, digestive problems, palpitations and chest tightness [27,29].

2.5.4. Stem Cell Therapy in MS Disease

While stem cells are used for the purpose of curing and treating some diseases, they are also involved in repairing the damage that occurs in the myelin sheath of the nerve cells. In this context, it is stated that some stem cell types contribute to neurological recovery and prevention of attacks, and also play a role in limiting neuronal damage [7,10,30].

2.5.5. Symptomatic Treatment in MS Disease

It is very important that symptomatic treatments to be applied in individuals with MS disease are preferred in line with the needs of the sick individuals. In addition, in this context, informing the patient about the possible side effects of the treatment and the predicted results for the treatment becomes an important situation. Symptomatic treatment options for MS disease vary according to the symptoms seen in the patient, but in general, they are aimed at increasing the quality of life of the individuals [8,13].

3. SLE Disease

Systemic lupus erythematosus (SLE) disease; is a chronic autoimmune disease that can affect the tissues and organs, cause organ damage, and whose etiology has not been clearly elucidated. It causes damage to the kidneys, skin, nervous system, joints and some organs, this situation is mediated by the immune complexes [31-33].

SLE disease, which can be seen in individuals of all ages, can be seen rarely in childhood. This disease is mostly seen in individuals between the ages of 20 and 40 years [34,35].

It can affect both genders, but is more common in females (mostly during childbearing) compared to the males [33,36,37].

It is thought that many factors have an effect on the occurrence of SLE, that's why different symptoms can occur [37,38].

3.1. Some Symptoms and Findings in SLE Disease

Various symptoms and signs may occur in individuals with SLE disease. Some of the symptoms seen in SLE disease include; kidney disease, some skin findings, neuropsychiatric symptoms, musculoskeletal system involvement, arthritis, headache and muscle pain, weakness, weight changes, fatigue, and fever [36,37,39].

While symptoms such as fatigue, fever and weakness are usually encountered in the early stages of the disease, the symptoms that occur in the organs are usually encountered in the later stages of the disease [31].

Vitamin D deficiency, anxiety, obesity, depression and some factors can be counted among the causes of fatigue problem encountered in SLE [31].

Skin lesions that may occur in SLE may increase with exposure to the sunlight. A rash usually occurs on the cheeks and nose area after the sun exposure [33,40].

Musculoskeletal symptoms are common in individuals with SLE. In this context, arthralgia, myalgia and joint arthritis that affect small or large joints may occur [33,37,39].

Neuropsychiatric symptoms are reported in some individuals with SLE. In this context; conditions such as mood disorders, depression and headaches can be seen [37,39].

Dermatological symptoms can also be seen during the course of SLE. In this direction, some skin rashes and skin lesions may also occur [37].

Kidney disease can be seen in some individuals with the disease. Kidney involvement can be seen in approximately half of the individuals suffering from SLE [36,39].

Cardiovascular effects such as myocarditis, pericarditis and endocarditis and gastrointestinal involvement (with symptoms such as abdominal pain and nausea) can also be observed in SLE patients [33].

3.2. Some Factors That Can Affect the Development of SLE

Although the etiology of SLE is not known with certainty, there are some factors that are thought to be associated with the development of the disease. Among these factors; genetic factors, environmental factors, immunological factors, hormonal factors can be listed as risk factors [33,38].

Presence of the disease in first-degree relatives may increase the probability of SLE disease development in the individual. In other words, it is thought that there is a relationship between genetic predisposition and SLE. It has been suggested that some environmental factors also play a role in the development of the disease. These environmental factors are; some drugs, smoking, stress, ultraviolet rays, some supplements, hormones, some infections, silica exposure, and some foods [32,33,36,40,41].

3.3. Pathogenesis of SLE

Although the etiopathogenesis of SLE has not been clearly elucidated, some factors are thought to be involved in the pathogenesis [40].

Impairment of the immune tolerance is very important in SLE development and severity. In this context, T cells have a major role [38].

Disturbances in regulatory T cell functions and some immunological abnormalities are among some of the pathological features of SLE. There is a relationship between SLE disease and dysfunctions in helper T cells [38,40].

It has been found that there is a decrease in TGF- β cytokine and an increase in IL-10 cytokine in individuals with SLE disease [41].

Some autoantibodies can also be identified in SLE patients [33].

3.4. Some Treatment Approaches in SLE

Treatment of SLE may differ depending on different factors such as the course of the disease and its severity. In this context, the drug classes used vary depending on the severity of the disease. However, some suggestions are given for individuals with lupus in general. These recommendations are; not smoking, applying the necessary nutrition program and protection from the sunlight. In addition, performing adequate and regular exercises, and providing protection against ultraviolet light are among some of the conditions that should be considered in this context [31,33,39].

3.4.1. Treatment with Antimalarial Agents in SLE

Some antimalarial agents have been useful in patients with SLE who have fatigue, fever and musculoskeletal symptoms. These anti-malarial agents suppress the symptoms associated with SLE [33,40].

Hydroxychloroquine can be used as part of this treatment. The hydroxychloroquine agent is known to be beneficial for arthritis and skin symptoms, it reduces the inflammation in those areas [32,33].

3.4.2. Glucocorticoid Treatment in SLE

Glucocorticoid therapy may be preferred to decrease the disturbing symptoms of the lupus disease. Glucocorticoid therapy can be applied at the different doses depending on the course of the disease [31,40].

3.4.3. Treatment with Immunosuppressive Agents in SLE

Depending on the course of the disease, immunosuppressive agents can be used within the scope of the treatment for the disease. Cyclophosphamide is among the immunosuppressive agents that have been mostly used in SLE patients [31,33].

4. Conclusion

Autoimmune disorders lead to the symptoms that reduce the patients' quality of life. Although treatment approaches for the autoimmune diseases have progressed significantly and positively, especially in recent years, these treatment approaches are generally applied to increase the quality of life of the patient and to reduce the symptoms seen in the course of the disease rather than enabling a total cure for the disease. Novel biocompatible drug candidates should be generated by the biotechnological tools to eliminate the main reasons behind the development of the disease rather than just focusing on the elimination of the symptoms [42]. Future studies should focus on the disease development mechanisms for different autoimmune disorders and how to interfere at each point of the progress in order to develop better treatment approaches.

Acknowledgement

This study was partly presented at the 4th Advanced engineering Days [43].

Funding

This research received no external funding.

Author contributions

Ceren Canatar: Conceptualized, wrote, reviewed. **Furkan Ayaz:** Edited the final version

Conflicts of interest

The authors declare no conflicts of interest.

References

1. Düzgün, N. (2014). İmmün sistemin tanıtımı. Ankara Üniversitesi Tıp Fakültesi, İç Hastalıkları Anabilim Dalı, Romatoloji Bilim Dalı, 97-122.
2. Songu, M., & Katılmış, H. (2012). Enfeksiyondan korunma ve immün sistem. Journal of Medical Updates, 2(1), 31-42.
3. Işıtmangil, G., & Demirtunç, R. (2012). Basic Terminology Of Immunogenetics. The Medical Journal Of Haydarpaşa Numune Training and Research Hospital, 52(1), 45-51.
4. Özbek, M. (2014). T Lenfositlerin Gelişimi. Mehmet Akif Ersoy University Journal of Health Sciences Institute, 2(2), 104-113.
5. Stojanovich, L., & Marisavljevich, D. (2008). Stress as a trigger of autoimmune disease. Autoimmunity reviews, 7(3), 209-213.
6. Ngo, S. T., Steyn, F. J., & McCombe, P. A. (2014). Gender differences in autoimmune disease. Frontiers in neuroendocrinology, 35(3), 347-369.
7. Efendi, H., Yandım Kuşcu, D. (2018). Multipl Skleroz Tanı ve Tedavi Kılavuzu.
8. Öztürk, S., Aytaç, G., Kızılay, F., Sindel, M. (2017). Multipl Skleroz. Akdeniz Tıp Dergisi, 3(3), 137-147.
9. Ghasemi, N., Razavi, S., & Nikzad, E. (2017). Multiple sclerosis: pathogenesis, symptoms, diagnoses and cell-based therapy. Cell Journal (Yakhteh), 19(1), 1.
10. Ulucan Karnak, F. (2020). Multipl Skleroz Hastalığına Karşı Tedavi Yaklaşımları. ERÜ Sağlık Bilimleri Fakültesi Dergisi, 7(2), 49-54.
11. Terzi, M., & Onar, M.K. (2009). Multipl Sklerozda klinik ve demografik özellikler. Journal of Experimental and Clinical Medicine, 21(4).
12. Goldenberg, M. M. (2012). Multiple sclerosis review. Pharmacy and therapeutics, 37(3), 175.
13. Özakbaş, S. (2011). Multipl Sklerozda Semptomatik Tedavi/Symptomatic Menagement in Multiple Sclerosis. Noro-Psikiyatri Arsivi, 48, 83.
14. Akkuş, Y., Kapucu, S. (2006). Multipl skleroz ve hasta eğitimi. Hacettepe Üniversitesi Hemşirelik Yüksekokulu Dergisi, 13(2), 57-63.
15. Karantay Mutluay, F. K. (2006). Multipl skleroz rehabilitasyonu. Türk Nöroloji Dergisi, 12(2), 134-143.
16. Özkarabulut, A.H., Onur, H.N., Yaşar, İ. (2018). Multiple Skleroz (MS) hastalığı öncesi ve sonrası beslenme alışkanlıklarının karşılaştırılması, yeterli ve dengeli beslenmenin ms ataklarına olan etkisinin irdelenmesi. İstanbul Gelişim Üniversitesi Sağlık Bilimleri Dergisi, (6), 535-550.
17. Garg, N., & Smith, T. W. (2015). An update on immunopathogenesis, diagnosis, and treatment of multiple sclerosis. Brain and behavior, 5(9), e00362.
18. Soyder Kuş, C.N., Zorlu, Y., Çoker, I., Şener, U., Altinel, Ö. (2004). RR Tip Multipl Skleroz Hastalarında HLA DQ Antijenlerinin Dağılımı. SSK Tepecik HastDerg, 14(2):95-100.
19. Mirza, M. (2002). The etiology and the epidemiology of multiple sclerosis. Erciyes Medical Journal, 24(1), 40-47.
20. Kılıç, H. (2009). Elazığ bölgesinde multipl skleroz tanısı ile izlenen hastaların epidemiyolojik, demografik özellikleri ve ailesel sıklığı/Epidemiological, demographical features and familial frequency of the patients with multiple sclerosis followed in region Elazığ. (Uzmanlık Tezi)
21. Huang, W. J., Chen, W. W., & Zhang, X. (2017). Multiple sclerosis: Pathology, diagnosis and treatments. Experimental and therapeutic medicine, 13(6), 3163-3166.

22. Karakulak, E. Z. (2018). Multipl skleroz hastalarında kronik özür lülük oluşturan semptomlar üzerinde transkranyal direk akımın (TDCS) etkilerinin araştırılması (Master's thesis, İstanbul Medipol Üniversitesi Sağlık Bilimleri Enstitüsü).
23. Özdemir, M., Ayaz, A. (2020). Multipl Skleroz'da K Vitamininin Rolü Var Mıdır? Kocatepe Tıp Dergisi, 21(4), 362-369.
24. Altıntaş, A., Esen, F. (2008). Multipl Skleroz İmmunopatogenezi. Nöropsikiyatri Arşivi
25. Sevim, S. (2016). Multipl skleroz atakları üzerine güncelleme: Tanım, patofizyoloji, özellikler, taklitçiler ve tedavi. Turk J Neurol, 22, 99-108.
26. Loma, I., Heyman, R. (2011). Multiple sclerosis: pathogenesis and treatment. Current neuropharmacology, 9(3), 409-416.
27. Dargahi, N., Katsara, M., Tselios, T., Androutsou, M. E., De Courten, M., Matsoukas, J., & Apostolopoulos, V. (2017). Multiple sclerosis: immunopathology and treatment update. Brain sciences, 7(7), 78.
28. Tüzün, E. (2011). Multipl Skleroz Patogenezinde B Hücrelerinin Rolü ve B Hücre Karşıtı. Archives of Neuropsychiatry, 48(2), 73-8.
29. Akman Demir, G. (2010). Multipl Skleroz Tedavisi. Klinik Gelişim, 23(1), 65-70.
30. Shroff, G. (2018). A review on stem cell therapy for multiple sclerosis: special focus on human embryonic stem cells. Stem cells and cloning: advances and applications, 11, 1.
31. Özkaraman A., Uzgör, F. (2019). Sistemik Lupus Eritematozus ve Hemşirelik Yönetimi ve Hemşirelik Yönetimi. Kocaeli Tıp Dergisi, 8(3), 69-79.
32. Fava, A., & Petri, M. (2019). Systemic lupus erythematosus: diagnosis and clinical management. Journal of autoimmunity, 96, 1-13.
33. Maidhof, W., & Hilas, O. (2012). Lupus: an overview of the disease and management options. Pharmacy and Therapeutics, 37(4), 240.
34. Pehlivanoglu, C., Bilge, I., Aksu, B., Yılmaz, A., Yıldırım, Z. Y., Yılmaz, Y., Kılıçaslan, I., Sevinç, Emre, S. (2015). Yaşamı Tehdit Eden Sistemik Lupus Eritematozus Vakasında Rituksimab Tedavisi. Çocuk Dergisi, 15(3), 107-110.
35. Serin, S., Tatar, K. K., & Saler, T. (2014). İnfektif Endokarditle Karışan Sistemik Lupus Eritematozus Olgusu. Medical Bulletin of Haseki/Haseki Tıp Bulteni, 52(3).
36. Manson, J.J., Rahman, A. (2006). Systemic lupus erythematosus. Orphanet Journal of Rare Diseases, 1:6.
37. Cojocar, M., Cojocar, I. M., Silosi, I., & Vrabie, C. D. (2011). Manifestations of systemic lupus erythematosus. Maedica, 6(4), 330-336.
38. Pan, L., Lu, M.P., Wang, J.H., XU, m., Yang, S.R. (2020). Immunological pathogenesis and treatment of systemic lupus erythematosus. World Journal of Pediatrics, 16(1), 19-30.
39. Kuhn, A., Bonsmann, G., Anders, H. J., Herzer, P., Tenbrock, K., & Schneider, M. (2015). The diagnosis and treatment of systemic lupus erythematosus. Deutsches Ärzteblatt International, 112(25), 423.
40. Yükselmiş, Ö. (2020). Hidroksiklorokin ile Uzun Süreli Tedavi Altında Olan sistemik Lupus Eritematozuslu Hastalarda Covid-19'un Prevelansı ve Klinik Seyri. International Anatolia Academic Online Journal Health Sciences, 7(1), 1-15.
41. Artım Esen, B., İnanç, M. (2005). Sistemik lupus eritematozus etyopatogenezinde virüslerin rolü. Journal of Istanbul Faculty of Medicine, 68(3), 85-91.
42. Chandrashekar, S. (2012). The treatment strategies of autoimmune disease may need a different approach from conventional protocol: a review. Indian journal of pharmacology, 44(6), 665.
43. Canatar, C., & Ayaz, F. (2022). Mast cells and their importance for the immune system. *Advanced Engineering Days (AED)*, 4, 18-19.





Detection of materials and material deterioration in historical buildings by spectroscopic and petrographic methods: The example of Mardin Tamir Evi

Lale Karataş¹, Aydın Alptekin², Murat Yakar³

¹Mardin Artuklu University, Department of Architecture and Urban Planning, Türkiye, lalekaratas@artuklu.edu.tr

²Mersin University, Faculty of Engineering, Department of Geological Engineering, Türkiye, aydinalptekin@mersin.edu.tr

³Mersin University, Faculty of Engineering, Department of Geomatics Engineering, Türkiye, myakar@mersin.edu.tr

Cite this study: Karataş, L., Alptekin, A, & Yakar, M. (2022). Detection of materials and material deterioration in historical buildings by spectroscopic and petrographic methods: The example of Mardin Tamir Evi. *Engineering Applications*, 1 (2), 170-187

Keywords

Material Analysis
Spectroscopic Analysis
Petrographic Analysis
Material Deterioration
Restoration

Research Article

Received: 30.09.2022

Revised: 30.10.2022

Accepted: 07.11.2022

Published: 14.11.2022



Abstract

The province of Mardin is an area where stone material is concentrated in terms of its geographical region, and it is a city that is under protection as a protected area with its historical buildings made of local Mardin stone extracted from the region. However, in the historical city of Mardin, as in the rest of the world, stone structures are subject to deterioration due to various effects and protection interventions are often needed in the region. The lack of information on the compatibility of materials used in the past years in Mardin, as in many other countries, has caused serious damage to historical textures and structures in many cases. Today, integrated studies of the analysis of available materials and the selection of restoration materials are often included in the restoration programs of monuments. The aim of this study is to document the characteristics of the local Mardin stone, the material problems it is exposed to, through stone material and mortar samples taken from a historical residence in Mardin, and thus to contribute to the selection of compatible restoration materials for the sustainable management of the structures in the geographical region. In this context, an examination was made on the materials and mortar samples used in the building, which constitutes a representative sample from the building. Analysis of proteins, fats and water-soluble salts with simple spot tests on samples defined by visual analysis and their conductivity, the amount of CaCO₃ with the loss of 105 °C and 550 °C by calcination analysis, the content and problems of the samples were investigated by determining the general texture and mineral content by stereo microscope and petrography analysis, and the quality and proportions of the aggregates of the acid-treated sample with stereomicroscope analysis. The results of this study are important in terms of creating a guideline for the use of compatible materials in the restoration stages in structures made with local Mardin stone in Mardin. Based on the analysis results obtained in the study, it is hoped that correct applications will be made in the selection of materials in the restoration applications to be made in the geographical region.

1. Introduction

Historical buildings deteriorate due to traditional building materials (stone, brick, air or hydraulic mortars, etc.), certain environmental loads and unsuitable materials (cement, polymeric materials, etc.) used in previous restoration interventions, and various restoration interventions are needed on the structures. In the restoration materials used in the interventions, the original materials used in the building should be taken into consideration, and in order to choose a compatible restoration material, the physical, chemical and mechanical behavior of the repair material should be compared with the original ones. In order to make this comparison, before proceeding to the repair phase in historical buildings, first of all, the properties of the materials should be determined in detail on the mortar and material samples, which form a representative sample from the monument [1,2]. Restoration

materials to be used for historical buildings and monuments are a frequently discussed topic in the repair phase of buildings in the world [3]. Today, integrated studies of the analysis of existing mortars and the design of restoration mortars are often included in the restoration programs of monuments [4,5]. The purpose of the analysis of historical materials is to obtain information about the physical and chemical composition of the materials as well as the production technology [6]. However, after this accumulation of knowledge, a detailed study on the synthesis of compatible mortars and materials in order to proceed with the restoration of the historical structure can lead to correct results in conservation applications [7].

Recently, scientific conservation studies have been carried out to clarify the deterioration factors by non-destructive diagnosis on the samples taken from the building based on the characteristics of the stones that make up it, in order to establish a systematic approach to the preservation of stone cultural heritage [8-12]. Petrographic and spectroscopic analyzes have proven useful in several studies to establish a guideline for the use of compatible materials in the restoration phase [13]. Patil et al [14] carried out microscopic studies such as petrographic and Scanning Electron Microscopy (SEM), Energy Dispersive X-ray spectroscopy (EDS) calculation for detailed characterization of stone degradation in Kopeshwar Temple and Panhala fort and found that these studies provided sufficient information about the nature and distribution of the mineralogical phases and elements within the basalt stone sample and the stone interface, which contributed to the identification of essential minerals and the behavior responsible for stone degradation. Columbu et al [15] used petrographic and mineralogical analyzes of stone materials to describe the chemical composition of rocks and to examine the surface properties of the stone and found these methods to be useful for identifying possible old treatments used to identify and maintain surface alteration processes. Campos-Suñol et al. [16] used Optical microscopy, scanning electron microscopy-energy dispersive x-ray spectrometry (SEM-EDX), x-ray diffraction, Raman spectroscopy, and infrared spectroscopy for the microstructural and compositional analysis of the dark yellow patinas seen on the substrate of the stone in the historical monuments of Úbeda and Baeza (Spain), and detected the types of deterioration on the patinas with these methods. Colao et al. [17] used laser-induced failure spectroscopy and found that spectroscopy measurements were a fast and effective method for detecting material deterioration. Theologitis et al. [18] analyzed the mortar and plaster samples taken from the Frangokastello Castle in Sfakia (Western Crete) and showed that the mechanical behavior of the restoration mortar can be compared with the historical ones. The data obtained as a result of the analysis of the materials in the building showed that they formed a laboratory guideline for the composition of the restoration material. It is stated that such applications have not yet been created on a regional scale in many countries, especially in Crete, and that these analysis catalogs should be created on the basis of geographical region in different countries.

In this study, it is requested to create a stone analysis catalog to be used in the restoration of stone structures in Mardin province, based on the necessity of creating the stone analysis catalogs specified in the literature on the basis of geographical region in different countries. The aim of the study in this context is to document the characteristics of the local Mardin stone and the material problems it is exposed to, through the stone material and mortar samples taken from a historical residence in Mardin, and thus to contribute to the selection of compatible restoration materials for the sustainable management of the structures in the geographical region.

The lack of information on the compatibility of mortars and raw materials in the historical stone structures of the city of Mardin, as in many countries, in many cases caused serious damage to the historical texture and structures. Mardin Tamir Evi, located in the city of Mardin, which is the subject of the study, is a masonry structure built of local Mardin stone, which has all the features of Mardin traditional houses selected within the scope of the Mardin House Conservation and Repair Project. In recent years, it is seen that the signs of deterioration in the structure have accelerated. Accurate identification of weathering forms and intensity is an important factor in determining conservation methods. In the case study of a traditional house, which is a stone historical building, in the Southeastern Anatolia region, stone material samples were analyzed and restoration materials compatible with the existing substrate were investigated. Petrographic and spectroscopic studies were performed for detailed characterization of stone degradation on stone samples collected from the study area to better understand the composition and formation of degradation products, and to identify contaminants and to evaluate their effects on limestone. These studies provided information about the local Mardin stone sample and the nature and distribution of the elements, the nature and distribution of the mineralogy phases within the stone interface, and the material degradation, which contributed to the identification of basic minerals and the behavior responsible for stone degradation. Microstructural analysis reveals that the degradation process has already begun inside the building blocks.

2. Material and Method

Within the scope of the "Mardin House Conservation and Restoration Project" carried out by the Cultural Heritage Preservation Association and the Mardin Archeology Museum, 3 wood samples, 12 stone samples, and from the deep between knitting stones 12 mortar samples, were taken from the Mardin House from a building in the Artuklu District of Mardin Province. The following analyzes were carried out in the Restoration-Conservation and Analysis Laboratory of the Mardin Museum.

Table 1. Stone samples

Sample No	Explanation
1-Z01 (Stone)	It is a solid example of a yellowish light brown colored stone with black deposited dirt on its surface, taken from the damaged part of the vault of the semi-open courtyard section of the house.
2-Z01 Ton. (Mortar)	It is a sample of brownish gray mortar, with white masses up to 4 mm in size, at least 4-8 mm in size, taken from among the masonry stones in the damaged part of the vault of the semi-open courtyard section of the house, which disintegrates while it is intact.
3-Z01 D.D. (Mortar)	It is a relatively solid sample of brownish gray mortar with white masses up to 2 mm in size, 3-5 mm in spatter, and taken from the wall of the semi-open courtyard section of the house.
4-Z02 K.C.D. (Mortar)	It is a sample of brown-colored mortar containing aggregates up to 10 mm in size, relatively solid in place, and dispersed when taken, taken from the south exterior (courtyard) façade of the house.
5-Z02 A.K.C. (Stone)	It is a very solid example of a yellowish-brown stone with a layer of black dirt on its surface, taken from the upper part of the niche of the well, located in the semi-open courtyard of the house.
6-Z02 A.K.C. (Mortar)	The south exterior (courtyard) façade of the house is a solid example of cream-colored mortar with aggregates up to 12 mm in size, taken from among the brickwork of the eastern window.
7-Z03 T.T.Y.T. (Stone)	It is an example of a solid yellowish-white stone, taken from the vault of the upper floor entrance room of the house, from the blooming (salting) area.
8-Z03 G.D. (Mortar)	The south wall of the upper floor entrance room of the house is a solid example of cream-colored, solid mortar with a small amount of aggregates up to 4 mm, taken from the wall between the windows and between the brickwork.
9-Z03 T.T.Y. (Stone)	The upper floor entrance room of the house is a solid example of light cream colored stone with yellow spots on the surface, taken from the flowering part of the beginning of the vault in the north.
10-Z03 B.D.D. (Mortar)	It is a relatively weak sample of brown-colored mortar, which was taken from the masonry of the west wall of the entrance room and the west wall of the house, containing aggregates up to 10 mm in size.
11-Z03 Y.D. (Stone)	It is a sample of solid, non-porous, cream-colored stone with yellow spots on the surface, taken from the ground floor of the house, entrance room floor.
12-Z04 T.D. (Mortar)	It is a weak mortar sample taken from the vault that forms the ceiling of the second room of the house, dark brown in color, the aggregates of which cannot be seen, but white masses up to 3 mm in size and a small amount of ceramic pieces between 5-10 mm in size can be seen.
13-Z04 T.K. (Stone)	It is an example of a very solid, non-porous colored stone with a yellowish light brown color, with brown deposits on the surface, taken from the arch of the vault that forms the ceiling of the ground floor and the second room of the house.
14-Z04 D.D. (Mortar)	It is a light gray colored mortar sample taken from the east wall of the ground floor, second room of the house, with white particles up to 4 mm in size and yellowish brown deposits on the surface.
15-Z05 Yüz. (Stone)	It is an example of a yellowish-cream colored, heavily fractured and cracked stone with dark yellow stained areas on the surface, taken from the middle part of the vault of the entrance floor, second room of the house.
16-102 T.T.O. (Stone)	It is a solid example of yellowish-cream colored stone with visible cracks and cracks, with a black colored dirt layer on the surface, taken from the vault of the second room of the house, from the surface of the place where the salinization occurs.
17-102 D.D.Y. (Stone)	The upper floor façade of the house is a solid example of a light brownish-cream colored stone with eroded surface and yellow stained areas from place to place, taken from its outer surface.
18-102 T.D. (Mortar)	It is a light gray and white colored solid mortar sample that has no aggregate but has a 6 mm white mass taken from the vault of the upper floor entrance room of the house.
19-102 G.D.Y. (Stone)	This is a solid example of a brownish yellow stone with algae formation on the surface, soot and accumulation pollution and a small amount of erosion, taken from the south wall of the upper floor entrance room of the house, under the skylight.
20-102 G.D.B. (Stone)	It is a solid stone sample taken from the south wall of the upper floor entrance room of the house, between the door and the window, in a brownish-cream color, with white areas up to 4 mm in size, with abundant flowering and a small amount of erosion on the surface.
21-102 B.D.D. (Mortar)	It is a brownish gray mortar sample taken from the west wall of the upper floor entrance room of the house, with aggregates up to 6 mm in size, solid in place, and dispersed while taking it.
22-102 G.D. (Stone)	It is a solid example of a light brownish-cream colored stone with creamy-white particles up to 5 mm in size and yellow deposited pollution on the surface, taken from the south wall of the upper floor entrance room of the house, over the window in the direction of the door.
23-103 B.D. (Mortar)	It is a sample of cream gray colored mortar, containing cream-white particles up to 2 mm in size, solid in place and disintegrating when taken, taken from the west wall of the upper floor entrance room of the house.
24-103 B.D.D. (Mortar)	It is a sample of brownish gray mortar, containing cream-white aggregates up to 6 mm in size, solid in place and disintegrating when taken, taken from the west wall of the upper floor entrance room of the house.
25 (Wood)	The lower floor of the house is a wood sample taken from the beams on the entrance door, with light yellow, dark colored rots, drying cracks and insect flight holes visible.
26 (Wood)	The lower floor of the house is a wood sample taken from the beam on the window, with yellow, dark rot and insect flight holes visible.
27 (Wood)	The upper floor of the house is a wood sample taken from the beams on the kitchen door, where light brown, dark rots, drying cracks and insect flight holes can be seen.



Figure 1. Samples taken from Tamir Evi

In this study, the content and problems of the samples whose definitions were made by the visual analysis were investigated. Conductivity was investigated with analysis of protein, oil, and water-soluble salts with simple spot tests, CaCO₃ amount was investigated with 105 C and 550 C loss with calcination analysis, general texture, and mineral content were investigated with a stereo microscope and petrography analysis, and quality and proportions of the acid-treated aggregates were investigated with stereo microscope analysis. In addition, as a result of examining the macroscopic properties of wood samples, the problems of wood were investigated, and by examining the transverse radial and tangential sections prepared from these samples under the microscope, the types of wood were investigated.

2.1. Protein and Fat Analysis with Water-Soluble Salts

Analyzes of simple spot tests were made to be able to determine the qualities of the water-soluble salts (chlorine (Cl⁻), sulfate (SO₄⁼), carbonate (CO₃⁼) and nitrate (NO₃⁻) salts), and their amounts, and to decide whether the addition of additives such as saponifiable oil and protein or not into the samples and the results are given in Table 1.

Table 1. Protein and Fat Analysis of Samples using Water-Soluble Salts

Sample	Cl ⁻	SO ₄ ⁻²	CO ₃ ⁻²	NO ₃ ⁻	Conductivity (µs)	Salt (%)	Ph	Protein	Oil
1	+	-	-	-	267	1.46	7.36	-	-
2	+	-	-	-	662	3.70	7.87	+	-
3	++	-	-	+++	1227	6.88	7.68	+	-
4	+	-	-	-	325	1.82	7.67	+	-
5	+	-	-	-	241	1.34	7.47	-	-
6	++++	±	-	++++	2863	16.03	7.50	-	-
7	+	-	-	+	507	2.83	7.89	-	-
8	++++	±	-	++++	2284	12.80	7.74	-	-
9	+	±	-	++	997	5.59	7.80	-	-
10	++++	-	-	++	1740	9.74	7.98	-	-
11	+++	-	-	±	556	3.11	7.79	-	-
12	++	-	-	-	345	1.93	8.04	+	-
13	+	-	-	-	273	1.52	7.83	-	-
14	++++	±	-	++	1540	8.62	7.43	-	-
15	++++	±	-	++	1586	8.89	7.65	-	-
16	++	-	-	±	419	2.34	7.88	-	-
17	++++	-	-	±	1122	6.29	7.84	-	-
18	++++	±	-	+	1000	5.60	8.32	+	-
19	++	-	-	-	427	2.40	8.08	+	-
20	++++	±	-	±	1336	7.49	7.91	-	-
21	+	-	-	-	724	4.05	8.38	+	-
22	+	-	-	-	259	1.45	8.34	-	-
23	++++	±	-	++	2193	12.29	7.66	-	-
24	++++	-	-	++++	3047	17.06	8.13	-	-

∓: Absent ±: Present/Absent +: Few ++: Little +++: A lot of ++++: Many

2.2. Loss of Ignition, Acid Treatment and Sieve Analysis

The calcination (heat loss) analysis results of the samples at 105 ± 5°C, 550 ± 5°C and 1050 ± 5°C, as well as the proportion of silicate aggregates that did not react and remained intact as a result of acid treatment, and the size distributions of these aggregates are given in Table 2.

2.3. Visual Analysis of Aggregates with a Stereo Microscope

The silicate aggregates of the samples, whose binders were destroyed by treatment with acid, were examined under a stereo microscope after sieve analysis and their visible properties are given in this part. In the definitions, the terms "very little" for less than 1% and "little" for 1-2% are used.

2.3.1. Sample 1-Z01(Stone)

5-10% of the 31.73% residue remaining after acid treatment of the sample is cream and brown colored, silt and clay, and the remaining part is unreacted calcarenite masses.

Table 2. Loss on Ignition and sieve analyzes of aggregates (*: Not applied)

#	Loss on ignition		Acid (%)			Retained material on sieve (%)								
	Moisture	550 C°	CaCO ₃	Loss	Residual	6300	4000	2500	1000	500	250	125	63	<63
1	0.05	0.44	98.59	68.27	31.73	*	*	*	*	*	*	*	*	*
2	1.61	8.88	71.27	90.37	9.63	0.00	0.00	0.00	2.29	3.82	5.34	38.17	38.93	11.45
3	3.11	6.34	75.11	84.01	15.99	0.00	2.09	0.19	3.98	6.07	24.10	42.69	19.92	0.95
4	14.02	3.13	78.84	51.24	48.76	68.20	3.40	1.33	4.37	4.37	4.61	9.47	4.25	0.00
5	0.35	0.54	93.46	89.87	10.13	*	*	*	*	*	*	*	*	*
6	9.87	7.46	83.80	76.39	23.61	54.88	3.55	0.55	0.67	2.99	9.42	18.63	7.76	1.55
7	1.00	2.71	101.10	97.06	2.94	*	*	*	*	*	*	*	*	*
8	11.01	7.66	82.53	80.48	19.52	0.00	0.00	0.00	3.74	21.76	17.36	47.03	9.23	0.88
9	1.93	2.13	94.88	98.11	1.89	*	*	*	*	*	*	*	*	*
10	7.48	3.35	82.54	75.75	24.25	53.74	10.10	1.21	0.40	1.41	5.05	16.16	10.30	1.62
11	2.09	1.28	98.40	97.71	2.29	*	*	*	*	*	*	*	*	*
12	20.76	2.02	76.20	88.20	11.80	0.00	0.00	0.00	0.00	0.00	52.20	46.44	1.36	0.00
13	0.26	0.21	98.50	96.47	3.53	*	*	*	*	*	*	*	*	*
14	10.00	3.07	86.50	88.87	11.13	0.00	0.00	0.00	0.41	5.33	20.90	36.07	26.23	11.07
15	16.47	2.84	73.19	74.58	25.42	*	*	*	*	*	*	*	*	*
16	0.92	0.89	91.83	98.69	1.31	*	*	*	*	*	*	*	*	*
17	2.87	2.16	98.82	98.54	1.46	*	*	*	*	*	*	*	*	*
18	0.91	4.24	91.92	97.41	2.59	0.00	0.00	0.00	0.00	15.63	25.56	31.25	23.44	3.13
19	0.14	1.65	99.00	99.28	0.72	*	*	*	*	*	*	*	*	*
20	2.44	1.63	99.92	98.98	1.02	*	*	*	*	*	*	*	*	*
21	1.02	3.16	65.40	87.34	12.66	0.00	3.19	0.35	3.90	4.61	17.38	46.45	18.09	6.03
22	0.12	0.94	99.25	76.85	23.15	*	*	*	*	*	*	*	*	*
23	7.41	2.87	93.55	95.04	4.96	0.00	*	0.00	5.60	7.20	13.60	51.20	19.20	3.20
24	8.24	6.79	81.56	88.92	11.08	0.00	0.00	0.00	0.81	6.85	12.90	45.56	28.63	5.24

2.3.2. Sample 2-Z01 Tons (Mortar)

The remaining aggregates smaller than 125µ of the sample after acid are only brick dust feldspar and muscovite, few are black slag particles, and the rest are gray colored portland cement feldspar.

Of the 125–1000 µ sized particles, few brick fragments and muscovite, very few black slag particles, 3-5% volcanic rock particles, 10-15% quartz, the remainder are gray colored Portland cement feldspar mass.

The small amount of coarse aggregates (greater than 1000 µm in size) up to 2 mm in size, only a few brick fragments, very few black slag particles, 5-10% volcanic rock particles, 25-30% gray Portland cement is feldspar mass, the remainder is quartz.

Aggregates of the sample remaining in the acid, 1 mm under sieve size, a single shard of brick and muscovite, very little black slag particles, 3-5% volcanic rock particles, 10-15% quartz, the rest gray portland cement feldspar and is its mass.

2.3.3. Sample 3-Z01 D.D. (Mortar)

The remaining aggregates smaller than 125µ of the sample after acid are only brick dust feldspar and muscovite, few are black slag particles, 15-20% are ash, the remainder are gray colored portland cement feldspar.

Of the 125–1000 µ sized particles, very few brick fragments and muscovite, very few black slag particles, 5-10% volcanic rock particles and quartz, the remainder are ash and gray colored Portland cement feldspar mass.

Of the coarse aggregates, 1 of which is 5 mm in size and generally up to 2 mm in size, a single piece of brick is broken, very little is black slag particles, 20-25% is volcanic rock particles and quartz, the rest is ash and gray colored portland cement feldspar mass.

1 of the aggregates remaining in the acid is 5 mm in size, generally in 2 mm under sieve size, only a few brick fragments and muscovite, very little black slag particles, 5-10% volcanic rock particles and quartz, 15-20% ash, the remainder is a gray colored Portland cement feldspar and mass.

2.3.4. Sample 4-Z02 K.C.D. (Mortar)

3-5% of aggregates smaller than 125µ remaining after acid are black slag particles, the rest is brown silt and clay.

Few of the 125–1000 µ sized particles are brick fragments, 3-5% are black slag particles, the remainder is brown clay and silt mass.

The coarse aggregates, generally up to 10 mm in size, consist of very few brick fragments, very few black slag particles, some volcanic rock particles and quartz, and the rest unreacted limestone particles.

Aggregates remaining in the acid, with a size of 10 mm under a sieve, very few brick fragments, some volcanic rock particles and quartz, 3-5% black slag particles, 10-15% brown clay and silt, the rest is unreacted limestone particles.

2.3.5. Sample 5-Z02 A.K.C. (Stone)

After the acid treatment of the sample, 10-15% of the remaining 10,13% residue is brownish yellow, silt and clay, and the remaining part is unreacted calcarenite masses.

2.3.6. Sample 6-Z02 A.K.C.(Mortar)

Few of the aggregates smaller than 125 μ remaining after acid are black slag particles and brick dust feldspar, the rest is light brown silt and clay.

Of the 125–1000 μ sized particles, very few are black slag particles, few are brick fragments, 3-5% are volcanic rock particles and quartz, and the remainder are dark brown clay and silt masses.

The coarse aggregates, generally up to 12 mm in size, consist of very few brick fragments, very few black slag particles, some volcanic rock particles and quartz, and the rest unreacted limestone particles.

Aggregates of the sample remaining in the acid are 12 mm under sieve size, very few brick fragments, very few black slag particles, few volcanic rock particles and quartz, 5-10% brown clay and silt and masses, the rest unreacted limestone particles.

2.3.7. Sample 7-Z03 T.T.Y.T. (Stone)

The remaining 2.94% residue after the acid treatment of the sample is dark brown colored silt and clay and a black oil-like gel-like substance.

2.3.8. Sample 8-Z03 G.D. (Mortar)

Few of the aggregates smaller than 125 μ remaining in the sample after acid are black slag particles and brick dust feldspar, the rest is dark brown silt and clay.

Of the 125–1000 μ -sized particles, very few are black slag particles, few are brick fragments, 2-3% are volcanic rock particles and quartz, and the remainder are dark brown clay and silt masses.

A small amount of coarse aggregates, very few of which are 2-4 mm in size and generally up to 2 mm in size, consist of only brick fragments, very few black slag particles, few volcanic rock particles and quartz, and the rest are unreacted limestone particles.

Aggregates of the sample remaining in the acid are 1-4 mm, generally 1 mm under sieve size, very few brick fragments, very few black slag particles, few volcanic rock particles and quartz, 10-15% brown clay and silt and their masses, the remainder are unreacted limestone particles.

2.3.9. Sample 9-Z03 T.T.Y. (Stone)

1.89% residue of the sample after acid treatment is cream-brown colored silt and clay.

2.3.10. Sample 10-Z03 B.D.D. (Mortar)

2-3% of the small sized aggregates of the sample after acid are black slag particles, the rest is brown silt and clay.

Of the 125–1000 μ sized particles, very few are brick fragments, few are black slag particles and quartz, and the rest are brown clay and silt masses.

The coarse aggregates, generally up to 8 mm in size, consist of only a few brick fragments, very few black slag particles, some volcanic rock particles and quartz, and the rest unreacted limestone particles.

Aggregates of the sample remaining in the acid are generally 8 mm under sieve size, very few brick fragments, some black slag particles, volcanic rock particles and quartz, 30-35% brown clay and silt and masses, the rest unreacted limestone particles.

2.3.11. Sample 11-Z03 Y.D. (Stone)

After the acid treatment of the sample, the residue of 2.29% is brown silt and clay and a black oil-like gel-like substance.

2.3.12. Sample 12-Z04 T.D. (Mortar)

The aggregates of the sample with a size less than 500 μ remaining after acid are black slag particles and brick dust feldspar, the rest is dark brown colored silt and clay. Brick pebbles visible in the raw sample were not included in the acid-treated part.

2.3.13. Sample 13-Z04 T.K. (Stone)

After the acid treatment of the sample, the residue of 3,53% is brown colored silt and clay and a black oil-like gel-like substance.

2.3.14. Sample 14-Z04 D.D. (Mortar)

2-3% of the small sized aggregates of the sample after acid are black slag particles, the rest is brownish gray colored portland cement feldspar.

Few of the 125–1000 μ sized particles are black slag particles, 25-30% are brownish gray colored portland cement feldspar mass, the remainder are volcanic rock particles and quartz.

Few of the coarse aggregates, which are insignificant and 1-2 mm in size, are black slag particles, 20-25% are brownish gray colored portland cement feldspar mass, the remainder are volcanic rock particles and quartz.

Aggregates of the sample remaining in the acid are generally 1 mm under sieve size, some of them are black slag particles, 25-30% are volcanic rock particles and quartz, and the rest is portland cement.

2.3.15. Sample 15-Z05 Yüz. (Stone)

After the acid treatment of the sample, 10-15% of the remaining 25.42% residue is cream yellow colored silt and clay, and the remaining part is unreacted calcarenite masses.

2.3.16. Sample 16-102 T.T.O.(Stone)

The 1.31% residue remaining after the acid treatment of the sample is dark gray and white colored silt and clay and a small amount of black oil-like gel-like substance.

2.3.17. Sample 17-102 D.D.Y. (STONE)

The 1.46% residue remaining after the acid treatment of the sample is cream colored and white colored silt and clay and a small amount of black oil-like gel-like substance.

2.3.18. Sample 18-102 T.D.(Mortar)

Most of the aggregates of the sample with a size less than 500 μ remaining after the acid are brick dust feldspar, some are quartz, 2-3% are black slag particles and the remainder are dark brown colored silt and clay.

2.3.19. Sample 19-102 G.D.Y. (Stone)

The 0.72% residue remaining after the acid treatment of the sample is cream and white colored silt and clay and a small amount of black oil-like gel-like substance.

2.3.20. Sample 20-102 G.D.B.(Stone)

The remaining 1.02% residue after the acid treatment of the sample is cream and white colored silt and clay and a small amount of black oil-like gel-like substance.

2.3.21. Sample 21-102 B.D.D.(Mortar)

3-5% of the small sized aggregates of the sample after acid are black slag particles, the rest is dark gray colored portland cement feldspar.

Of the 125–1000 μ size particles, 3-5% are black slag particles, 5-10% are volcanic rock particles and quartz, and the rest is dark gray portland cement feldspar.

The small amount of coarse aggregates, which are generally 4 mm in size, consist of black slag particles, 20-25% brown clay and silt and their masses, the rest is volcanic rock particles and quartz.

Aggregates of the sample remaining in the acid are less than 1-4 mm in size, generally 1 mm in size under a sieve, 3-5% of black slag particles, 20-25% of brown clay and silt masses and volcanic rock particles and quartz, the rest is dark gray. colored portland cement feldspar and mass.

2.3.22. Sample 22-102 G.D. (Stone)

After the acid treatment of the sample, the remaining 23.12% residue is colored with a small amount of black oil-like gel material, 10-15% is creamy yellow colored silt and clay, and the remaining part is unreacted calcarenite masses.

2.3.23. Sample 23-103 B.D.(Mortar)

Few of the aggregates smaller than 125 μ remaining in the sample after acid are black slag particles, the rest is cream colored feldspar.

Few of the 125–1000 μ sized particles are black slag particles, 5-10% are white colored particles, and the remainder are cream colored feldspar masses.

Few of the small amount of coarse aggregates, which are 2 mm in size, are black slag particles, 5-10% are white colored particles, and the rest are cream colored feldspar masses.

The aggregates of the sample remaining in the acid are 1-2 mm, generally 1 mm in size under a sieve, very little black slag particles, 5-10% white colored particles that have not reacted with acid, and the rest are cream colored feldspar and its masses.

2.3.24. Sample 24-103 B.D.D. (Mortar)

Less than 125 μ sized aggregates of the sample remaining after acid are brick dust feldspar, 3-5% are black slag particles, the rest is dark gray colored portland cement feldspar.

Of the 125–1000 μ sized particles, very few are brick fragments, few are black slag particles and quartz, 5-10% are white colored particles, and the remainder are dark gray colored portland cement feldspar.

Of the insignificant amount of coarse aggregates, which are generally 2 mm in size, very few are black slag particles and the rest are white colored particles.

Aggregates of the sample remaining in the acid are generally 1 mm under sieve size, very few brick fragments, few black slag particles and quartz, 5-10% white colored particles, the rest is dark gray colored Portland cement feldspar and mass.

2.3.25. Sample 25

It is a wood sample and this analysis was not done.

2.3.26. Sample 26

It is a wood sample and this analysis was not done.

2.3.27. Sample 27

It is a wood sample and this analysis was not done.

2.4. Petrographic Analysis of Samples

The textural and aggregate properties of the shiny (thick) sections prepared from the mortar and plaster samples embedded in epoxy were determined by examining under a stereo microscope (single nicol) and the mineral contents and roughly ratios of thin sections were examined under a polarizing microscope (double nicol) and the results are given below. In defining the pore ratios of the samples, the terms "slight" for pores up to 5%, "moderate" for pores of 5-15%, and "abundant" for pores greater than 15% were used. In addition, the type of wood was investigated by examining the prepared transverse, radial and tangential sections of the wood samples under the microscope.

2.4.1. Sample 1-Z01(Stone)

After the acid treatment of the sample, 5-10% of the remaining 31.73% residue is cream and brown colored, silt and clay, and the remaining part is unreacted calcarenite masses.

2.4.2. Sample-2-Z01 Ton. (Mortar)

The sample, which has a binding area of 20-25% and a brownish gray color, has aggregates up to 4 mm in cross-sectional area. For example, aggregates of which few are black slag particles and brick shards and dust, 3-5% are volcanic rock particles and quartz are 1 mm under sieve, and the remaining aggregates with limestone fragments are 4 mm under sieve size. The binder phase and binder aggregate phase of the sample, which has moderate pores up to 0.5 mm in size, are good.

2.4.3. Sample 3-Z01 D.D. (Mortar)

The sample, which has a binding area of 20-25% and a brownish light gray color, has aggregates up to 5 mm in cross-sectional area. Very little part of the sample is brick shards and dust, 2-3% is black slag particles, 3-5% is volcanic rock particles and quartz aggregates are 2 mm under sieve, the rest is limestone fragments and other aggregates are 5 mm under sieve size. The sample, which has moderate pores up to 1 mm in size, has good binding phase and binding aggregate phase.

2.4.4. Sample 4-Z02 K.C.D.(Mortar)

The sample, which has a binding area of approximately 25% and a brownish-cream color, has aggregates up to 10 mm in cross-sectional area. Very little of the sample is brick fragments and dust, some black slag particles and volcanic rock particles and quartz, 5-10% graywacke particles and aggregates with 1 mm under sieve, the rest with limestone fragments is 10 mm under sieve size. The binder phase and binder aggregate phase of the sample, which has moderate pores up to 0.5 mm in size, are good.

2.4.5. Sample 5-Z02 A.K.C. (Stone)

It is known as Urfa stone, with a light brownish yellow texture, grain sizes up to 0.5 mm, abundant macrofossils, micro cracks and veins, secondary calcite crystals as well as clay fillings and dyeings, porous up to 0.5 mm in size. It is an Eocene-Oligocene aged biomicritic clastic calcarenite limestone. On the surface of the sample, there are brownish black, organic origin impurities.

2.4.6. Sample 6-Z02 A.K.C.(Mortar)

The bond area is 35-40% and the cream-colored sample has aggregates up to 12 mm in cross-sectional area. Very little of the sample is brick fragments and dust, some of it is black slag particles and volcanic rock particles and quartz, 3-5% of the aggregates with graywacke particles and dust are 2 mm under sieve and the rest of the aggregates with limestone fragments are 12 mm under sieve size. The binder phase and the binder aggregate phase of the sample, which has 3-5% of 1-3 mm in size voids and a moderate amount of pores up to 0.5 mm in size, are good.

2.4.7. Sample 7-Z03 T.T.Y.T. (Stone)

Eocene-Oligocene aged micritic, also known as Urfa stone, with a yellowish cream-colored texture and grain sizes up to 0.5 mm, with no veins visible, but clay fillings and dyes between calcite crystals, small amount and porous up to 0.1 mm. it is limestone. On the surface of the sample, there is a yellowish accumulation of pollution from place to place.

2.4.8. Sample 8- Z03 G.D. (Mortar)

The bond area is 35-40% and the cream-colored sample has aggregates up to 10 mm in cross-sectional area. Very little of the sample is brick fragments and dust, a few black slag particles and volcanic rock particles and quartz, 3-5% of graywacke particles and aggregates are 1 mm under sieve and the rest of the aggregates with limestone fragments are 4 mm under sieve size. The binder phase and binder aggregate phase of the sample, which has abundant pores up to 0.5 mm in size, are good.

2.4.9. Sample 9- Z03 T.T.Y. (Stone)

It is an Eocene-Oligocene aged micritic limestone, also known as Urfa stone, with a yellowish-cream color, grain size up to 0.5 mm, veins are not visible, but there are clay fillings and dyes between calcite crystals, and porous up to 0.1 mm in size. On the surface of the sample, there is a yellowish accumulation of pollution from place to place.

2.4.10. Sample 10- Z03 B.D.D. (Mortar)

The sample, which has a binding area of approximately 25% and a brownish-cream color, has aggregates up to 10 mm in cross-sectional area. Very little of the sample is broken brick and dust, some of it is black slag particles and volcanic rock particles and quartz, 10-15% of the aggregates with graywacke particles and dust is 8 mm under sieve, and the rest of the aggregates with limestone fragments are 10 mm under sieve size. For example, with moderate pores up to 0.5 mm in size, the binder phase and binder aggregate phase are good.

2.4.11. Sample 11-Z03 Y.D. (Stone)

It is an Eocene-Oligocene aged micritic limestone, also known as Urfa stone, with a yellowish-cream color, grain size up to 0.5 mm, veins not visible, but clay fillings and dyes between calcite crystals, small amount and porous up to 0.1 mm. On the surface of the sample, there are yellow-brown colored, stain-like, accumulated impurities on the surface.

2.4.12. Sample 12-Z04 T.D. (Mortar)

The sample, which has a binding area of 30-35% and a creamy white color, has aggregates up to 1 mm in cross-sectional area. Very little of the sample is brick fragments and dust, a few black slag particles and volcanic rock particles and quartz, 5-10% graywacke particles and dust aggregates are 0.5 mm under sieve, the rest is 1 mm under sieve size. The binder phase and binder aggregate phase of the sample, which has abundant pores up to 0.5 mm in size, are relatively weak.

2.4.13. Sample 13-Z04 T.K. (Stone)

Eocene-Oligocene aged, also known as Urfa or Mardin stone, with a yellowish-brown texture and partially recrystallized, very small and semi-euhedral grain sizes, with secondary calcite crystals and clay dyeings in the veins and around the fragments, porous up to 0.1 mm in size. It is a limestone composed of micrite sized calcites. On the surface of the sample, there is a brownish, slightly crusty accumulation of impurity.

2.4.14. Sample 14- Z04 D.D. (Mortar)

The sample, which has a binding area of 25-30% and a light gray color, has aggregates up to 4 mm in cross-sectional area. Very little of the sample is brick shards and dust and black slag particles, 3-5% of volcanic rock particles and quartz aggregates are 1 mm under sieve and the remaining aggregates with limestone fragments are 4 mm under sieve size. Binder phase and binder aggregate phase of the sample, which has abundant pores up to 0.5 mm in size, are quite good.

2.4.15. Sample 15- Z05 Yüz. (Stone)

Eocene-Oligocene, also known as Urfa or Mardin stone, with a light yellowish cream color texture, average grain size of 0.5 mm, filled with secondary calcite crystals, abundant micro-cracks and clay stains in places, porous up to 0.2 mm. It is a calc-arenite limestone consisting of aged micrite-sized calcites. On the surface of the sample, there are dark yellow brown colored and less black colored deposited crustal impurities in places.

2.4.16. Sample 16- 102 T.T.O.(Stone)

Eocene-Oligocene aged micritic limestone, also known as Urfa stone, with a yellowish-cream color, grain size up to 0.5 mm, crack-like veins and secondary calcite crystals and clay staining around the crumbs, porous up to 0.1 mm in size.

2.4.17. Sample 17-102 D.D.Y.(Stone)

Eocene-Oligocene aged micritic limestone, also known as Urfa stone, with a yellowish light brown texture and grain sizes up to 0.5 mm, with no veins visible, but clay fillings and dyes between calcite crystals, small amount and porous up to 0.1 mm.

2.4.18 Sample 18-102 T.D. (Mortar)

The sample, which has a binding area of 30-35% and a creamy white color, has aggregates up to 1 mm in cross-sectional area. Very little of the sample is broken brick and dust, volcanic rock particles and quartz and black slag

particles, aggregates with few graywacke particles and dust are 0.5 mm under sieve, while the rest of the aggregates with limestone fragments are 6 mm under sieve size. For example, the binder phase and binder aggregate phase are good, with abundant pores up to 0.5 mm in size.

2.4.19. Sample 19-102 G.D.Y. (Stone)

It is also known as Urfa stone, with a brownish yellow texture and grain sizes up to 0.5 mm, with abundant macrofossils, with no veins visible, but with clay filling and dyeing between the calcite crystals, with a small amount of pores up to 0.5 mm in size, is an Eocene-Oligocene aged biomicritic limestone. On the surface of the sample, there are yellow-brown-black colored, soot, moss and organic origin, crust-like, accumulated impurities.

2.4.20. Sample 20- 102 G.D.B. (Stone)

Eocene-Oligocene aged biomicritic limestone., also known as Urfa stone, with a brownish yellow texture and grain sizes up to 0.5 mm, with abundant macrofossils, with clay filling and dyeing between calcite crystals, with abundant macrofossils, up to 0.5 mm in size. On the surface of the sample, there are very light, brownish yellow, organic origin impurities.

2.4.21. Sample 21-102 B.D.D. (Mortar)

The aggregates in the cross-sectional area are up to 6 mm in the sample, which has a binding area of 25-30% and a creamy white color. The sample contains very little brick fragments and dust, some black slag particles, 3-5% volcanic rock particles and quartz, 5-10% graywacke particles and dust aggregates 0.5 mm under sieve, and other aggregates with limestone fragments. Is 6 mm under sieve size. The binder phase and binder aggregate phase of the sample, which has abundant pores up to 0.5 mm in size, are relatively weak.

2.4.22. Sample 22-102 G.D. (Stone)

Its texture is brownish yellow and partially recrystallized, its grain sizes are very small and semi-euhedral, it has secondary calcite crystals and clay dyeings in the veins and around the fragments, as well as abundant fossils, it is porous up to 0.5 mm in size, also known as Urfa or Mardin stone. It is calrenite limestone with biomicrite clastics, composed of Eocene-Oligocene aged micrite-sized calcites. On the surface of the sample, there is dark yellow – brown colored, organic origin, deposited crustal contamination.

2.4.23. Sample 23-103 B.D. (Mortar)

The bond area is 35-40% and the cream colored sample has aggregates up to 2 mm in cross-sectional area. Very little of the sample is broken brick and dust, some of it is black slag particles and volcanic rock particles and quartz, 3-5% of the aggregates with graywacke particles and dust is 1 mm under sieve, the rest of it is 2 mm under sieve size. The binder phase and binder aggregate phase of the sample, which has small pores up to 1 mm in size, are good.

2.4.24. Sample 24-103 B.D.D. (Mortar)

The binder area is approximately 20% and the gray colored sample has aggregates up to 6 mm in cross-sectional area. Very little of the sample is brick fragments and dust, less of it is black slag particles, 3-5% is volcanic rock particles and quartz aggregates are 1 mm under sieve, the rest is limestone fragments and other aggregates are 6 mm under sieve size. For example, the binder phase and binder aggregate phase are good, with abundant pores up to 0.5 mm in size.

2.4.25. Sample 25-Wood

It has been determined that the light yellow colored wood sample has a scattered trachelia structure in its cross-section, and gradually decreases in the number and diameter of the tracheas from the spring wood to the summer wood layer. In the radial section, the perforation tables are of simple type and sometimes as tuelles has been determined. In the tangential section, it has been determined that the pith rays are single-lined, their heights are very different, and they range from 3-5 cells high to 30 cells high.

2.4.26. Sample 26-Wood

It has been determined that the yellow colored wood sample has a scattered tracheia structure in its cross-section, and gradually decreases in the number and diameter of the trachea as we go from the spring wood to the summer wood layer. In the radial section, perforation tables are seen as simple type and sometimes as tules. In the tangential section, it has been determined that the pith rays are single-lined, their heights are very different, and they range from 3-5 cells high to 30 cells high.

2.4.27. Sample 27-Wood

It has been determined that the light brown wood sample has a ringed tracheal structure in its cross-section, the trachea in the summer wood layer are arranged in a radial and diagonal arrangement, it forms a flame-like structure, the longitudinal parenchymas are in the apotraheal scattered and tangential stripe order, and there are paratraheal parenchymas. It has been determined that the core rays are homogeneous in the radial section, the perforation tables are simple type, the meeting passages of the core rays and the trachea are large, round and oval. In the tangential section, it has been determined that the core rays are in two different widths, very wide and single cell width.

3. Results

When all these results are brought together, 12 mortar samples taken from the traditional house of Mardin selected within the scope of the "Mardin House Conservation and Repair Project" were classified into 2 main groups according to the analysis results, binders and aggregates remaining after acid treatment.

The binder of the mortar samples numbered 4, 6, 8, 10, 12, 18, 21 and 23, which is classified as the first main group, is air lime (cream lime) and is divided into 2 subgroups according to the binder lime ratios. While an average of 35% cream lime was used as binder in samples 6, 8, 12, 18, 21 and 23, which are classified as subgroup 1A, an average of 25% cream lime was used in samples no. 4 and 10, classified as subgroup 1B. While samples 8, 12 and 21 belonging to subgroup 1A, average 5mm under-sieve size limestone fragments were used as aggregate, in samples 12 and 23 2-mm under sieve size limestone fragments and in sample 6 12-mm under-sieve size limestone fragments and pebbles were used as aggregate. In samples 4 and 10 belonging to subgroup 1B, 10 mm under-sieve size limestone fragments were used as aggregate. It is thought that the graywacke particulate sands and volcanic rock particles and quartz sands, which are determined in the aggregates of almost all of the samples and which amount to 5-10% in total, are found in the source where the limestone broken sand is obtained. According to their binding nature, the mortars belonging to subgroup 1A were considered to be original, while the mortars belonging to subgroup 1B were considered to belong to the complements and/or repairs made during or after the construction process.

Mortar No. 2, 3, 14 and 24, which is classified as the second main group, is a sample binder, Portland cement with 10-15% lime added, varying between 100-200 doses, and its aggregates are 5 mm in average under sieve size and 3-5% volcanic fracture of limestone, which is rock particles and quartz. In the 3rd sample of this group, approximately 5% ash was added additionally. It has been understood that the mortars of this group, depending on their binding nature, were used in the extensive and/or individual repairs made in the middle or the second half of the 20th century. It has been visually determined that all of the plasters applied on the vaults of the house, which did not need to be taken as samples, were recent plasters with portland cement binder (Figure 1,2).



(a)



(b)

Figure 1a. In the vault of the space in the semi-open courtyard of the house
Figure 1b. Upstairs, recent repair plasters with portland cement binder in the kitchen vault



(a)



(b)

Figure 2a. Upstairs of the house, recent repair plaster with portland cement binder in the vault of the entrance room

Figure 2b. Plant formations and stains caused by water on the inner surface of the south wall

In addition, it is determined that in the construction of the house, partially clayey and/or recrystallized micritic limestones consisting of Eocene-Oligocene micrite-sized calcites, also known as Urfa or Mardin stone, whose mineralogical properties are given above, were used as masonry material, biomicritic limestones with abundant fossils, micrite or biomicrite clastic calcarenite limestones were used. It has been determined that a significant part of these stones contain a small amount of petroleum-like, non-saponifiable (mineral-based) oil.

The stones in the ground floor of the house and the rock-cut section were found to be micritic limestone with plenty of cracks, which has not yet completed its petrification, looks like greywacke and has plenty of clay. It has been determined that there are surface erosions on the inner and outer surfaces of the walls of the house, especially in the areas of water evaporation, there are chloride and nitrate salts from the repair mortars and plasters with portland cement binder in general, and from the sewage in places, from the water leaking from the walls and roof (roof) of these salts, from the flowering cycle of these salts. In addition to these surface problems, as a result of the overflow of the water tank on the roof of the house, wetting on the outer surface of the south wall of the house, accordingly the formation of herbaceous plants on the exterior, woody plant formations on the garden wall, as well as the moisture problem in the entire building has been seen. As a result of these wetting and drying cycles, there has been an increase in flowering and surface erosion of the mesh stones (Figure 3,4).



(a)



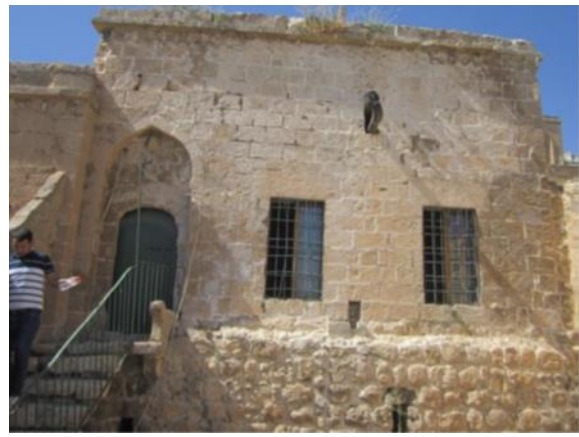
(b)

Figure 3a. On the outer wall surface of the house, with herbaceous plant formations due to wetting

Figure 3b. General views of the woody plant formation on the garden wall



(a)



(b)

Figure 4a. General view of efflorescence (salt deposits) occurring in the evaporation zone on the interior wall surfaces of the house

Figure 4b. General view of efflorescence (salt deposits) occurring in the evaporation zone on the exterior wall surfaces of the house

In addition, poplar (*Papulus Nigra L.*) wooden elements were used on the beams on the doors and windows on the lower floor of the house, while oak (*Queras SPP.*) wooden elements were used on the beams on the doors and windows of the upper floor ([Figure 5](#)).



(a)



(b)

Figure 5a. General view of the wooden elements used on the door tops and the damage caused by rot and insect infection on these wooden elements

Figure 5b. General view of the wooden elements used on the window tops and the rot and insect infection damage on these wooden elements

In addition, according to the gallery type, *Anobium Punctatum* (Furniture Beetle) is used on the wooden main carriers that carry the wooden elements, which are exposed to brown-colored rot in various intensities due to humidity and individual wetting in general, and which carry the connecting wall of the place between the bagdadi laths and the Z02 space of the Observatory and the connection corridor.) were found to be infected by insects, which are understood to be of the genus. In addition to the problems in the building materials of the house, it has been visually determined that there are structural static problems in the walls and rock-carved vaults of the house, although not much. In addition, it is seen that there is a very serious structural crack in the wall of the neighboring house, which is understood to have been partially destroyed and repaired before ([Figure 6](#)).



Figure 6a. General view of static problems on the interior wall of the house
Figure 6b. General view of static problems on the wall of the neighboring house

4. Discussion and Conclusion

In this study, it is aimed to document the characteristics of the local Mardin stone, the material problems it is exposed to, through the stone material and mortar samples taken from a historical residence in Mardin, and thus to contribute to the selection of compatible restoration materials for the sustainable management of the structures in the geographical region. In this context, an examination was made on the materials and mortar samples used in the building, which constitutes a representative sample from the building. The results of this study are important in terms of creating a guideline for the use of compatible materials in the restoration stages in structures made with local Mardin stone in Mardin. According to the analysis results obtained in the study, it is seen that material deterioration can be detected by spectroscopic and petrographic methods. This finding obtained from the study supports the results of the study, which determined that the petrographic and spectroscopic analyzes determined in various studies in the literature are useful for creating a guideline for the use of compatible materials in the restoration phase [8-13].

Based on the analysis results obtained in the study, it is hoped that correct applications will be made in the selection of materials in the restoration applications to be made in the geographical region. According to the evaluation made by combining these results, it is necessary to eliminate the static problems seen in the walls of the house and the vaults of the rock-carved sections, or to take measures (suspension, support, etc.) against these problems. After the necessary static measures are taken, it is recommended to remove the modern Portland cement binder vault plasters, which are determined to be in the near term, by scraping, although it is the project decision whether to remove these plasters (because it has been applied throughout the vaults). If it is decided to remove the Portland cement binder vault plasters, it would be appropriate to carry out this application sensitively by mechanical method. If it is decided to preserve the Portland cement binder vault plasters (to complete the existing state without scraping), the light accumulation of dirt and salt crystals on the interior and exterior surfaces of these plasters and other walls should be removed first by using a plastic brush and vacuum cleaner, then once (It would be appropriate to continue cleaning with pulp impregnated with 5% ammonium bicarbonate solution (twice) or twice if the stain does not come off, and finally, salt cleaning should be done twice with clean (drinkable quality) water-impregnated pulp.

It would be appropriate to remove the recently made Portland cement bonded joints by scraping them with precision and mechanical method. It would be appropriate to remove the rotten and infected woods and the insect-infested wooden beams on the door and window beams, or all or all of the rotten and infected woods. It would be appropriate to complement and/or renew the partially and/or completely removed woods that have lost their function with wood of the same type (poplar on the lower floor, oak type on the upper floor), and impregnation of the new woods with a vacuum system.

In the walls and vaults of the house to be completed or newly built, cut and/or half-hewn Mardin stone as stone, it would be appropriate to use a mixture of 1 part air lime ($50 \pm 2\%$ hydrated cream lime) as a binder, 0.25 part pozzolan as an additive, 2 mm as aggregate 0.5 part quartz black sand as under sieve size, 2.25 parts limestone crumb and dust (or carbonate aggregates to be obtained from sand quarries) with 10 mm under sieve size, and trowel finishing on the joints where plaster application will not be applied. In new joint applications to be made on the walls and vaults of the house, it will be appropriate to use a mixture of 1 part air lime ($50 \pm 2\%$ hydrated cream lime) as binder, 0.25-part pozzolan as additive, 0.5-part quartz black sand as aggregate, 2 mm under sieve

size. of 2 parts of limestone crushed and dust (or carbonate aggregates to be obtained from sand quarries), 6 mm (or in narrow joints, not exceeding half of the joint gap) under sieve size and trowel finishing. In reinforcing the existing plasters of the house (on vaults and partially on the wall surfaces), it would be appropriate to use a mixture of 1-part hydraulic lime (NHL 3,5), 0.25-part pozzolan as additive, 0.5-part quartz black sand, 4 mm under sieve size, as aggregate, 1.75 parts of limestone flakes and dust (or carbonate aggregates from sand quarries) and trowel the surface. If the 3rd article is applied, in the application of the plaster to be rebuilt on the vault and partly wall surfaces of the house, the binder is 1 part air lime (50% \pm 2 hydrated cream lime), the additive is 0.25 part pozzolan, its aggregate is 4 mm under sieve size. It would be appropriate to use a mixture of 0.5 part quartz black sand, 2 parts limestone fragments and dust (or carbonate aggregates to be obtained from sand quarries) and trowel the surface.

It is recommended to use casein added whitewash with pigment(s) that will provide the color that will determine the project, as paint on interior (applied on vaults and walls) plaster surfaces whose cleaning and repair applications have been completed.

Acknowledgement

We would like to thank T. C. Ministry of Culture and Tourism Mardin Museum Directorate for providing us with the necessary experimental data for this study.

Funding

This research received no external funding.

Author contributions

Lale Karataş: Conceptualization, Methodology, Software, Visualization, Investigation, Writing-Reviewing **Aydın Alptekin:** Editing, Writing-Reviewing **Murat Yakar:** Editing, Reviewing.

Conflicts of interest

The authors declare no conflicts of interest.

References

1. Moropoulou, A., Bakolas, A., & Bisbikou, K. (2000). Investigation of the technology of historic mortars. *Journal of Cultural Heritage*, 1(1), 45-58. [https://doi.org/10.1016/s1296-2074\(99\)00118-1](https://doi.org/10.1016/s1296-2074(99)00118-1)
2. Papayianni, I. (2006). The longevity of old mortars. *Applied Physics A*, 83(4), 685-688. <https://doi.org/10.1007/s00339-006-3523-2>
3. Karataş, L., Alptekin, A., Kanun, E., & Yakar, M. (2022). Tarihi kârgir yapılarda taş malzeme bozulmalarının İHA fotogrametrisi kullanarak tespiti ve belgelenmesi: Mersin Kanlıdivane ören yeri vaka çalışması. *İçel Dergisi*, 2(2), 41-49.
4. Moropoulou, A., Maravelaki-Kalaitzaki, P., Borboudakis, M., Bakolas, A., Michailidis, P., & Chronopoulos, M. (1998). Historic mortars technologies in Crete and guidelines for compatible restoration mortars. In *PACT* (No. 55, pp. 55-72). Conseil de l'Europe.
5. Karataş, L. (2023). Investigating the historical building materials with spectroscopic and geophysical methods: A case study of Mardin Castle. *Turkish Journal of Engineering*, 7(3), 266-278.
6. Karataş, L., Alptekin, A., & Yakar, M. (2022). Creating Architectural Surveys of Traditional Buildings with the Help of Terrestrial Laser Scanning Method (TLS) and Orthophotos: Historical Diyarbakır Sur Mansion. *Advanced LiDAR*, 2(2), 54-63.
7. Karataş, L., Alptekin, A., & Yakar, M. (2022). Determination of Stone Material Deteriorations on the Facades with the Combination of Terrestrial Laser Scanning and Photogrammetric Methods: Case Study of Historical Burdur Station Premises. *Advanced Geomatics*, 2(2), 65-72.
8. Avdelidis, N. P., & Moropoulou, A. (2004). Applications of infrared thermography for the investigation of historic structures. *Journal of Cultural Heritage*, 5(1), 119-127.
9. Fitzner, B., Heinrichs, K., & La Bouchardiere, D. (2004). The Bangudae Petroglyph in Ulsan, Korea: studies on weathering damage and risk prognosis. *Environmental Geology*, 46(3), 504-526.

10. Lee, C. H., Lee, M. S., Kim, Y. T., & Kim, J. (2006). Deterioration assessment and conservation of a heavily degraded Korean Stone Buddha from the ninth century. *Studies in conservation*, 51(4), 305-316.
11. Lee, C. H., & Yi, J. E. (2007). Weathering damage evaluation of rock properties in the Bunhwangsa temple stone pagoda, Gyeongju, Republic of Korea. *Environmental Geology*, 52(6), 1193-1205.
12. Nuzzo, L., Calia, A., Liberatore, D., Masini, N., & Rizzo, E. (2010). Integration of ground-penetrating radar, ultrasonic tests and infrared thermography for the analysis of a precious medieval rose window. *Advances in Geosciences*, 24, 69-82.
13. McK. Clough, T. H., & Woolley, A. R. (1985). Petrography and stone implements. *World Archaeology*, 17(1), 90-100.
14. Patil, S. M., Kasthurba, A. K., & Patil, M. V. (2022). Damage assessment through petrographic and microscopic studies of stone monuments. *Journal of Building Pathology and Rehabilitation*, 7(1), 1-12. <https://doi.org/10.1007/s41024-022-00223-9>
15. Stefano, C., Carboni, S., Pagnotta, S., Lezzerini, M., Raneri, S., Stefano, L., ... & Usai, A. (2018). Laser-Induced Breakdown Spectroscopy analysis of the limestone Nuragic statues from Mont'e Prama site (Sardinia, Italy).
16. Campos-Suñol, M. J., Domínguez-Vidal, A., & la Torre-López, D. (2008). Renaissance patinas in Úbeda (Spain): mineralogic, petrographic and spectroscopic study. *Analytical and bioanalytical chemistry*, 391(3), 1039-1048. <https://doi.org/10.1007/s00216-008-2086-9>
17. Colao, F., Fantoni, R., Ortiz, P., Vazquez, M. A., Martin, J. M., Ortiz, R., & Idris, N. (2010). Quarry identification of historical building materials by means of laser induced breakdown spectroscopy, X-ray fluorescence and chemometric analysis. *Spectrochimica Acta Part B: Atomic Spectroscopy*, 65(8), 688-694. <https://doi.org/10.1016/j.sab.2010.05.005>
18. Theologitis, A., Kapridaki, C., Kallithrakas-Kontos, N., Maravelaki-Kalaitzaki, P., & Fotiou, A. (2021). Mortar and plaster analysis as a directive to the design of compatible restoration materials in Frangokastello (Crete). *Mediterranean Archaeology & Archaeometry*, 21(1), 109-120



© Author(s) 2022. This work is distributed under <https://creativecommons.org/licenses/by-sa/4.0/>